Vol. 73, Part I, 2003

ISSN 0369-8211

Proceedings of the National Academy of Sciences India

SECTION A — PHYSICAL SCIENCES

National Academy of Sciences, India, Allahabad
राष्ट्रीय विज्ञान अकादमी, भारत, इलाहाबाद

The *Proceedings of the National Academy of Sciences, India,* is published in two Sections: Section A (Physical Sciences) and Section B (Biological Sciences). Four parts of each section are published annually (since 1960).

The Editorial Board in its work of examining papers received for publication is assisted, in an honorary capacity by a large number of distinguished scientists. The Academy assumes no responsibility for the statements and opinions advanced by the authors. The papers must conform strictly to the rules for publication of papers in the *Proceedings*. A total of 25 reprints is supplied free of cost to the author or authors. The authors may ask for a reasonable number of additional reprints at cost price, provided they give prior intimation while returning the proof.

Communication regarding contributions for publication in the *Proceedings,* books for review, subscriptions etc. should be sent to the Managing Editor, The National Academy of Sciences, India, 5 Lajpatrai Road, Allahabad-211 002 (India).

Annual Subscription for both Sections : Rs. 500.00; for each Section Rs. 250.00; Single Copy : Rs. 100.00. Foreign Subscription : (a) for one Section : US $100, (b) for both Sections U.S.$ 200.

(Air-Mail charges included in foreign subscription)

Co-Sponsored by C.S.T., U.P. (Lucknow)

PROCEEDINGS

OF THE

NATIONAL ACADEMY OF SCIENCES, INDIA

2003

VOL LXXIII 'SECTION–A PART I

A review on elasto-dynamic problems in couple-stress theory of elasticity

P. R. SENGUPTA[1], SISIR NATH and ASIT MANDAL

[1]*Department of Mathematics, University of Kalyani, Kalyani-741 235, India.*

Received July 10, 2001; Revised Feb. 20, 2002; Accepted May 31, 2002

Abstract

An attempt has been made in this review paper to study the effect of couple-stress on some problems of classical elasto-dynamics. Using the linearized asymmetric theory of couple-stress, presented by Mindlin and Tiersten, the authors have reported the following investigations on elastic waves and distribution of stresses in solid elastic material. In Cosserat's pseudo-continuum, the propagation of surface waves is considered paying special attention to Rayleigh, Love and Stonele type of waves. The propagation of waves in a solid elastic layer has been studied thoroughly in the arena of couple-stress theory of elasticity. Axis symmetric Lamb's problem is also studied in this review paper Remembering the engineering significance the effect of couple-stress on steady-state response to moving loads in a semi-infinite elastic medium is studied in details considering the three possible cases – supersonic, subsonic and transonic, depending on Mach numbers. Wave velocity equations are deduced and in particular in the last problem integral transform technique has been adopted and finally the expressions for displacements and stresses in improper integrals are evaluated and written in terms of real functions. The results obtained during the investigation in this review paper are in fair agreement with the results of the corresponding classical problem when the couple-stress parameter tends to zero.

(Keywords : couple-stress/Cosserat's pseudo-continuum/ asymmetric theory of elasticity/ Galilean-transformation/Mach numbers).

Introduction

The classical theory of elasticity is based on an ideal model of an elastic continuous medium in which the loading is transmitted through an infinitesimal area element in the body by means of stress vector only. The deformations thus take place is characterized by the symmetric strain tensors. The symmetric stress and strain tensors are interrelated by the generalized Hooke's law. Though the results obtained for homogeneous, isotropic materials with the application of the classical theory of elasticity are in harmony with experiments, in many cases, remarkable discrepancies between theory and experiments have been observed. The discrepancy between the classical theory of elasticity and experiment is striking where the stress concentration takes place in solid elastic medium i.e. in the neighbourhood of holes, notches, grooves, cracks and also in case of ultrasonic waves. The classical theory of elasticity eventually fails in the study of vibration of grain bodies and polymer[1].

It is expected from the mechanical point of view that the forces across a hypothetical plane within the solid should be statistically equivalent to a force and a couple. Such an assumption relays the fact that not only force stresses but also the couple stresses are transmitted through an area element, both of them obviously are asymmetric in nature. The corresponding deformations are also characterized by two asymmetric tensors namely strain tensor and curvature twist tensor. These are the main theme of couple-stress theory of elasticity.

The concept of couple-stress was originally introduced by Viogt[2]. The complete theory of asymmetric elasticity was developed in 1909 by the Cosserat brothers[3]. In this theory, which was non-linear in the beginning, they assumed to each molecule a perfectly rigid trihedron which during the process of deformation underwent not only the displacement but also the rotation. The material medium is termed as Cosserat continuum or micropolar elastic medium. In spite of the novelty of the idea, the work of Cosserat brothers was not duly appreciated during their life time and unnoticed for a good while.

After a long time, the interests of research workers were concentrated on the simplified Cosserat theory of asymmetric elasticity of the so-called Cosserat Pseudo-continuum. By this same we understand a continuum for which the symmetric stress (force stress and couple-stress) may occur while the displacement of a body is described by a single displacement vector only. The modern derivation of the Cosserat's theory has been given by Truesdell and Toupin[4], Toupin[5], Aero and Kuvshinki[6,7], Grioli[8], Mindlin[9], Mindlin and Triesten[10] and Cohen[11]. Following the linearized form of constitutive equations in couple-stress theory studied by Mindlin

and Tiersten some problem of elasto-dynamics have been studied in this review paper.

The investigation of propagation of waves (surface waves and waves in a layer) in solid, elastic, homogenous and isotropic medium is one of the main feature of classical elasto-dynamics. Both the problems have been studied by a good number of investigators[12-24]. Regarding Lamb problem, it is noted that Sengupta and Ghosh[25] studied the axis symmetric Lamb problem in couple-stress theory of elasticity and Nowacki and Nowacki[26,27] studied the plane and axis symmetric Lamb problem in micropolar theory of elasticity. In classical theory of elasticity, the problem of moving load over a solid elastic semi-space has been studied by Cole and Huth[28], Lamb[29] and Sneddon[30]. The designs of highways or airport runways, as well as the foundation problems in soil mechanics, particularly when the earth-mass supports a moving load over its free plane surface lead to the investigations of the dynamic stress distribution associated with the problems. It is also noted that Nath and Sengupta[31] investigated steady-state response to moving loads in solid elastic media considering the supersonic-supersonic case.

Sengupta and this research collaborators have studied different problems of elastic waves and vibrations in couple-stress theory of elasticity[32-40]. In this connection it is mentioned that another part of asymmetric elasticity, namely the mircopolar theory of elasticity has been developed by many authors[4156].

The present review paper is concerned with the general linear theory of Cosserat medium. We confine ourselves to the problem of elastic, homogeneous, isotropic and centro-symmetric bodies. Here like the classical, in the linear asymmetric theory of elasticity we assume that the deformations are small and square and product of the deformation are negligible with the respect to the linear terms. It is also assumed that the relation between the state of strain and stress are linear and the increase of temperature is inconsiderable. Lastly, we shall consider the theory of couple stress as macroscopic theory like the classical theory of elasticity and distance considered within its frame are much greater than the intermolecular distance. Hence, it may be assumed that the action radius of the intermolecular forces is negligible and equals to zero.

Basic Equations and Relations :

We shall consider the following basic equations and relations in studying different problems in this review paper. The states of stresses and couple-stresses are given in terms of the Cartesian tensor notation[10].

$$\tau_{ij}^{s} = 2\mu e_{ij} + \lambda e_{kk}\delta_{ij}\ ;\ \mu_{ij}^{D} = 4\eta x_{ij} + 4\eta' x_{ji} \tag{1}$$

where the local strain $e_{i,j}$, rotation ω_i and curvature twist tensor χ_{ij} are expressed in terms of the displacement u_i as

$$e_{ij} = \{u_{i,j} + u_{i,j})/2\};\ \omega_I = -\{\varepsilon_{ijk}\ u_{jk})/2\};\ \chi_{ij} = \omega_{j,i} \tag{2}$$

where λ, μ are Lame's constants, δ_{ij} is Kronecker delta, η and η' are the material constraints associated with resistance to curvature, ε_{ijk} is the unit alternating tensor and comma denotes the partial differential with respect to the space co-ordinates.

The deviation of the couple stress tensor μ_{ij}^{D} and symmetric stress τ_{ij}^{s} are given by

$$\mu_{ij}^{D} = \mu_{ij} - \{(\mu_{kk}\delta_{ij})/3\},\ \tau_{ij}^{s} = \{(\tau_{ij} + \tau_{ij})/2\} \tag{3}$$

The stress equation of motion, couple stress equation of motion and linearized stress equation of motion are given by the vector form[10] as

$$\bar{\nabla}.\bar{\tau} + \rho\bar{f} = \rho\ddot{\bar{u}}\ ; \qquad \bar{\nabla} \equiv \bar{i}\frac{\partial}{\partial x} + \bar{j}\frac{\partial}{\partial y} + \bar{k}\frac{\partial}{\partial z} \tag{4}$$

$$\bar{\nabla}.\bar{\mu} + \rho\bar{c} + \bar{\tau} \times \bar{I} = 0$$

$$\bar{\nabla}.\bar{\tau}^{s} + (1/2)\bar{\nabla} \times \bar{\nabla}.\bar{\mu}^{D} + \rho\bar{f} + (1/2)\rho\bar{\nabla} \times \bar{c} = \rho\ddot{\bar{u}} \tag{5}$$

where I ($\equiv \bar{\nabla} r$) is the unit spatial dyadic, $\bar{f}$ denotes the body force vector, $\bar{c}$ is the body couple vector and dot denotes the time derivative Inserting (1) in (5) we get the displacement equation of motioin[10] as

$$\mu\nabla^2\bar{u} + (\lambda + \mu)\bar{\nabla}\bar{\nabla}.\bar{u} + \eta\nabla^2\bar{\nabla} \times \bar{\nabla} \times \bar{u} + \rho\bar{f} + (1/2)\rho\bar{\nabla} \times \bar{c} = \ddot{\bar{u}} \tag{6}$$

The equations of motion given by (4) and (6) may be written in terms of tensor notations as

$$\begin{aligned} &\tau_{ij,j} + \rho f_i = \rho\ddot{u}_i \\ &\varepsilon_{ijk}\tau_{jk} + \mu_{ji,j} + \rho c_i = 0 \end{aligned} \quad \left| \quad \left[\begin{aligned} &(i, j = 1, 2, 3) \\ &\nabla^2 \equiv \frac{\partial^2}{\partial x^2} + \frac{\partial^2}{\partial y^2} + \frac{\partial^2}{\partial z^2} \end{aligned} \right] \right. \tag{7}$$

$$\mu\nabla^2 u_i + (\lambda+\mu) u_{j,ji} + \eta\nabla^2(u_{j,ji} - \nabla^2 u_i) + \rho f_i - \frac{\rho}{2}\varepsilon_{ijk} c_{j,k} = \rho\ddot{u}_i \tag{8}$$

We shall deal mainly with the following displacement equations of motion in absence of body forces and body couples [putting $f_i = c_i = 0$ (i =1, 2, 3) in equiation (8)] in studying this review paper.

$$\mu\nabla^2 u_i + (\lambda+\mu) u_{j,ji} + \eta\nabla^2(u_{j,ji} - \nabla^2 u_i) = \rho\ddot{u}_i \quad (i, j = 1, 2, 3) \tag{9}$$

Effect of Couple Stress on Surface Waves :

Let us consider two homogeneous elastic medium M_1 and M_2 welded in contact (or sufficiently rough enough to prevent any sliding on common surface) at their common surface of separation. The two medium are separated by a plane horizontal boundary extended to infinity and M_2 being above M_1. As a reference coordinate system, a set of orthogonal Cartesian axes $Ox_1x_2x_3$, the origin O being any point of the boundary and Ox_3 pointing normally into M_2 is taken.

Let us consider the possibility of a wave traveling in the direction Ox_1 in such a manner that (a) the disturbance is largely confined to the neighbourhood of the boundary, and (b) at any instance all particles in any line parallel to Ox_2 have equal displacements. Due to (a), the wave is a surface wave; and due to (b), the case we have taken is analogous to the plane waves. Then the displacement components, u_1 and u_3, at any point may be expressed in the form

$$u_1 = \Phi_{,1} + \psi_{,3},\ u_3 = \Phi_{,3} - \psi_{,1}, \tag{10}$$

so that $\nabla^2\Phi = 0$, $\nabla^2\psi = u_{1,3} - u_{3,1}$ $\nabla^2 \equiv \dfrac{\partial^2}{\partial x_1^2} + \dfrac{\partial^2}{\partial x_3^2}$

where Φ and ψ are functions of coordinates x_1, x_3 and time t.

The displacement equations of motion are from (9)

$$\mu\nabla^2 u_i + (\lambda+\mu) u_{j,ji} + \eta^*\nabla^2(u_{j,ji} - \nabla^2 u_i) = \rho\ddot{u}_i \quad (i, j = 1, 2, 3) \tag{11}$$

Then, in presence of couple-stresses we obtain, in view of (10) and (11), the following relations in M_1 :

$$\nabla^2\Phi - \ddot{\Phi}/\alpha_1^2 = 0, \quad \nabla^2\Psi - \ell_1^2\,\nabla^4 = \ddot{\Psi}_2/\beta_1^2, \nabla^2 u_2 - \ell_1^2\,\nabla^4 u_2 = \ddot{u}_2/\beta_1^2, \tag{12}$$

where ρ_1, λ_1, μ_1 denote the properties of the media M_1 and

$$\alpha_1^2 = \{(\lambda_1 + 2\mu_1)/\rho_1\}, \qquad \beta_1^2 = \mu_1/\rho_1 \text{ and } \ell_1^2 = \eta_1^*/\mu_1, \tag{13}$$

η_1^* being a constant characterizing the effect of couple-stress in the medium M_1. Similar relations hold good in M_2 with ρ_1, λ_1, μ_1 ℓ_1, α_1 β_1 replaced by ρ_2, λ_2, μ_2 ℓ_2, α_2 β_2.

To solve the equations (12) and similar equations for the medium M_2, we assume

$$\Phi = f(x_3)e^{i\xi(x_1-ct)}, \qquad \Psi = g(x_3)e^{i\xi(x_1-ct)}, u_2 = h(x_3)e^{i\xi(x_1-ct)} \tag{14}$$

On substituting equation (14) in (12) and similar equations for the medium M_2, and on simplification we get the solutions satisfying conditions for surface waves, as follows:

In the medium M_1

$$\left.\begin{aligned} \Phi &= Ae^{i\xi\left(-r_1x_3+x_1-ct\right)}, \\ \Psi &= \left[Be^{-\eta_1x_3} + Ce^{\varsigma_1x_3}\right]e^{i\xi(x_1-ct)}, \\ u_2 &= \left[B^*e^{-\eta_1x_3} + C^*e^{\varsigma_1x_3}\right]e^{i\xi(x_1-ct)}. \end{aligned}\right\} \tag{15}$$

In the medium M_2

$$\left.\begin{aligned} \Phi &= De^{i\xi(r_2x_3+x_1-ct)}, \\ \Psi &= \left[Ee^{\eta_2x_2} + Fe^{-\varsigma_2x_3}\right]e^{i\xi(x_1-ct)}, \\ u_2 &= \left[E^*e^{\eta_2x_3} + F^*e^{-\varsigma_2x_3}\right]e^{i\xi(x_1-ct)}. \end{aligned}\right\} \tag{16}$$

where A, B, C, D, E, F, B^*, C^*, F^* are all arbitrary constants and r_j, η_j (j = 1, 2) are all positive imaginaries and ζ_j are positive real numbers given by

$$\left.\begin{aligned} r_j &= \left(\frac{\rho_j c^2}{\lambda_j + 2\mu_j} - 1\right)^{1/2}, \eta_j = \left(p_j^2 - \xi^2\right)^{1/2}, \ \zeta_j = \left(q_j^2 + \xi^2\right)^{1/2} \\ p_j^2 &= \frac{1}{2\ell_j^2}\left\{\left(1 + 4\frac{\rho_j}{\mu_j}\xi^2 c^2 \ell_j^2\right)^{1/2} - 1\right\}, \ q_j^2 = \frac{1}{2\ell_j^2}\left\{\left(1 + 4\frac{\rho_j}{\mu_j}\xi^2 c^2 \ell_j^2\right)^{1/2} + 1\right\} \end{aligned}\right\} \quad (17)$$

The above system of equations (15) and (16) will lead us to a particular solution corresponding to a group of simple harmonic waves of wave-length $2\pi/\xi$ traveling forward with speed c.

To obtain the velocity equations we have now to apply the following boundary conditions :

(i) The displacement at the common boundary surface between M_1 and M_2 must be continuous at all times and places.

(ii) The rotation components ω_1, ω_2 and ω_3 where $\omega_1 = -\frac{u_{2,3}}{2}$, $\omega_2 = \nabla^2\psi$, $\omega_3 = -\frac{u_{2,1}}{2}$ must be continuous on the common boundary.

(iii) The stresses σ_{31}, σ_{32}, σ_{32} and couple-stress μ_{31}, μ_{32}, μ_{33}, where

$$\left.\begin{aligned} \sigma_{31} &= \mu_1\left(2\Phi_{,13} - \Psi_{,11} + \Psi_{,33}\right) - \eta_1^*\nabla^4\Psi, \\ \sigma_{32} &= \mu_1 u_{2,3} - \eta_1^*\left(u_{2,333} + u_{2,311}\right), \\ \sigma_{33} &= \lambda_1\nabla^2\Phi + 2\mu_1\left(\Phi_{,33} - \Psi_{,13}\right), \\ \mu_{31} &= -2\eta_1^* u_{,33}, \quad \mu_{32} = 2\eta_1^*\nabla^2\psi_{,3}, \end{aligned}\right\} \quad (18)$$

and similar expressions for M_2, across the boundary surface between M_1 and M_2 must be continuous at all times and places. Using (10), (15), (16) and the condition (i), we obtain

$$\xi A - \eta_1 B - i\zeta_1 C = \xi D + E + \eta_2 E + i\zeta_2 F, \quad (19)$$

$$-r_1 A - (B + C) = r_2 D - (E + F), \quad (20)$$

$$B^* + C^* = E^* + F^*$$

Again, substituting (15) and (16) into (19) and using condition (iii), we obtain

$$\begin{aligned} &2\mu_1 r_1 \xi^2 A + \left\{\left(\xi^2 - \eta_1^2\right)\mu_1 - \eta_1^*\left(\eta_1^2 + \xi^2\right)^2\right\}B + \left\{\left(\xi^2 + \zeta_1^2\right)\mu_1 - \mu_1^*\left(\zeta_1^2 - \xi^2\right)^2\right\}C \\ &= -2\mu_2 r_2 \xi^2 D + \left\{\left(\xi^2 - \eta_2^2\right)\mu_2 - \eta_2^*\left(\eta_2^2 + \xi^2\right)^2\right\}E + \left\{\left(\xi^2 + \zeta_2^2\right)\mu_2 - \eta_2^*\left(\zeta_2^2 - \xi^2\right)^2\right\}F; \end{aligned} \tag{22}$$

$$\left\{\eta_1^*\eta_1\left(\eta_1^2 + \xi^2\right) + \eta_1\mu_1\right\}B^* + i\left\{\eta_1^*\zeta_1\left(\xi^2 - \zeta_1^2\right) + \zeta_1\mu_1\right\}C^* =$$

$$= -\left\{\eta_2^*\eta_2\left(\eta_2^2 + \xi^2\right) + \eta_2\mu_2\right\}E^* - i\left\{\eta_2^*\zeta_2\left(\xi^2 - \zeta_2^2\right) + \zeta_2\mu_2\right\}F^*; \tag{23}$$

$$\left\{\lambda_1\left(r_1^2 + 1\right) + 2\mu_1 r_1^2\right\}\xi^2 A + 2\mu_1\xi\eta_1 B + 2\mu_1\xi\zeta_1 iC =$$

$$= \left\{\lambda_2\left(r_2^2 + 1\right) + 2\mu_2 r_2^2\right\}\xi^2 D - 2\mu_2\xi\eta_2 E - 2\mu_2\xi\zeta_2 iF; \tag{24}$$

$$i\eta_1\left(\eta_1^2 + \xi^2\right)\eta_1^* B + \zeta_1\left(\zeta_1^2 - \xi^2\right)\eta_1^* C = -i\eta_2\left(\eta_2^2 + \xi^2\right)\eta_2^* E - \zeta_2\left(\zeta_2^2 - \xi^2\right)\eta_1^* F; \tag{25}$$

$$\eta_1^*\left(-i\eta_1 B^* + \zeta_1 C^*\right) = \eta_2^*\left(i\eta_2 E^* - \zeta_2 F^*\right), \tag{26}$$

and from the condition (ii), we obtain

$$i\eta_1 B^* + \zeta_1 C^* = i\eta_2 E^* - \zeta_2 F^*, \tag{27}$$

$$-\left(\eta_1^2 + \xi^2\right)B + \left(\zeta_1^2 - \xi^2\right)C = -\left(\eta_2^2 + \xi^2\right)E + \left(\zeta_2^2 - \xi^2\right)F, \tag{28}$$

and other component ω_2 contributes the same equation as (21).

From the equations (21), (23), (26) and (27) we find that only possible values of B^*,C^*, E^* and F^* are zeros. Thus there is no propagation of the displacements u_2.

Again, equation (25) will be satisfied if

$$C=-\frac{ip_1^2\eta_1}{q_1^2\zeta_1}B+\frac{K}{q_1^2\zeta_1\eta_1^*}\text{ and }F=-\frac{ip_2^2\eta_2}{q_2^2\zeta_2}E+\frac{K}{q_2^2\zeta_2\eta_2^*} \tag{29}$$

where K is a constant which depends on the parameters of the couple-stress of the media. From the equations (28) and (29), we obtain

$$K=v_1p_1^2B-v_2p_2^2E\,, \tag{30}$$

where

$$v_1=(1+i/\varsigma_1)\Big/\left(\frac{1}{\zeta_1\eta_1^*}+\frac{1}{\varsigma_2\eta_2^*}\right),\qquad v_2=(1+i/\zeta_2)\Big/\left(\frac{1}{\zeta_1\eta_1^*}+\frac{1}{\zeta_2\eta_2^*}\right) \tag{31}$$

In view of (31) the equations (19), (20), (22) and (24) can be written as

$$\left.\begin{aligned}
&\xi A-\left(\eta_1\frac{\eta_1p_1^2}{q_1^2}-iv_1p_1^2a\right)B-\xi D-\left(\eta_2\frac{\eta_2p_2^2}{q_2^2}+iv_2p_2^2a\right)E=0\\
&r_1A+\left(1-\frac{i\eta_1p_1^2}{\varsigma_1q_1^2}+v_1p_1^2b\right)B+r_2D-\left(1-\frac{i\eta_2p_1^2}{\zeta_2q_2^2}+v_2p_2^2b\right)E=0\\
&2\mu_1r_1\xi^2A+\left[\left\{\left(\xi^2-\eta_1^2\right)\mu_1-\eta_1^*p_1^4\right\}-i\left\{\left(\xi^2+\zeta_1^2\right)\mu_1-\eta_1^*q_1^4\right\}\frac{\eta_1p_1^2}{\zeta_1q_1^2}+v_1p_1^2c\right]\\
&B+2\mu_2r_2\xi^2D-\left[\left\{\left(\xi^2-\eta_2^2\right)\mu_2-\eta_2^*p_2^4\right\}-i\left\{\left(\xi^2+\varsigma^2\right)\mu_2-\eta_2^*q_2^4\right\}\frac{\eta_2p_2^2}{\varsigma_2q_2^2}+v_2p_2^2c\right]E=0\\
&\left\{\left(\lambda_1+2\mu_1\right)\left(r_1^2+1\right)-2\mu_1\right\}\xi A+\left\{2\mu_1\left(\eta_1+\frac{\eta_1p_1^2}{q_1^2}\right)+iv_1p_1^2d\right\}B-\\
&\left\{\left(\lambda_2+2\mu_2\right)\left(r_2^2+1\right)-2\mu_2\right\}\xi D+\left\{2\mu_2\left(\eta_2+\frac{\eta_2p_2^2}{q_2^2}\right)-iv_2p_2^2d\right\}E=0,
\end{aligned}\right\} \tag{32}$$

where

$$\left.\begin{aligned} a &= \frac{1}{q_1^2\eta_1^*} - \frac{1}{q_2^2\eta_2^*}, \quad b = \frac{1}{\zeta_1 q_1^2\eta_1^*} + \frac{1}{\zeta_2 q_2^2\eta_2^*}, \\ c &= \left\{\left(\xi^2+\zeta_1^2\right)\mu_1 - \eta_1^*\left(\zeta_1^2-\xi^2\right)^2\right\}\frac{1}{\zeta_1 q_1^2\eta_1^*} + \left\{\left(\xi^2+\zeta_2^2\right)\mu_2 - \eta_2^*\left(\zeta_2^2-\xi^2\right)^2\right\}\frac{1}{\zeta_2 q_2^2\eta_2^*}, \\ d &= \frac{2\mu_1}{q_1^2\eta_1^*} - \frac{2\mu_2}{q_2^2\eta_2^*} \end{aligned}\right\} \tag{33}$$

Eliminating A, B, D and E from the equations (32), we obtain the modified wave-velocity equation of the surface waves under the influence of couple-stresses,

$$\begin{vmatrix} \xi - \left\{\left(\eta_1 + \frac{p_1^2}{q_1^2}\right) - iv_1 p_1^2 a\right\} & -\xi - \left\{\left(\eta_1 + \frac{p_2^2}{q_2^2}\right) - iv_2 p_2^2 a\right\} \\ r_1\left(1 - \frac{i\eta_1 p_1^2}{\zeta_1 q_1^2} + v_1 p_1^2 b\right) & r_2\left(-1 - \frac{i\eta_2 p_2^2}{\zeta_2 q_2^2} + v_2 p_2^2 b\right) \\ 2\rho_1\beta_1 r_1\xi^2\left[\begin{matrix}\rho_1\beta_1^2\left\{\left(\xi^2-\eta_1^2\right) - \ell_1^2 p_1^4\right\} - 2\rho_2\beta_2 r_2\xi^2 - \\ i\left\{\left(\xi^2-\zeta_1^2\right) - \ell_1^2 q_1^4\right\}\times\frac{\eta_1 p_1^2}{\zeta 1} q_1^2\rho_1\beta_1^2 + v_1 p_1^2 c\end{matrix}\right] & 2\rho_2\beta_2 r_2\xi^2\left[\begin{matrix}\left\{\left(\xi^2-\eta_2^2\right) - \ell_2^2 p_2^4\right\}\times\rho_2\beta_2^2 - \rho_2 \\ \left\{\left(\xi^2+\zeta_2^2\right) - \ell_2^2 q_2^4\right\}\beta_2^2\frac{\eta_2 p_2^2}{\zeta_2 q_2^2} + v_2 p_2^2 c\end{matrix}\right] \\ \left[\rho_1\left\{\alpha_1^2\left(r_1^2+1\right)2\rho_1\beta_1^2\left(\eta_1 + \frac{\eta_1 p_1^2}{q_1^2}\right) + iv_1 p_1^2 d - 2\beta_1^2\right\}\xi\right] & \left[-\rho_2\left\{\alpha_2^2\left(r_2^2+1\right)\right\}2\rho_2\beta_2^2\left(\eta_2 + \frac{\eta_2 p_2^2}{q_2^2}\right) + iv_2 p_2^2 d\right] \\ -2\beta_1^2\}\xi] & -2\beta_2^2\}\xi] \end{vmatrix} \tag{34}$$

$$= 0$$

where α_j^2, β_j^2 and ℓ_j^2 are given by (13) and $j = 1,2$.

If the parameters of couples=stress ℓ_1 and ℓ_2 vanish, the wave-velocity equation (34) as obtained above is in agreement with the corresponding classical result, which may be written in the simplified form.

$$c^4[(\rho_1-\rho_2)^2+(\rho_1 r_2+\rho_2 r_1)]+2Qc^2[r_1\eta_1\rho_2-r_2\eta_2\rho_1+\rho_2-\rho_1]+Q^2(r_1\eta_1+1)(r_2\eta_2+1)=0, \tag{35}$$

where $q=2(\rho_1\beta_1^2-\rho_2\beta_2^2)=2(\mu_1-\mu_2)$ and $r_j=\left\{\left(c^2/\alpha_j^2\right)-1\right\}^{1/2}$, $\eta_j=\left\{\left(c^2/\beta_j^2\right)-1\right\}^{1/2}$

Particular cases :

Ralieigh waves : The particular case of the foregoing problem is to investigate the possibility of Rayleigh waves in an elastic solid under the influence of couple-stress. In this particular case the plain boundary must be a free surface so that M_2 is replaced by vacuum. In view of (22), (24) and (25) we obtain :

$$2\mu_1 r_1\xi^2 A+\left[\left\{\left(\xi^2-\eta_1^2\right)\mu_1-\eta_1^* p_1^4\right\}-i\left\{\left(\xi^2+\zeta_1^2\right)\mu_1-\eta_1^* q_1^4\right\}\eta_1 p_1^2/\zeta_1 q_1^2\right]B=0, \tag{36}$$

$$\left\{\left(\lambda_1+2\mu_1\right)\left(r_1^2+1\right)-2\mu_1\right\}\xi A+2\mu_1\left\{\eta_1+\left(\eta_1 p_1^2/q_1^2\right)\right\}B=0. \tag{37}$$

Eliminating A and B from (36) and (37), we obtain :

$$4\mu_1^2 r_1\xi\left\{\eta_1+\left(\eta_1 p_1^2/q_1^2\right)\right\}-\left\{\left(\lambda_1+2\mu_1\right)\left(r_1^2+1\right)-2\mu_1\right\}\left[\left\{\left(\xi^2-\eta_1^2\right)\mu_1-\eta_1^* p_1^4\right\}-i\left\{\left(\xi^2+\zeta_1^2\right)\mu_1-\eta_1^* q_1^4\right\}\eta_1 p_1^2/\zeta_1 q_1^2\right]=0 \tag{38}$$

Equation (38), in view of (17) becomes

$$4\left(\frac{c^2}{\alpha_1^2}-1\right)^{\frac{1}{2}}\left(\frac{p^2}{\xi^2}-1\right)^{\frac{1}{2}}\left(1+\frac{p_1^2}{c_1^2}\right)=\left(\frac{c^2}{\beta_1^2}-2\right)\left(2-\frac{c^2}{\beta_1^2}\right)\left(1-i\frac{\eta_1 p_1^2}{\zeta q_1^2}\right) \tag{39}$$

Equation (39) determines the velocity of the Rayleigh surface wave under the influence of couple-stress.

If the parameter ℓ_2 of couple-stress be zero, we obtain the classical result[19]

$$\{2-(c^2/\beta_1^2)\}^2 = 4\{1-(c^2/\alpha_1^2)\}^{1/2}\{1-(c^2/\beta_1^2)\}^{1/2}$$

The equation (39) can be analysed to study the effect of couple-stress on the said classical problem by assuming the couple-stress parameter ℓ_2 to be so small that its cubes and higher powers are always neglected. Thus the approximate form of equation (39) is

$$\left(2-\frac{c^2}{\beta_1^2}\right)^2 = 4\left(1-\frac{c^2}{\alpha_1^2}\right)^{\frac{1}{2}}\left(1-\frac{c^2}{\beta_1^2}+\frac{c^4}{\beta_1^4}\xi^2\ell_1^2\right)^{\frac{1}{2}} = \left(1+\frac{\xi^2c^2}{\beta_1^2}\ell_1^2\right) \tag{40}$$

Squaring both the sides of (40) and re-arranging we obtain

$$\frac{c^2}{\beta_1^2}\left[\frac{c^6}{\beta_1^6}-8\frac{c^4}{\beta_1^4}+c^2\left(\frac{24}{\beta_1^2}-\frac{16}{\alpha_1^2}\right)-16\left(1-\frac{c_2^2}{\alpha_1^2}\right)-16\xi^2\ell_1^2\frac{c^2}{\beta_1^2}\times\left(1-\frac{c_2^2}{\alpha_1^2}\right)-32\xi\ell^2\left\{1-\left(\frac{c_2^2}{\alpha_1^2}+\frac{c_2^2}{\beta_1^2}\right)+\frac{c_4}{\alpha_1^2\beta_1^2}\right\}\right]=0 \tag{41}$$

We assume $\lambda = \mu$ (i.e. $\nu = ¼$), then $\alpha_1 = \sqrt{3}\beta_1$, and we obtain from equation (41)

$$\left(\frac{c^6}{\beta_1^6}-8\frac{c^4}{\beta_1^4}+\frac{56}{3}\frac{c^2}{\beta_1^2}-\frac{32}{3}\right)-\frac{16}{3}\xi^2\ell_1^2\left(3-\frac{c^2}{\beta_1^2}\right)\left(2-\frac{c^2}{\beta_1^2}\right)=0 \tag{42}$$

The above equation is a cubic equation in c^2/β_1^2 and has three real and positive roots. One of the roots lies between 0.8453 and 2. In order to satisfy the condition of Rayleigh waves the value of $\xi^2\ell_1^2$ must be less than or equal to 0.09, and the acceptable roots for the real existence of Rayleigh waves have been computed numerically. It is thus observed that the velocity of Rayleigh waves increases due to the influence of couple-stress.

Numerical result :

In Table 1 the values of c/β_1 have been computed for different values of $\xi^2\ell_1^2$ in equatin (42), and thus it has been exhibited that the velocity of Rayleigh waves in presence of couple-stresses increases.

Table 1– Computed of c/β_1 for different values of the couple-stress parameter

$\xi^2\ell_1^2$	10^{-2}	10^{-3}	10^{-4}	10^{-5}	10^{-6}
c/β_1	0.92915	0.92288	0.92199	0.919411	0.9194025

Love waves :

Let us suppose that the medium M_2 is bounded by two horizontal plane surface at finite distance H apart, the upper plane being free, while the lower plane surface forms the medium M_1.It is sufficient to consider the displacement u_2 only. The notable fact here is that the displacement in M_2 may no longer dimnish with distance from the boundary between M_1 and M_2, so that for the medium M_2 we presence the full solution as

$$u_2 = \left[\left(A_1 e^{i\eta_2 x_3} + A_2 e^{-i\eta_2 x_3}\right) + \left(B_1 e^{-\zeta_2 x_3} + B_2 e^{\zeta_2 x_3}\right) e^{i\xi(x_1 - ct)}\right], \tag{43}$$

and for the medium M_1, the solution is

$$u_2 = \left[\left(B^* e^{-i\eta_2 x_3} + C^* e^{\zeta_1 x_3}\right)\right] e^{i\xi(x_1 - ct)}, \tag{44}$$

where η_2 is not necessarily imaginary, while for M_1 we see that η_1 is an imaginary and ζ_1, ζ_2 are positive quantities.

In addition to the three boundary conditions (i), (ii) and (iii) for general surface waves we have the conditions that there shall be no stress and couple-stress across the free surface $x_3 = H$. Hence, in view of (43), (44) the boundary conditions may be written as

$$B^* + C^* = (A_1 + A_2) + (B_1 + B_2), \tag{45}$$

$$i\eta_1 B^* + \zeta_1 C^* = i\eta_2 (A_1 - A_2) - \zeta_2 (B_1 - B_2), \tag{46}$$

$$-i\eta_1\mu_1\left(1 + \ell_1^2\beta_1^2\right) B^* + \mu_1\zeta_1\left(1 - \ell_1^2 q_1^2\right) C^*$$

$$= i\eta_2\mu_2\left(1 + \ell_2^2 p_2^2\right)\left(A_1 - A_2\right) - \mu_2^2\zeta_2\left(1 - \ell_1^2 q_2^2\right)\left(B_1 - B_2\right) \tag{47}$$

$$\left(-\eta_1^2 B^* + \zeta_1^2 C^*\right)\mu_1\ell_1^2 = \left\{-\eta_2^2\left(A_1 + A_2\right) + \zeta_2^2\left(B_1 + B_2\right)\right\}\mu_2\ell_2^2 \tag{48}$$

$$i\eta_2\left(1+\ell_2^2p_2^2\right)\left(A_1e^{i\eta_2H}-A_2e^{-i\eta_2H}\right)=\zeta_2\left(1-\ell_2^2q_2^2\right)\left(B_1e^{-\zeta_2H}-B_2e^{\zeta_2H}\right)=0 \tag{49}$$

$$-\eta_2^2\left(A_1e^{i\eta_2H}+A_2e^{-i\eta_2H}\right)+\zeta_2^2\left(B_1e^{-\zeta_2H}-B_2e^{\zeta_2H}\right)=0 \tag{50}$$

From (48) we, get

$$C^*=\frac{K}{\mu_1\ell_1^2\zeta_1^2}+\frac{\eta_1^2}{\zeta_1^2}B^*,\ B_1+B_2=\frac{K}{\mu_2\ell_2^2\zeta_1^2}+\frac{\eta_2^2}{\zeta_2^2}\left(A_1+A_2\right), \tag{51}$$

where K is an arbitrary constant which depends on the parameters.

Equation (49) and (50) are satisfied if

$$\left(\eta_2^2/\zeta_2^2\right)A_1e^{i\eta_2H}=\left(\eta_2^2/\zeta_2^2\right)A_2e^{-i\eta_2H}=B_2e^{\zeta_2H}=B_1e^{-\zeta_2H}, \tag{52}$$

which gives $\dfrac{A_2-A_1}{A_1+A_2}=i\tan\eta_2H$ and $B_1-B_2=(B_1+B_2)\tan h\zeta_2H$ (53)

In view of (46), (51) and the second equation of (53), we obtain

$$K=(1/a)\{bB^*+c(A_1+A_2)\},$$

$$\left.\begin{aligned}&K=(1/a)\left\{bB^*+c\left(A_1+A_2\right)\right\}\\&\text{where } a=\left(\frac{\tan h\zeta_2H}{\mu_2\ell_2^2\zeta_1}+\frac{1}{\mu_1\ell_1^2\zeta_2}\right),\ b=i\eta_1^2+\frac{\eta_1^2}{\zeta_1},\ c=\frac{\eta_2^2}{\zeta_2^2}\tan h\zeta_2H+\eta_2\tan\eta_2H\end{aligned}\right\} \tag{54}$$

In view of (51), (54), we obtain from (45) and (47)

$$\begin{aligned}&\mu_1\left\{-i\eta_1\left(1+\ell_1^2p_1^2\right)+\frac{1-\ell_1^2q_1^2}{\zeta_1^2}\eta_1^2+b_2\right\}\frac{1+\left(\eta_2^2/\zeta_2^2\right)+c_1}{1+\left(\eta_1^2/\zeta_1^2\right)-b_1}\left(A_1+A_2\right)\\&=\mu_2\left[i\eta_2\left\{1+\ell_2^2p_2^2\left(A_1-A_2\right)\right\}-\left\{1-\ell_2^2q_2^2\left(\eta_2^2/\zeta_2^2\right)\tan h\zeta_2H+c_2\right\}\left(A_1+A_2\right)\right]\end{aligned} \tag{55}$$

where

$$\left.\begin{aligned} b_1 &= \frac{b}{a}\left(\frac{1}{\mu_2\ell_2^2\zeta_2^2}-\frac{1}{\mu_1\ell_1^2\zeta_1^2}\right), c_1 = \frac{c}{a}\left(\frac{1}{\mu_2\ell_2^2\zeta_2^2}-\frac{1}{\mu_1\ell_1^2\zeta_1^2}\right) \\ \mu_1 b_2 &= \frac{b}{a}\left\{\frac{\zeta_1\left(1-\ell_1^2q_1^2\right)}{\ell_1^2\zeta_1^2}-\frac{\zeta_2\left(1-\ell_2^2q_2^2\right)\tan h\zeta_2 H}{\ell_2^2\zeta_2^2}\right\}, \\ \mu_2 c_2 &= \frac{c}{a}\left\{\frac{\zeta_1\left(1-\ell_1^2q_1^2\right)}{\ell_1^2\zeta_1^2}-\frac{\zeta_2\left(1-\ell_2^2q_2^2\right)\tan h\zeta_2 H}{\ell_2^2\zeta_2^2}\right\}. \end{aligned}\right\} \tag{56}$$

Equation (54), in view of the first equation of (52), becomes

$$\begin{aligned} &\mu_1\left\{-i\eta_1\left(1+\ell_1^2p_1^2\right)+\left(1-\ell_1^2q_1^2/\zeta_1^2\right)\eta_1^2+b_2\right\}\frac{1+\left(\eta_2^2/\zeta_2^2\right)+c_1}{1+\left(\eta_1^2/\zeta_1^2\right)-b_1} \\ &=\mu_2\left[\eta_2\left\{\left(1+\ell_2^2p_2^2\right)\right\}\tan\zeta_2H-\left\{\left(1-\ell_2^2q_2^2\right)\left(\eta_2^2/\zeta_2^2\right)\tan h\,\zeta_2H+c_2\right\}\right] \end{aligned} \tag{57}$$

The above equation gives the S. H. surface waves of velocity under the inluece of couple-stress. If the parameters of couple-stresses, ℓ_1 and ℓ_2 vanish, the wave-velocity equation is in agreement with the classical equation of Love waves. Hence, equation (57) shows the remarkable effect of couple-stresses on the Love waves.

The modified equation can be analysed to study the effect of couple-stresses on the classical problem by assuming the parameters of couple-stresses, ℓ_1 and ℓ_2, to be small so that their cubes and higher powers are always neglected. Hence, on the above assumption, we obtain the following approximate form of equation (57):

$$\mu_1\left[-i\eta_1\left\{1+\left(c^2/\beta_1^2\right)\xi^2\ell_1^2\right\}\right]=\mu_2\left[\eta_2\left\{1+\left(c^2/\beta_2^2\right)\xi^2\ell_2^2\right\}\tan\eta_2H\right],$$

where $$\eta_i=\xi\left\{\left(c^2/\beta_i^2\right)-\left(c^4/\beta_i^4\right)\xi^2\ell_1^2-1\right\}(i=1,2) \tag{59}$$

Equation (58) yields a real value of c if η_1 are imaginary and real respectively. The requirement that η_1, should be imaginary and η_1 be real is, by (59),

$$\beta_2\left(1+\xi^2\ell_2^2\right)<c<\beta_1\left(1+\xi^2\ell_1^2\right) \tag{60}$$

which shows that for a particular ξ the range of c increase under the influence of couple-stresses. In other words, the velocity c of Love waves increases under the influence of couple-stresses.

Stoneley waves :

In the classical theory Stoneley waves are a generalized form of Rayleigh waves propagating along the common boundary of M_1 and M_2. Hence, Stoneley waves along the common boundary of the media M_1 and M_2 under the influence of couple-stresses are determined by the roots of the wave equation (25). When the couple-stress parameters vanish, we get equation (26), which is the frequency equation of Stoneley waves in the classical theory.

Effect of couple-stress on waves in a layer :

Let us introduced a Cartesian frame of reference $ox_1x_2x_3$ taking the origin in the middle plane of the elastic layer; the middle plane coincides with the plane ox_1x_2. We consider the effect of couple-stresses on the propagation of waves in an elastic layer of thickness $2h$. The planes bounding the layer are $x_3 = \pm h$ and are supposed to be free of stress. There exists a plane wave moving with the constant velocity c in the direction of x_1. Both the longitudinal and transverse waves in the infinitely extended layer would be propagated. The boundary surfaces of the elastic space leads evidently to a distortion of the state of stress, which influences the velocity of propagation of elastic waves. From the nature of the problem the non-zero displacement u_1 and u_3 at any point may be expressed in the form.

$$u_1 = \phi_{,1} - \psi_{,3}, \qquad u_3 = \phi_{,3} + \psi_{,1} \tag{61}$$

where ϕ and ψ are displacement potentials, functions of the coordinates x_1, x_3 and time.

The displacement equations of motion are

$$\eta\nabla^2 u_i + (\lambda+\mu)u_{j,ji} + \eta^2\nabla^2(u_{j,ji} - \nabla^2 u_i) = \rho\ddot{u}_i \qquad [i,j = 1, 2, 3] \tag{62}$$

The equation of motion (62) in view of (61), yield the following equations

$$\nabla^2\phi - c_1^2\ddot{\phi} = 0; \qquad \nabla^2\psi - \ell^2\nabla^4\psi = c_2^2\ddot{\psi} \tag{63}$$

where $c_1^2 = (\lambda + 2\mu)/\rho$, $c_2^2 = \mu/\rho$, $\ell^2 = \eta/\mu$,

η is a constant characterizing the existence of couple-stresses and λ, μ are Lame's elastic constants. If ℓ, the parameter of couple-stress, be zero the classical result of the corresponding problem follows at once.

Our problem here is to seek solutions of the equations (63) subject to the boundary conditions

$$\sigma_{33} = \sigma_{31} = \mu_{32} = 0 \text{ in the plane } x_3 = \pm h \tag{64}$$

The stresses σ_{ij} and couple-stresses μ_{ij} are given by[1]

$$\left.\begin{array}{ll} \sigma_{33} = 2\mu e_{33} + \lambda(e_{11} + e_{33}), & \sigma_{11} = 2\mu e_{11} + \lambda(e_{11} + e_{33}) \\ \sigma_{13} + \sigma_{31} = 4\mu e_{13}, & \mu_{32} = 4\eta(e_{31,3} - e_{33,1}) \\ \sigma_{13} + \delta\sigma_{31} = -\mu_{13,1} + \mu_{32,3} & \mu_{12} = 4\eta(e_{11,3} - e_{13,1}) \end{array}\right\} \begin{pmatrix} i = 1,3 \\ j = 1,3 \end{pmatrix} \tag{65}$$

On substituting for μ_1 and μ_3 from (61) in (65) we get

$$\left.\begin{array}{ll} \sigma_{11} = 2\mu(\phi_{,11} - \psi_{,13}) + \lambda\nabla^2\phi, & \sigma_{33} = 2\mu(\phi_{,33} - \psi_{,13}) + \lambda\nabla^2\phi \\ \sigma_{13} = \mu(2\phi_{,13} - \psi_{,33} + \psi_{,11}) - \eta\nabla^4\psi & \sigma_{31} = \mu(2\phi_{,31} - \psi_{,33} + \psi_{,11}) + \eta\nabla^4\psi \\ \mu_{32} = -2\eta\nabla^2(\psi_{,3}) & \mu_{12} = -2\eta\nabla^2(\psi_{,1}) \end{array}\right\} \begin{pmatrix} i = 1,3 \\ j = 1,3 \end{pmatrix} \tag{66}$$

To solve the equation (63), we assume

$$\phi(x_1, x_3, t) = f(x_1, x_3)e^{i\omega t} \quad ; \quad \psi(x_1, x_3, t) = g(x_1, x_3)\, e^{i\omega t} \tag{67}$$

Owing to (67), equations (63) take the form

$$\nabla^2 f + k_1^2 f = 0 \quad ; \quad \nabla^2 g + k_2^2 g - \ell^2\nabla^4 g = 0 \tag{68}$$

where $k_1^2 = (\omega^2/c_1^2)$, $k_2 = (\omega^2/c_2^2)$

The solution of the equation (67) are

$$f = f^*(x_3)\,e^{-i\alpha x_1} \qquad ; \qquad g = g^*(x_3)\,e^{-i\alpha x_1} \tag{69}$$

Introducing (69) into (68), we arrive at two ordinary differential equations

$$\left(\frac{d^2}{dx_3^2}\right) f^* - \left(\alpha^2 - k_1^2\right) f^* = 0 \left[\ell^2\left(\frac{d^2}{dx_3^2}\right) - \alpha^2\right]^2 - \left(\frac{d^2}{dx_3^2}\right) - \alpha^2 - k_1^2 \Big\} g^* = 0 \tag{70}$$

the solution of which are

$$\left.\begin{aligned} f^* &= A\sinh \nu_1 x_3 + B\cosh \nu_1 x_3 \\ g^* &= C\sinh \nu_2 x_3 + D\cosh \nu_2 x_3 + E\sinh \nu_3 x_3 + F\cosh \nu_3 x_3 \end{aligned}\right\} \tag{71}$$

where

$$\nu_1 = \sqrt{\alpha^2 - k_1^2}, \quad \nu_2 = \sqrt{\alpha^2 - p^2}, \quad \nu_3 = \sqrt{\alpha^2 - q^2},$$
$$p^2 = \left(1/2\ell^2\right)\left[\left(1 + 4k_2^2\ell^2\right)^{1/2} - 1\right]; \; q^2 = \left(1/2\ell^2\right)\left[\left(1 + 4k_2^2\ell^2\right)^{1/2} - 1\right]$$

By virtue of equations (71), (69) and (67), we finally obtain

$$\left.\begin{aligned} \phi &= \left(A\sinh \nu_1 x_3 + B\cosh \nu_1 x_3\right)^{i(\omega t - \alpha x_1)} \Big\} \\ \psi &= \left(C\sinh \nu_2 x_3 + D\cosh \nu_2 x_3 + E\sinh \nu_3 x_3 + F\cosh \nu_3 x_3\right)^{i(\omega t - \alpha x_1)} \Big\} \end{aligned}\right\} \tag{72}$$

we consider the particular case

$$\left.\begin{aligned} \phi_1 &= B\cosh \nu_1 x_3^{\,i(\omega t - \alpha x_1)} \Big\} \\ \psi_1 &= \left(C\sinh \nu_2 x_3 + E\sinh \nu_3 x_3 + F\cosh \nu_3 x_3\right)^{i(\omega t - \alpha x_1)} \Big\} \end{aligned}\right\} \tag{73}$$

Introducing (73) into (61), it is readily observed that in this case the displacement are symmetric with respect to $x_3 = 0$, so are the stresses σ_{33}, σ_{31} and couple-stress μ_{32}. Besides, the stress σ_{13} and the couple-stress μ_{12} are antisymmetric with respect to the plane $x_3 = 0$.

Substituting from (73) into the boundary conditions (64), we get,

$$\left.\begin{aligned}(\rho\omega^2-2\mu\alpha^2)B\cosh\nu_1 h+2i\mu\alpha\left(C\nu_2\cosh\nu_2 h+E\nu_3\cos h\nu_3 h\right)=0\\ 2i\alpha\nu_1 B\sin h\nu_1 h+C\left\{\left(\nu_2^2+\alpha^2\right)-\ell^2\left(\nu_2^2+\alpha^2\right)^2\right\}\sin h\nu_2 h\\ +E\left\{\left(\nu_3^2+\alpha^2\right)-\ell^2\left(\nu_3^2+\alpha^2\right)^2\right\}\sin h\nu_3 h=0\\ C\nu_2\left(\nu_3^2-\alpha^2\right)\cos h\nu_2 h+E\nu_3\left(\nu_3^2-\alpha^2\right)\cos h\nu_3 h=0\end{aligned}\right\} \quad (74)$$

Since ℓ is small, the system of equations (74) takes the form

$$\left.\begin{aligned}\left[\alpha\left\{\left(c^2/c_2^2\right)-2\right\}\cos h\nu_1 h\right]B+2i\left(C\nu_2\cos h\nu_2 h+E\nu_3\cos h\nu_3 h\right)=0\\ 2iB\alpha\nu_1\sinh\nu_1 h+C\left(2\alpha^2-k_2^2\right)\sinh\nu_2 h+E\left(2\alpha^2-k_2^2\right)\sinh\nu_3 h=0\\ -C\nu_2 p^2\cosh\nu_2 h+E\nu_3 q^3\cosh\nu_3 h=0\end{aligned}\right\}(c=\omega/\alpha) \quad (75)$$

These equations lead to the transcendental equation

$$\frac{\tanh\nu_1 h}{\tanh\nu_2 h}=\left[\left\{2-\left(c^2/c_2^2\right)\right\}\left(2\alpha^2-k_2^2\right)\Big/4\nu_1\nu_2\left\{1+\left(p^2/q_2^2\right)\right\}\right]\left(1+\left(\nu_2 p^2/\nu_3 q^2\right)\frac{\tanh\nu_3 h}{\tanh\nu_2 h}\right) \quad (76)$$

It is readily observed that the wave velocity equation (76), as derived above for the propagation of waves in an elastic layer, contains the couple-stress parameter ℓ. Assuming the couple-stress parameter ℓ to small so that is cubes and higher powers are always neglected. To discuss the result of the wave velocity equation (76) in the following cases.

Case I: If the length of the wave is large compared with the thickness of the layer 2h, the quantities $\nu_1 h$, $\nu_2 h$ and αh can be regarded as small and the hyperbolic tangents can be replaced by their arguments. But $\nu_3 h$ is not small. So the equation (76) becomes

$$4\nu_1^2\left\{1+\left(p^2/q^2\right)\right\}=\left\{2-\left(c^2/c_2^2\right)\right\}\left(2\alpha^2-k_2^2\right)\left\{1+\left(p^2/q^2\right)\frac{\tanh\nu_3 h}{\tanh\nu_3 h}\right\} \quad (77)$$

Equation (77) determines the velocity c of the plane wave under the influece of couple-stress in an infinitely layer.

If the parameter ℓ of couple-stress vanishes, we get from equation (77)

$$4\left\{1-\left(c^2/c_1^2\right)\right\}-\left\{2-\left(c^2/c_2^2\right)\right\}=0$$

i.e. $c^2c_1^2=4c_2^2\left(c_1^2-c_2^2\right)$ which is in agreement with the classical result of Rayleigh[57] and Lamb[58].

Since the parameter ℓ of couple-stresses is small, we get the following approximate form of the equation (77)

$$4v_1^2\left(1+k_2^2\ell^2\right)=\left(2-c^2/c_2^2\right)\left(2\alpha^2-k_2^2\right)$$

which can be rewritten as

$$4\left(1-c^2/c_1^2\right)\left\{1+\left(c^2/c_2^2\right)\alpha^2\ell^2\right\}=\left(2-c^2/c_2^2\right)^2 \quad (78)$$

we assume $\lambda = \mu$;($\nu = 1/4$); then $c_1^2=3c_2^2$, and $c^2/c_2^2=\frac{8}{3}\left(1+\frac{1}{6}\alpha^2\ell^2\right)$

which shows that the symmetrical mode of vibration c/c_2 increases due to the presence of couple-stress. On the other hand the velocity c of the propogation of waves in the elastic layer increases due to the presence of couple-stress.

Case II :If, again, the length of the wave is very small compared with the thickness of the layer $2h$, the quantities v_1h, v_2h, v_3h and αh are large and we may assume that the ratio of hyperbolic tangents in equation (76) approaches unity and equation (76) becomes

$$4\left(1-c^2/c_1^2\right)^{1/2}\left(1-p^2/\alpha^2\right)^{1/2}=\left(1+p^2/q^2\right)\left(2-c^2/c_2^2\right)^2\left\{1+\left(v_2p^2/v_3q^2\right)\right\} \quad (79)$$

Equation (79) determines the velocity of the Rayleigh surface wave under the influence of couple-stress. If $\ell=0$, couple-stress vanish and we get the classical result

$$\left(2-c^2/c_2^2\right)^2=4\left\{1-\left(c^2/c_1^2\right)\right\}^{1/2}\left\{1-\left(c^2/c_2^2\right)^{1/2}\right\}$$

The couple-stress parameter ℓ being small we get the following approximate form of the equation (79),

$$\left(c^2/c_2^2\right)\left[\begin{array}{l}\left(c^6/c_2^6\right)-8\left(c^4/c_2^4\right)+c^2\left\{\left(24/c_2^2\right)-\left(16/c_1^2\right)\right\}-16\left\{1-\left(c_2^2/c_1^2\right)\right\}-16\left(c^2/c_2^2\right)\alpha^2\ell^2\times \\ \qquad\times\left\{1-\left(c^2/c_1^2\right)\right\}-32\alpha^2\ell^2\left\{1-\left(\frac{c^2}{c_1^2}+\frac{c^2}{c_2^2}\right)+\frac{c^4}{c_1^2c_2^2}\right\}\end{array}\right]=0 \tag{80}$$

We assume $\lambda = \mu$ (i.e. $\nu = 1/4$), then $c_1 = \sqrt{3}c_2$ and obtain from the above equation (80)

$$\left(\frac{c^6}{c_2^6}-9\frac{c^4}{c_2^4}+\frac{56}{3}\frac{c^2}{c_2^2}-\frac{32}{3}\right)-\frac{16}{3}\alpha^2\ell^2\left(3-\frac{c^2}{c_2^2}\right)\left(2-\frac{c^2}{c_2^2}\right)=0 \tag{81}$$

The above cubic equation in c^2/c_2^2 has three real and positive roots. One of the roots lies between 0.8453 and 2. In order to satisfy the condition of Rayleigh waves the value of $\alpha^2\ell^2$ must be less than 0.09 and the acceptable root for the real existence for Rayleigh wave been computed numerically. It is thus observed that the velocity of Rayleigh waves increases due to the influence of couple-stress.

Numerical result :

In the following table the values of c/c_2 have been computed for different values of $\alpha^2\ell^2$ in equation (81) and thus it has been exhibited that the velocity of Rayleigh waves in presence of couple-stresses increases and the velocity of Rayleigh waves under the influence of couple-stress, approaches to the classical value 0.9194019 c_2 with the diminution of the value of the parameter of couple-stress.

Table 2– Computation of c/c_2 for different values of couple-stress parameter.

$\alpha^2\ell^2$	10^{-2}	10^{-3}	10^{-4}	10^{-5}	10^{-6}
c/c_2	0.92915	0.92288	0.92199	0.919411	0.9194025

Let us consider another set of interesting solutions given by

$$\phi_2 = A\sinh\nu_1 x_3 e^{i(\omega t-\varepsilon x_1)};\qquad \psi_2 = \left(D\cosh\nu_2 x_3 + D\cosh\nu_3 x_3\right)e^{i(\omega t-\varepsilon x_1)} \tag{82}$$

Introducing (82) into (61), it is readily observed that the displacement u_1, u_3, the stresses σ_{11}, σ_{33} and couple-stress μ_{32} are antisymmetric with respect to the plane $x_3 = 0$, while the stresses σ_{13}, σ_{31} and the couple-stress μ_{12} are symmetric with respect to this plane.

Introducing (82) into the boundary condition (64) and making use of equation (66), we obtain the following three linear equations for A, D and F.

$$\left.\begin{aligned}(\rho\omega^2-2\mu\alpha^2)A\sinh\nu_1h+2i\mu\alpha(D\nu_2\sinh\nu_2h+F\nu_3\sinh\nu_3h)=0\\ 2i\alpha\nu_1A\cosh\nu_1h+D\left\{(\nu_2^2+\alpha^2)-\ell^2(\nu_2^2-\alpha^2)^2\right\}\cosh\nu_2h\\ +F\left\{(\nu_3^2+\alpha^2)-\ell^2(\nu_3^2-\alpha^2)^2\right\}\cosh\nu_3h=0\\ D(\nu_2^2-\alpha^2)\nu_2\sinh\nu_2h+F(\nu_3^2-\alpha^2)\nu_3\sinh\nu_3h=0\end{aligned}\right\}. \tag{83}$$

Since ℓ is small, elimination of A, D and F from the equation (83) leads to the equation

$$\frac{\tanh\nu_1h}{\tanh\nu_2h}=4\nu_1\nu_2\{1+(p^2/q^2)\}/(2\alpha^2-k_2^2)\{2-(c^2/c_2^2)\}\left(1+\frac{p^2\nu_2}{q^2\nu_3}\frac{\tanh\nu_2h}{\tanh\nu_3h}\right) \tag{84}$$

Case I. If the length of the wave is very small compared with the thickness of the layer, equation *84) reduces to (79) and yields the velocity of propagation of Rayleigh surface waves under the influence of couple-stress. If the parameter of couple-stress is zero, the classical result follows.

Case II : If the length of the wave be large compared with the thickness of the layer, quantities ν_1h, ν_2h and αh can be regarded as small and hyperbolic tangents $\tanh\nu_1h$, $\tanh\nu_2h$ can be replaced by the first two terms of their expansions into series. Then equation (84) becomes

$$\frac{\nu_1\{1-(\nu_1^2h^2/3)\}}{\nu_2\{1-(\nu_2^2h^2/3)\}}=\frac{4\nu_1\nu_2\{1+(p^2/q^2)\}}{(2\alpha^2-k_2^2)\{2-(c^2/c_2^2)\}\left\{1+\dfrac{p^2\nu_2^2\{1-(\nu_2^2h^2/3)\}h}{q^2\nu_3\tanh\nu_3h}\right\}} \tag{85}$$

If $\ell=0$ we get, on simplification,

$$(c^2/c_2^2)=\frac{4}{3}\alpha^2h^2\{1-(c_2^2/c_1^2)\},\ c=(\omega/\alpha)$$

which is the classical result of Rayleigh[57] and Lamb[58] since ℓ is small, we obtain the following approximation of equation (85)

$$\left(c^2/c_2^2\right)=\left(4\alpha^2h^2/3\right)\left\{1-\left(c_2^2/c_1^2\right)\right\}+4\alpha^2\ell^2 \tag{86}$$

which shows that the value of c/c_2 increase in presence of couple-stress. In other words the velocity c of the propagation of waves in the elastic layer increases due to the presence couple stress.

Axis symmetric Lamb's problem in couple stress theory :

We consider a time varying loading $z(r,t) = p(r)\exp(i\omega t)$ acting on the elastic semi-space bounded by the $z = 0$ plane z axis being pointed into the medium. The loading being axially symmetrical, it produces in the semi-space state of stress and deformation and the cylindrical co-ordinates (r,ϕ,z) is used to investigate the problem.

We consider the displacement equation of motion in absence of body forces and body couple as

$$\mu\nabla^2\overline{u}+\left(\lambda+\mu\right)\overline{\nabla}\overline{\nabla}\overline{u}+\eta\nabla^2\overline{\nabla}\times\overline{\nabla}\times\overline{u}=\rho\ddot{u} \tag{87}$$

we express the displacement $\overline{u}$ into its lameller and solenoidal components

$$u=\overline{\nabla}\phi+\overline{\nabla}\times\overline{H} \qquad \overline{\nabla}.\overline{H}=0 \tag{88}$$

Then the above equation of motion reduces to the following equation

$$c_1^2\nabla^2\phi=\ddot{\phi}\,; \qquad c_2^2\left(1-\ell^2\nabla^2\right)\nabla^2\overline{H}=\ddot{H} \tag{89}$$

where $\ell^2=n/\mu$, $c_1^2=\left(\lambda+2\mu\right)/\rho$, $c_2^2=\mu/\rho$

For harmonic waves we insert $\phi=\overline{\phi}\exp(i\omega t)$ and $H=\overline{H}\exp(i\omega t)$in (89) to obtain

$$\left(\nabla^2+\sigma_1^2\right)\overline{\phi}=0 \quad ; \quad \left(\nabla^2+\beta_1^2\right)\left(\nabla^2-\beta_2^2\right)\overline{H}=0 \tag{90}$$

where $\sigma_1=\omega/c_1$; $\beta_1=2^{-1/2}\ell^{-1}\left[\left(1+4\ell^2\sigma_2^2\right)^{1/2}-1\right]^{1/2}$

$$\sigma_2 = \omega/c_2 \qquad ; \quad \beta_{21} = 2^{-1/2}\ell^{-1}\left[\left(1+4\ell^2\sigma_2^2\right)^{1/2}+1\right]^{1/2}$$

Then, considering $\overline{H} = \overline{H}' + \overline{H}''$ the complete solution becomes

$$\overline{u} = \overline{\nabla}\overline{\phi} + \overline{\nabla}\times\underline{\overline{H}}' + \overline{\nabla}\times\underline{\overline{H}}'' \tag{91}$$

where $\overline{\phi}$, $\underline{\overline{H}}'$ and $\underline{\overline{H}}''$ are governed by the Helmholtz equations

$$\left(\nabla^2+\sigma_1^2\right)\overline{\phi} = 0 \qquad ; \quad \left(\nabla^2+\beta_1^2\right)\overline{H}' = 0 \quad ; \quad \left(\nabla^2-\beta_2^2\right)\overline{H}'' = 0 \tag{92}$$

Boundary conditions : The boundary conditions on $z = 0$

$$\tau_{zz} = -p(r)e^{i\omega t} \qquad ; \qquad p_r = p_\phi = \mu_{z\phi} = \mu_{zr} = 0 \tag{93}$$

where[10]

$$p_r = \tau_{zr}^s - \frac{1}{2}\left(\frac{\partial}{\partial r}\mu_{r\phi} + \frac{1}{r}\frac{\partial}{\partial\phi}\mu_{\phi\phi}^D + \frac{\partial}{\partial z}\mu_{z\phi} + \frac{\mu_{r\phi}+\mu_{\phi r}}{r} - \frac{1}{r}\frac{\partial}{\partial\phi}\mu_{\phi\phi}^D\right)$$

$$p_\phi = \tau_{z\phi}^s + \frac{1}{2}\left(\frac{\partial}{\partial r}\mu_{rr}^D + \frac{1}{r}\frac{\partial}{\partial\phi}\mu_{\phi r} + \frac{\partial}{\partial z}\mu_{zr} + \frac{\mu_{rr}^D-\mu_{\phi\phi}^D}{r} - \frac{\partial}{\partial r}\mu_{zz}^D\right)$$

we consider the particular case in which the external loading and the displacement vector $\overline{u}$ are independent of ϕ, the body forces and body couples being discarded. In this case $w_r = w_z = 0, p_r = \mu_{zr} = 0$.

Hence, the boundary conditions reduce to

$$\left.\begin{aligned} &\tau_{zz}^s - \frac{1}{2}\left(\frac{\partial}{\partial r}\mu_{r\phi} + \frac{\partial}{\partial z}\mu_{z\phi} + \frac{\mu_{r\phi}+\mu_{\phi r}}{r}\right) = 0 \\ &\tau_{zz} = -p(r)e^{i\omega t} \;;\; \mu_{z\phi} = 0 \end{aligned}\right\} \tag{94}$$

With the boundary conditions (94), we seek solutions of (92). In this particular case $\overline{H}_r = \overline{H}_z = 0$. Hence the equations (92) take the following forms

$$\left(\nabla^2+\sigma_1^2\right)\overline{\phi}=0,\ \left(\nabla^2-\frac{1}{r^2}+\beta_1^2\right)\overline{H}_\phi'=0\ \ ;\ \ \left(\nabla^2-\frac{1}{r^2}+\beta_2^2\right)\overline{H}_\phi''=0 \tag{95}$$

Applying in equations of 95), the Hankel transformation defined by

$$\phi^*(\alpha,z)=\int_0^\infty r\overline{\phi}(r,z)J_0(\alpha r)dr\ \ ;\ \psi^*(\alpha,z)=\int_0^\infty r\overline{\psi}(r,t)J_0(\alpha r)dr \tag{96}$$

$$\overline{H}_\phi'=-\frac{\partial}{\partial r}\overline{\psi}_1\qquad,\overline{H}_\phi''=-\frac{\partial}{\partial r}\overline{\psi}_2$$

we obtain $\phi^*=Ae^{-\alpha z},\quad \psi_1^*=Be^{-\nu_1 z},\quad \psi_2^*=Ce^{-\nu_2 z}$ (97)

where $\sigma=\left(\alpha^2-\sigma_1^2\right)^{1/2},\quad \nu_1=\left(\alpha^2-\beta_1^2\right)^{1/2},\quad \nu_2=\left(\alpha^2+\beta_2^2\right)^{1/2}$

Hence in view of (88), (91) and (97) we obtain

$$u_r=\exp(i\omega t)\int_0^\infty\left\{-\alpha Ae^{-\alpha z}+\alpha\left(\nu_1Be^{-\nu_1 z}+\nu_2ce^{-\nu_2 z}\right)\right\}\alpha J_1(\alpha r)d\alpha \tag{98}$$

$$u_z=\exp(i\omega t)\int_0^\infty\left\{-\alpha Ae^{-\alpha z}+\alpha\left(\nu_1Be^{-\nu_1 z}+ce^{-\nu_2 z}\right)\right\}\alpha J_0(\alpha r)d\alpha \tag{99}$$

Substituting (98) and (99) in the boundary conditions (94) we obtain

$$\left.\begin{aligned}2\sigma A-\left\{\left(\nu_1^2+\alpha^2\right)-\ell^2\left(\nu_1^2-\alpha^2\right)^2\right\}\alpha B-\left\{\left(\nu_1^2+\alpha^2\right)-\ell^2\left(\nu_2^2-\alpha^2\right)^2\right\}\alpha C=0\\ \left(2\alpha^2-\sigma_2^2\right)A-2\alpha^2\left(\nu_1B+\nu_2C\right)=-p^*(\alpha)/\mu\\ \alpha\nu_1\left(\alpha^2-\nu_1^2\right)B-2\nu_2\left(\alpha^2-\nu_2^2\right)C=0\end{aligned}\right\}$$

where we have expressed the loading $p(r)$by the Hankel interal

$$P(r)=\int_0^\infty P^*(\alpha)\alpha J_0(\alpha r)d\alpha\ ;\qquad P^*(\alpha)=\int_0^\infty rP(r)J_0(\alpha r)dr \tag{101}$$

Solving the system of equation (100) we obtain

$$A(\alpha)=-\frac{KP^*}{R(\alpha)\mu} \qquad B(\alpha)=-\frac{2\sigma}{R(\alpha)}\frac{P^*}{\mu,}, \qquad c(\alpha)=\frac{\nu_1}{\nu_2}\frac{\beta_1^2}{\beta_2^2} \tag{102}$$

where

$$R(\alpha)=K\left(2\alpha^2-\sigma_2^2\right)-4\alpha^2\nu_1\sigma\left(1+\frac{\beta_1^2}{\beta_2^2}\right),\ K=\left(2\alpha^2-\sigma_2^2\right)\left(1+\frac{\nu_1}{\nu_1}\frac{\beta_1^2}{\beta_2^2}\right)$$

Hence for a concentrated force $z(r,t)$

$$\left.\begin{aligned} u_r &= \frac{P_0 e^{i\omega t}}{2\pi\mu}\int_0^\infty\left\{K\alpha e^{-\alpha z}-2\sigma\nu_1\alpha\left(e^{-\nu_1 z}+\frac{\beta_1^2}{\beta_2^2}e^{-\nu_2 z}\right)\right\}\frac{\alpha J_1(\alpha r)}{R(\alpha)}d\alpha \\ u_z &= \frac{P_0 e^{i\omega t}}{2\pi\mu}\int_0^\infty\left\{K\alpha e^{-\alpha z}-2\sigma\alpha^2\left(e^{-\nu_1 z}+\frac{\nu_1}{\nu_2}\frac{\beta_1^2}{\beta_2^2}e^{-\nu_2 z}\right)\right\}\frac{\alpha J_0(\alpha r)}{R(\alpha)}d\alpha \end{aligned}\right\} \tag{103}$$

$$z(r,t)=\left\{P_0\delta(r)/2\pi r\right\}e^{i\omega t} \qquad P^*(\alpha)=P_0/2\pi$$

Thus the displacement given by (103) under the influence of couple stress being know we can determine the stresses and the couple stresses from equation (1). If ℓ tends to zero the classical results follow[18].

Effect of couple-stress on steady-state response to moving loads :

We consider a homogeneous, isotropic elastic semi-space selecting the origin on the free plane boundary and x_2-axis pointing into the medium, the Cartesian co-ordinates of a point of the semi-space $x_2 \geq 0$ are supposed to be (x_1, x_2, x_3) the corresponding displacement components are designated by (u_1, u_2, u_3). As regards the line load we suppose that on plane boundary of the semi-space there acts the loading $p\delta(x_1+ut)$ where P is a constant and $\delta(t)$ is the Dirac-delta function.

We assume that a plane strain state prevails and the elastic displacements u_1, u_2, $(u_3 = 0)$ are derivable from the displacement potentials $\phi(x_1, x_2)$ and $\psi(x_1, x_2)$ so that

$$u_1 = \phi_{,1} - \psi_{,2}, \qquad u_2 = \phi_{,2} + \psi_{,1} \tag{104}$$

Displacement equations of motion in absence of body forces and body couples are

$$\mu\nabla^2\mu_i + (\lambda+\mu)\mu_{j,ji} + \eta\nabla^2(\mu_{j,ji} - \nabla^2\mu_i) = \rho\ddot{u}_i \quad (i,j = 1,2,3) \tag{105}$$

$$\nabla^2\phi - c_1^{-2}\ddot{\phi} = 0 \quad ; \quad \nabla^2\psi - \ell^2\nabla^4\psi = c_2^{-2}\ddot{\psi} \tag{106}$$

where $c_1^2 = (\lambda+2\mu)/\rho$, $c_2^2 = \mu/\rho$ $\ell^2 = \eta/\mu$

η is a constant characterzing the existence of couple-stresses and λ, μ are Lame's elastic constants. If $\ell = 0$ the couple-stress vanishes and the classical result follows at once.

Expressions for stresses and couple-stress in terms of ϕ and ψ are

$$\tau_{11} = 2\mu(\phi_{,11} - \psi_{,12}) + \lambda\nabla^2\phi \quad ; \quad \tau_{22} = 2\mu(\phi_{,22} + \psi_{,12}) + \lambda\nabla^2\phi,$$

$$\tau_{12} = \mu(2\phi_{,12} + \psi_{,11} - \psi_{,22}) - \eta\nabla^4\psi \quad ; \quad \tau_{21} = \mu(2\phi_{,12} + \psi_{,11} - \psi_{,22}) + \eta\nabla^4\psi \tag{107}$$

$$\tau_{13} = 2\eta\nabla^2(\psi_{,1}), \ \mu_{23} = 2\eta\nabla^2(\psi_{,2})$$

Now, in the problem stated above, the load moves in the negative direction of x_1-axis at a constant speed u. An observer moving with the load at the same speed would see the load as stationary. We introduce a Galilean transformation[59].

$$x_1' = x_1 + ut, \qquad x_2' = x_2 \qquad t' = t \tag{108}$$

then the boundary conditions would be independent of t'. For a concentrated line load the boundary conditions are in the moving co-ordinates, are

$$\tau_{22} = -p\delta(x_1'), \qquad \tau_{21} = \mu_{23} = 0. \tag{109}$$

Now, as the response in the elastic semi-space is in a steady state, ϕ and ψ will be independent of t' as seen by an observer moving with the load. In other words, x_1, and t enter ϕ and ψ in combination $x_1 + ut$. Under this assumption, equations (106) become

$$\left.\begin{aligned} \nabla'^2\phi &= c_1^{-2}u^2\frac{\partial^2\phi}{\partial x_1'^2} \\ \nabla'^2 - \ell^2\nabla'^4\psi &= c_2^{-2}u^2\frac{\partial^2\psi}{\partial x_1'^2} \end{aligned}\right\} \qquad \left[\nabla'^2\frac{\partial^2}{\partial x_1'^2}+\frac{\partial^2}{\partial x_2'^2}\right] \tag{110}$$

On introducing the Mach numbers[59]

$$M_1 = u/c_1; \qquad M_2 = u/c_2 \tag{111}$$

and the parameters,

$$\overline{\beta}_1 = \sqrt{1-M_1^2} \quad ; \quad \overline{\beta}_2 = \sqrt{1-M_2^2} \qquad \text{if } M_1<1,\ M_2<1. \tag{112}$$

$$\beta_1 = \sqrt{M_1^2-1} \quad ; \quad \beta_2 = \sqrt{M_2^2-1} \qquad \text{if } M_1>1,\ M_2>1. \tag{113}$$

we obtain the following partial differential equations

$$\left.\begin{aligned} \overline{\beta}_1^2\frac{\partial^2\phi}{\partial x_1'^2}+\frac{\partial^2\phi}{\partial x_1'^2} &\qquad \textbf{if } M_1<1 \\ \overline{\beta}_2^2\frac{\partial^2\psi}{\partial x_1'^2}+\frac{\partial^2\psi}{\partial x_2'^2}-\ell^2\nabla'^4\psi=0 &\qquad \textbf{if } M_2<1 \end{aligned}\right\} \tag{114}$$

and

$$\left.\begin{aligned} \beta_1^2\frac{\partial^2\phi}{\partial x_1'^2}-\frac{\partial^2\phi}{\partial x_1'^2}=0 &\qquad \text{if } M_1>1 \\ \beta_2^2\frac{\partial^2\psi}{\partial x_1'^2}+\frac{\partial^2\psi}{\partial x_2'^2}-\ell^2\nabla'^4\psi=0 &\qquad \text{if } M_2<1 \end{aligned}\right\} \tag{115}$$

In view of (110) and (111), the stresses and couple-stresses given by (107) reduce into

$$\left.\begin{aligned} &\frac{\tau_{11}}{\mu}=\left(M_2^2-2M_1^2+2\right)\frac{\partial^2\phi}{\partial x_1'^2}-2\frac{\partial^2\psi}{\partial x_1'^2\partial x_2'}; \quad \frac{\tau_{22}}{\mu}=\left(M_2^2-2\right)\frac{\partial^2\phi}{\partial x_1'^2}-2\frac{\partial^2\psi}{\partial x_1'\partial x_2'} \\ &\frac{\tau_{12}}{\mu}=M_2^2\frac{\partial^2\psi}{\partial x_1'^2}-2\frac{\partial^2\psi}{\partial x_2'^2}+2\frac{\partial^2\phi}{\partial x_1'\partial x_2'}; \quad \frac{\tau_{21}}{\mu}=2\frac{\partial^2\phi}{\partial x_1'\partial x_2'}-\left(M_2^2-2\right)\frac{\partial^2\phi}{\partial x_1'^2} \\ &\mu_{13}=2\eta\nabla'^2\left(\frac{\partial\psi}{\partial x_1'}\right) \quad ; \quad \mu_{23}=2\eta\nabla'^2\left(\frac{\partial\psi}{\partial x_2'}\right) \end{aligned}\right\} \tag{116}$$

The boundary conditions (109) become, at $x_2' = 0$

$$\left.\begin{aligned} &(M_2^2-2)\frac{\partial^2\phi}{\partial x_1'^2}+2\frac{\partial^2\psi}{\partial x_1'^2\partial x_2'}=-\frac{p}{\mu}\delta(x_1') \\ &2\frac{\partial^2\phi}{\partial x_1'^2\partial x_2'}-(M_2^2-2)\frac{\partial^2\psi}{\partial x_1'^2}=0 \quad ;\nabla^{14}\left(\frac{\partial\psi}{\partial x_2'}\right)=0 \end{aligned}\right\} \tag{117}$$

Now, we have to determine the functions ϕ and ψ which satisfy the differential equations (114) or (115), the boundary conditions on the free surface (117) and the appropriate (114) or (115), the boundary conditions on the free surface (117) and the appropriate radiation and finiteness conditions at infinity.

The nature of the solution depends on the Mach numbers M_1, M_2. Three cases can be distinguished :

(a) $M_2 > M_1 > 1$, (Supersonic)

(b) $M_2 > M_1 > 1$, (Transonic)

(c) $1 > M_2 > M_1$, (Subsonic)

Since $C_2 > C_1$, so that $M_2 > M_1$, the three above exhaust all possibilities.

Supersonic Case [$M_2 > 1, M_2 > 1$] :

In this case, we must solve the equations (115), we take the solutions as

$$\phi(x_1', x_2') = A_1(x_2')\, e^{i\lambda x_1'} \quad ; \quad \psi(x_1', x_2') = A_2(x_2')\, e^{i\lambda x_1'} \tag{118}$$

$$A_1(x_2') = A\, e^{-\eta_1 x_2'} \tag{119}$$

$$A_2(x_2') = B\, e^{-\eta_2 x_2'} \tag{120}$$

where

$$\left.\begin{aligned} &\eta_1 = \beta_1\lambda, \quad \eta_2 = \sqrt{\lambda^2 - p^2}, \quad \eta_3 = \sqrt{\lambda^2 - q^2} \\ &p^2 = \frac{1}{2\ell^2}\left[\left\{1+\left(1+\beta_2^2\right)4\ell^2\lambda^2\right\}^{\frac{1}{2}} - 1\right] \\ &q^2 = \frac{1}{2\ell^2}\left[\left\{1+4\left(1+\beta_2^2\right)\ell^2\lambda^2\right\}^{\frac{1}{2}} + 1\right] \end{aligned}\right\} \tag{121}$$

where λ, A, B and C are arbitrary constants. Hence, the solution are

$$\phi = Ae^{i\lambda x_1' - i\eta x_2'} \quad ; \quad \psi = \left(Be^{-\eta_2 x_2'} + Ce^{-\eta_3 x_2'}\right) = e^{1\lambda x_2'} A_2\left(x_2'\right) \tag{122}$$

which satisfy the radiation condition at infinity only backward running waves are admitted. The other possible solutions, of the form $e^{i(\lambda x_1' + \eta_1 x_2')}$ are rejected on the basis of the radiation condition because they represent disturbance which originate at infinity and coverage towards the load. We assume a general in the form

$$\begin{aligned} \phi\left(x_1', x_2'\right) &= \frac{1}{2\pi}\int_{-\infty}^{\infty} A(\lambda)\, e^{-i\eta_1 x_2' + i\lambda x_1'} d\lambda \\ \psi\left(x_1', x_2'\right) &= \frac{1}{2\pi}\int_{-\infty}^{\infty} \left\{B(\lambda)\, e^{-i\eta_2 x_2'} + C(\lambda)\, e^{-i\eta_3 x_2'}\right\} e^{i\lambda x_1'} d\lambda \end{aligned} \tag{123}$$

The boundary conditions (117) give

$$\begin{aligned} &(i\lambda)^2\left(M_2^2 - 2\right)A(\lambda) - 2i\lambda\left\{\eta_2 B(\lambda) + \eta_3 C(\lambda)\right\} = P(\lambda) \\ &2\eta_1 A(\lambda) + \left(M_2^2 - 2\right)\left\{B(\lambda) + C(\lambda)\right\}\lambda = 0 \\ &C(\lambda) = \frac{-\eta_2\left(\eta_2^2 - \lambda^2\right)}{\eta_3\left(\eta_3^2 - \lambda^2\right)} B(\lambda) \end{aligned} \tag{124}$$

where $P(\lambda)\ (= -P/\mu)$ is the Fourier transform of $-(P/\mu)\delta(x_1'')$.

Hence, from (124) we get on simplification

$$A(\lambda) = \left(M_2^2 - 2\right)\left(1 + \frac{\eta_2}{\eta_3}\frac{p^2}{q^2}\right)\lambda P^*(\lambda)/\Delta^* \quad ; \quad B(\lambda) = -2\eta_1 P^*(\lambda)/\Delta^* \tag{125}$$

where $$\Delta^* = \left(M_2^2 - 2\right)^2\left(1 + \frac{\eta_2}{\eta_3}\frac{p^2}{q^2}\right) i\eta^2 + \eta_1\left(1 + \frac{p^2}{q^2}\right) \tag{126}$$

In view of (125) and (126) becomes

$$\phi(x_1', x_2') = \frac{M_2^2 - 2}{2\pi} \int_{-\infty}^{\infty} \left\{ \left(1 + \frac{\eta_2 p^2}{\eta_3 q^2} \right) \frac{\lambda P^*(\lambda)}{\Delta^*} e^{i(\lambda x_1' + \eta_1 x_2')} \right\} d\lambda$$

$$\psi(x_1', x_2') = -\frac{1}{2\pi} \int_{-\infty}^{\infty} \frac{2\eta_1 P^*(\lambda)}{\Delta^*} \left\{ e^{i\lambda x_1' - \eta x_2'} - \frac{\eta_2 p^2}{\eta_3 q^2} \times e^{i\lambda x_1' - \eta_2 x_2'} \right\} d\lambda. \tag{127}$$

Since the parameter of the couple-stress 'ℓ' is small, we may neglect its cubes and higher powers. Then the approximate forms of ϕ and ψ are follows.

$$\phi(x_1', x_2') = \frac{M_2^2 - 2}{4\pi\Delta} \left\{ \int_{-\alpha}^{\alpha} \frac{P^*(\lambda)}{i\lambda} e^{i\lambda(x_1' - \beta_1 x_2')} d\lambda + \Delta_1 \ell^2 \int_{-\infty}^{\infty} \frac{\lambda^2 P^*(\lambda)}{i\lambda} e^{i\lambda(x_1' - \beta_1 x_2')} d\lambda \right\} \tag{128}$$

$$\psi(x_1', x_2') = \frac{2\beta_1}{2\pi\Delta} \left[\int_{-\infty}^{\infty} \frac{e^{i\lambda(x_1' - \beta_2 x_2')}}{i\lambda^2} + 2\ell^2 \lambda^2 \Delta_1 \frac{e^{i\lambda(x_1' - \beta_2 x_2')}}{i\lambda^2} + \frac{(1+\beta_2^2)}{2\beta_2} \ell^2 x_2' \lambda e^{i\lambda(x_1' - \beta_2 x_2')} \right] \lambda P^*(\lambda) d\lambda \tag{129}$$

where $\Delta = (M_2^2 - 2) + 4\beta_1\beta_2$; $\Delta_1 = \frac{2\beta_1(1+\beta_2^2)}{\beta_2\Delta}(1-\beta_2^2)$ (130)

$$u_1 = \frac{P}{\mu\Delta} \{(2 - M_2^2) H(x_1' - \beta_1 x_2') + 2\beta_1\beta_2 H(x_1' - \beta_1 x_2')\} + \frac{P}{\mu\Delta} \ell^2$$

$$\left[\Delta_1 (2 - M_2^2) F_1(x_1' - \beta_1 x_2') - \left\{ 2\beta_1\beta_2\Delta_1 - \frac{2\beta_1}{2\beta_2}(1+\beta_2^2) \right\} F_2(x_1' - \beta_1 x_2') - \right.$$

$$\left. \beta_1 (1+\beta_2^2)^2 x_2' \frac{\partial}{\partial x_1'} F_2(x_1' - \beta_2 x_2') \right] \tag{131}$$

$$u_2 = -\frac{P}{\mu\Delta} \{\beta_1 (2 - M_2^2) H(x_1' - \beta x_2') - 2\beta_1 H(x_1' - \beta x_2')\} - \frac{P\beta_1}{\mu\Delta} \ell^2$$

$$\left[(2 - M_2^2) \Delta_1 F_1(x_1' - \beta_1 x_2') + 4\Delta_1 F_2(x_1' - \beta_2 x_2') + \right.$$

$$\left. \frac{(1+\beta_2^2)^2}{\beta_2} x_2' \frac{\partial}{\partial x_1'} F_2(x_1' - \beta_2 x_2') \right]$$

$$\tau_{22} = \frac{P}{\Delta}\left[(2-M_2^2)\{2+(\lambda/\mu)M_1^2\}\delta(x_2') + \frac{4\beta_1\beta_2}{\Delta}\delta(x_1'-\beta x_2')i\right] +$$

$$+\frac{P}{\Delta}\ell^2\left[\Delta_1\frac{\partial}{\partial x_2'}F_1(x_1-\beta x_2')\left(2+\frac{\lambda}{\mu}M_1^2\right)(2-M_2^2) - 4\beta_1\beta_2\left\{2\Delta_1\frac{\partial}{\partial x_1'}F_2(x_1'-\beta_2 x_2') +\right.\right.$$

$$\left.\left.+\frac{(1+\beta_2^3)^2}{2\beta_2}x_2'\frac{\partial^2}{\partial x_1'^2}F(x_1'-\beta_2 x_2')\right\} + \frac{4\beta_1(1+\beta_2^2)}{2\beta_2}\frac{\partial}{\partial x_1'}F_2(x_1'-\beta_2 x_2')\right]$$

$$\tau_{11} = \frac{P}{\Delta}\left[(2-M_2^2)\left(2\beta_1^2+\frac{\lambda}{\mu}M_1^2\right)\delta(x_1'-\beta_1 x_2') - 4\beta_1\beta_2\delta(x_1'-\beta_2 x_2')\right]$$

$$+\frac{P}{\mu}\frac{\ell^2}{\Delta}\left[\Delta_1(2-M_2^2)\frac{\partial}{\partial x_1'}F(x_1'-\beta')(2\beta_1^2)\left(2\beta_1^2+\frac{\lambda}{\mu}M_2^2\right)\beta_2^2 +\right.$$

$$+4\beta_1\beta_2\left\{2\Delta_1\frac{\partial}{\partial x_1'}F_2(x_1'-\beta_2 x_2')\right\} + \frac{(1+\beta_2^2)^2}{2\beta_2}x_2'\frac{\partial^2}{\partial x_2'^2}F_2(x_1'-\beta_2 x_2') -$$

$$\left.-\frac{4\beta_1(1+\beta_2^2)^2}{2\beta_2}\frac{\partial}{\partial x_1'}F_2(x_1'-\beta_2 x_2')\right]$$

$$\tau_{12} = -\frac{2P}{\Delta}\beta_1(2-M_2^2)[\delta(x_1'-\beta_2 x_2') - \delta(x_1'-\beta_2')] - \frac{2P}{\mu}.\frac{\ell^2}{\Delta}[\beta_1(2-M_2^2)\Delta_1 F_1(x_1'-\beta_1 x_2') +$$

$$+\beta_1\left\{2\Delta_1\frac{\partial}{\partial x_1}F_2(x_1'-\beta_2 x_2') + \frac{(1+\beta_2^2)}{2\beta_2}x_2'\frac{\partial^2}{\partial x_2'^2}F_2(x_1'-\beta_2 x_2')\right\}(2-M_2^2)]$$

where[60]

$$F_1 = \delta^{(1)}(x_1'-\beta_1 x_2') = -(x_1'-\beta x_2')^{-1}\delta(x_2'-\beta_1 x_2')$$

$$\frac{\partial}{\partial x_1'} F_1 = \delta^{(2)}(x_1' - \beta_1 x_2') = 2(x_1' - \beta_1 x_2')^{-2} \delta(x_1' - \beta_1 x_2')$$

$$\frac{\partial}{\partial x_1^2} F_1 = \delta^{(3)}(x_1' - \beta_1 x_2') = -(x_1' - \beta_1 x_2)_{31}^{-3} \delta(x_1' - \beta_1 x_2'), (i = 1,2)$$

In case of the above relations (128–132), there is a term containing the parameter of couple-stress 'ℓ' with the classical part. hence the displacements and stresses are slightly changed due to the effect of couple stresses.

The difference of shear stresses

$$\tau_{12} - \tau_{21} = -2\eta \nabla'^4 \psi = -4 \frac{P}{\Delta} \beta_1 (1 + \beta_2^2)^2 \ell^2 \frac{\partial}{\partial x_1'} F_2(x_2' - \beta_2 x_2')$$

Is significant along the line $x_1=\beta_2 x_2$ due to influence of couple stress. In the similar way subsonic and transonic cases may be studied.

Discussion

The Rayleigh and Love type of surface waves are increased under the action of couple stress. As the couple stress parameters 1 is small, the change in the wave velocity C is also small. The waves in the layer are also affected by couple stress as studied in this review paper. The stress distribution due to the presence of moving load in the solid elastic semispace may be considered worthy for numerical calculations as the improper integrals have been evaluated and they are written in terms of different functions.

But it is to be mentioned that, this asymmetric theory does not have yet the complete or through experimental verification. We know merely the order of magnitudes and mutual relation between the material constants in studying most of the dynamic problem. However the complete correspondence of the experiment and theory exists in the case of discrete media (spatial grillages) where all the material constants may be uniquely determined. When passing from such a grillage to a continuous medium we obtain exactly Cosserat's continuum. The couple-stress theory of elasticity, which is now even considered as an Utopian theory by some sections of

research workers, will enhance the speed of development in science and technology in the future. We must remember that the phenomenon 'Utopian to reality' occurs as a repeated feature in the history of science.

References

1. Nowacki, W. (1970) *Theory of micropolar elasticity,* courses and lecture no. 25, International center for mechanical sciences, udine, Springer-Verlag.
2. Voigt, W. (1987) *Abh. Gesch Wiss* **34.**
3. Cosserat, E. & Cosserat, F. (1909) *Theorie des Corps deformables* A Herman Fils, paris.
4. Truesdell, C. & Toupin, R. A. (1960) The classical field theories, *Encyclopaedia of physics,* Vol. 3/1, Heidelberg, Springer, Berlin-Gottingen.
5. Toupin, R. A. (1962) *Arch. Rat. Mech. Anal.* **11** : 385.
6. Aero, A. L. & Kuvashinki, E. V. (1960) *Fizika Tvordogo Tela* **2** : 1399.
7. Aero, A. L. & Kuvashinki, E. V. (1961) *Trans. Soviet Physics Solid State* **2** : 1272.
8. Grioli, G. (1960) *Ann. Mat Pura et appl. Ser* **50(4)** : 389.
9. Mindlin, R. D. (1963) *Expl. Mech.* **3** : 1.
10. Mindlin, R. D. & Tiersten, H. F. (1962) *Arch. Rat. Mech. Anal.* **11** : 415.
11. Cohen, H. (1966) *J. Match. Phys.* **45(1)** : 35.
12. Love, A. E. H. (1953) *A treatise on the mathematical theory of elasticity,* 4th Ed., Cambridge University Press.
13. Love, A.E.H. (1911) *Some problems of Geodynamics, Dover Publications,* New York.
14. Ewing, W. M., jardetsky, W. S. & press, F. (1957) *Elastic wavesin layered media,* McGraw-Hill, Newyork.
15. Bullen, K. E. (1963) *An introduction to the theory of seismology,* 3rd Ed., Camb. Univ. press.
16. Jefferys, H. (1959) *The Earth,* Fourth Edition, Cambridge University Press.
17. Eringen, A. C. & Suhubi, E. S. (1974) *Elastodynamics* (I, II) Academic Press, Newyork.
18. Nowacki, W. (1963) *Dynamics of elastic system,* Chapman and Hall, London.
19. Rayleigh, Lord. (1885) *Proc. Land. Math. Soc.* **17** : 4.
20. Stonely, R. (1924) *Proc. Roy. Soc. A,* **106** : 416.
21. Jeffreys, H. (1925) *Mon. Not. R. Astr. Soc. Geophys Suppl.* **1** :282.
22. Buchwald, V. T. (1961) *Quart. Jour. Mech. Appl. Math.*, **14** : 293.
23. Suhubi, E. S. (1965) *Int. Jour. Engg. Sci.*, **2** : 441.

24. Chadwick, P. (1960) *Progress in solid mechanics,* ed. Sneddon, I.N. and Hill, R., North Holland Publishing Company, Amsterdam.
25. Sengupta, P. R. & Ghosh,, B. C. (1977) *Indian Journal of Pure and Applied Mathematics,* **8(9)** : 1032.
26. Nowacki, W. (1969) *Arch. Mech. Stos.,* **21** : 241.
27. Nowacki, W. & Nowacki, W. K. (1969) *proc. Vibr. Probl.,* **10** : 97.
28. Cole, J. & Huth, J. (1958) *J. Appl. Mech.,* **25** : 433.
29. Lamb, H. (1904) *Phil. Trans. Roy. Soc. Ser* A, **208** : 1.
30. Sneddon, I. N. (1951) *Fourier Transforms,* McGraw-Hill, New York.
31. Nath, S. & Sengupta, P. R. (1999) *Indian J. Pure appl. Math.* **30(3)** : 317.
32. Sengupta, P. R. & Ghosh, B. C. (1974) *Gerlands Beitr. Geophysik, Leipzig,* **83,4(S)** : 309.
33. Sengupta, P. R. & Ghosh, B. C. (1974) *Pure and Appl. Geophysics,* **112** : 331.
34. Sengupta, P. R. & Ghosh, B. C. (1980) *The Mathematics Student,* **48(2)** : 183.
35. Das, T. K., Sengupta, P. R. & Debnath, L. (1979) *Internat. J. Math. and Math. Sci.* **14(3)** : 553.
36. Bandyopadhyay, D. K. (1979) *Gerlands Beitr. Geophysik,* Leipzig, **88,5(S)** : 394.
37. Benerjee, D. K. & Sengupta. P. R. (1978) *Indian J. Pure appl. Math.* **9(1)** : 17.
38. Sengupta, P. R. & Chakraborty, J. (1979) *Gerlands Beitr. Geophysik, Leipzig,* **88,6(S)** : 492.
39. Sengupta, P. R. & Chel, J. (1984) *Gerlands Beitr. Geophysik, Leipzig,* **93,3(S)** : 223.
40. Sengupta, P. R. & Chel, J. (1986) *Bull. Acad. Polon Sci. Ser. Sci. Techn.,* **34(1,2)** : 29.
41. Nowacki, W. (1970) *Arch. Mech. Stos.,* 22 : 3.
42. Nowacki, W. & Nowacki W. K. (1969) *Bull. Acad. Polon Sci. Ser. Sci. Techn.,* **17** : 75.
43. Nowacki, W. & Nowacki W. K. (1969) *Bull. Acad. Polon Sci. Ser. Sci. Techn.,* **17** : 49[65].
44. Eringen, A. C. (1966) *J. Math. Mech,* **15** : 909.
45. Eringen, A. C. (1967) *Int. J. Engg. Sci,* **5** : 191.
46. Eringen, A. C. (1968) *Theory of micropolar elasticity,* ed. Liebowith, H., Academic Press, New York.
47. Eringen, A. C. & Suhubi, E. S. (1964) *Int. J. Engg. Sci,* **2** : 189.
48. Palmov, N. A. (1964) *Priki. Mat. Mech.* **28** : 401.
49. De, S. & Sengupta, P. R. (19.....) *Bull. De L Acad. Pol. Des. Sci.* **22(3)** : 137.
50. Sengupta, P. R. & Ghosh, B.C. (1976) *Indian Journal of Mechanics and Mathematics,* **14(2)** : 11.
51. Sengupta, P. R. & Ghosh, B.C. (1977) *Arch. Mech. Stos.,* **29(2)** : 273.
52. Sengupta, P. R. & Ghosh, B.C. (1978) *Bull. De L Acad. Pol. Des. Sci.,* **26(5)** : 285.

53. Sengupta, P. R. & Ghosh, B.C. (1978) *Acta. Ciencia Indica,* **5(2).**

54. Sengupta, P. R. & Chakraborty, J. (1979) *Bull. De L Acad Pol. Des. Sci.,* **27(1)** : 8.

55. Sengupta, P. R. & Chakraborty, J. (1979) *Bull. De L Acad Pol. Des. Sci.,* **27(2)** : 67.

56. Sengupta, P. R. & Chakraborty, J. (1979) *Bull. De L Acad Pol. Des. Sci.,* **27(5,6)** : 195.

57. Reyleigh, F. W. (1889) *Proc. London. Math. Soc.* **20.**

58. Lamb, H. (1916) *Proc. Roy. Soc.* **5** : 93.

59. Fung, Y. C. (1968) *Foundations i solid Mechanics, Prentice-Hall, New Delhi.*

60. Sneddon, I. N. (1974) *The use of integral transforms,* Tata-McGraw Hill, New Delhi.

PROC. NAT. ACAD. SCI. INDIA, 73 (A), I, 2003

Difference in NO bonding mode in $[Fe(NO)(S_2CNEt_2)_2]$ and $[Co(NO)(S_2CNEt_2)_2]$: EHMO and normal coordinate analysis

P.K. GOGOI* and R. KONWAR

Department of Chemistry, Dibrugarh University, Dibrugarh-786 004, India.

Received September 21, 2000; Revised June 8, 2001; Accepted September 29, 2001

Abstract

The Extended Huckel Molecular Orbital (EHMO) calculation and the Normal Coordinate Analysis (NCA) have been carried out on pentacoordinated nitrosyl adducts of iron and cobalt diethyldithiocarbamates with the linear and bent metal-N-O groups respectively. It is observed that the geometry of the metal-N-O group depends on the symmetries of the HOMOs and LUMOs of NO and the parent dithiocarbamate fragments, the energies of metal *d* orbitals relative to σ_n and π^* of NO as well as the electron density on the metla atom. This observation has been substantiated by the force constants of N-O, Co-N, Fe-N, Co-S, Fe-S and S-C bonds evaluated by NCA.

(**Keywords** : EHMO/NCA/nitrosobis(diethyldithiocarbamato) iron(II)/nitrosobis(diethyldithiocarbamato) cobalt(II)

Introduction

Bis(N, N-dimethyldithiocarbamato)nitrosyl iron(II), $[Fe(NO)(S2CNMe_2)_2]$[1] and its cobalt analogue, $[Co(NO)(S_2CNMe_2)_2]$[2] have the uncommon square pyramidal five coordinated configuration as predicted theoretically by Daudel and Bucher[3]. Although these two isomorphous[4] complexes have the same basal ligands yet their metal-(NO) bonding systems are found to be different. Unlike the linear Fe-N-O system in the iron complex, the Co-N-O system is significantly bent (~127°)[1] with unsymmetrical Co(NO) π bond which is absent in the former. General discussions[5-9] on pentacoordinated nitrosyls revealed that the bending of the metal-N-O group depends upon the different coordination modes (NO^+, NO and NO^-) of NO, the energies of the metal *d* orbitals relative to nitrosyl σ_n and π^*, electron donating capability of the basal ligands and the position of the metal in the periodic table. A comparative molecular orbital (MO) study of the bonding of NO groups in two nitrosyl complexes, $[Fe(NO)(S_2CNEt_2)_2]$ and $[Co(NO)(S_2CNEt_2)_2]$ will hence, be of heuristic value. It may be expected that the bonding and the structural differences in the M-NO groups (M = Fe or Co) of these complexes should be reflected on the symmetry properties of their frontier orbitals as well as the N-O, M-N and M-S force constants.

Qualitative MO calculations have been done by Extended Huckel Molecular Orbital (EHMO) method and the results thus obtained have been substantiaed by relevant force constants evaluated by Normal Coordinate Analysis (NCA).

Materials and Method

The complexes were prepared by the method reported earlier[10]. The FTIR spectra (3000-400 cm^{-1}) of the complexes as KBr pellets were recorded using a Perkin-Elmer 32100 FT-IR spectrophotometer.

EHMO Calculation : EHMO calculation was done with ICON 8 computer program[11]. The mean values of the structural parameters for the complexes (A&B) were taken from the published data[1,4] of their methyl analogues assuming that the alkyl substituents have

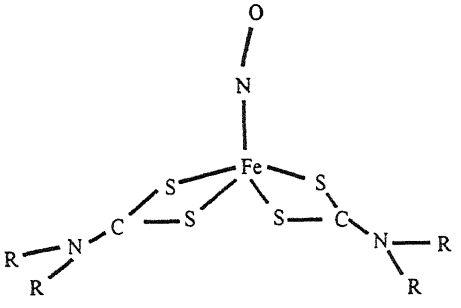

(A)

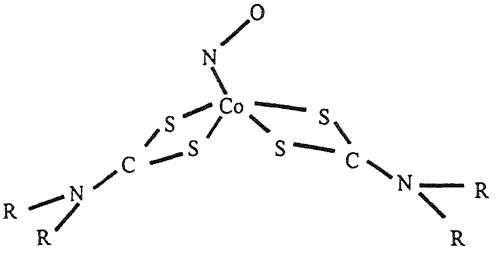

(B)

little effect on the distant M-N-O moiety which is the main centre of interest. Hydrogen atoms were excluded to simplify the calculation. The orbital exponents (ξ), corresponding relative weights of *d* orbitals, the ionization potentials (H_{ii}) and the Huckel constant (*K*) were obtained from published works[12-14]. The energy levels of the molecular orbitals of main interest are furnished in Fig. (1 & 2).

Normal Coordinate Analysis : The simplified models C and D of the complexes A and B were considered for the NCA assuming each ethyl group to behave as a single atom R. The 21 normal vibrations (3N-6; N = 9) of each of these 9 atomic models of C_S symmetry were found to be within the two symmetry species A′ and A″ and were classified as

$$\Gamma_{vib} = 14A' + 7A''$$

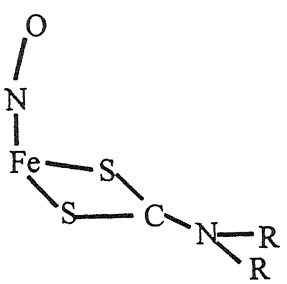

(C)

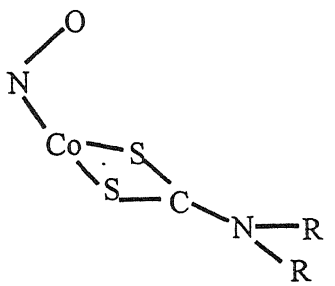

(D)

The Wilson GF matrix method[15] was used to solve the secular equation using QCMP 067 computer program[16]. The F matrix was constructed by using Urey-Bradley type force field[17]. The initial sets of force constants were taken from earlier literature on similar system[18] which were refined by the procedure of Nelder and Mead[19] to get the final sets of force constants [Table 1(a) & (b)]. The observed and calculated frequencies along with the band assignments and potential energy distributions (PED) are furnished in Table 2.

Results and Discussions

EHMO : As both the complexes have the same basal dithiocarbamate ligand, discussion will cover mainly the bodning scheme of the M-N-O groups. Cambi[20] reported the cobalt complex to be diamagnetic indicating a dsp^3 type hybridization. The iron complex with one electron less is paramagnetic as confirmed by e.s.r. studies[9]. Depending upon the behaviour of the antibonding orbital (Π^*), three different coordinating forms of nitric oxide, *viz.*, NO^+, NO and NO^- are observed in nitrosyl complexes[4]. It is common to consider the linear nitrosyls as complexes of NO^+ and bent molecules as complexes of NO^{-9}. Generally nitric oxide is like carbon monoxide in forming complexes with transition metals. The extra antibonding electron of NO is usually transferred to the metal atom to give the nitrosyl cation, $N{\equiv}O^+$. Typical complexes are $[Fe(CN)_5NO]^{2-}$ and $[Fe(H_2O)_5NO]^{2+}$ [21]. The spectral and magnetic properties of $[Fe(NO)(S_2CNMe_2)_2]$ revealed that nitrosyl bonds formally as NO^+ [22], consistent with the observation of an infrared band at 1735 cm^{-1} usually assigned to coordinated NO^+ [23]. In their theoretical study, Alderman and Owston[24] suggested the π^* (NO) $\rightarrow$ Co electron flow scheme. However, in some complexes, such as $[Co(NH_3)_5NO]^{2+}$, in presence of highly basic other ligands, an electron may be transferred from metal to NO[21]. The present EHMO calculation shows that the NO groups of

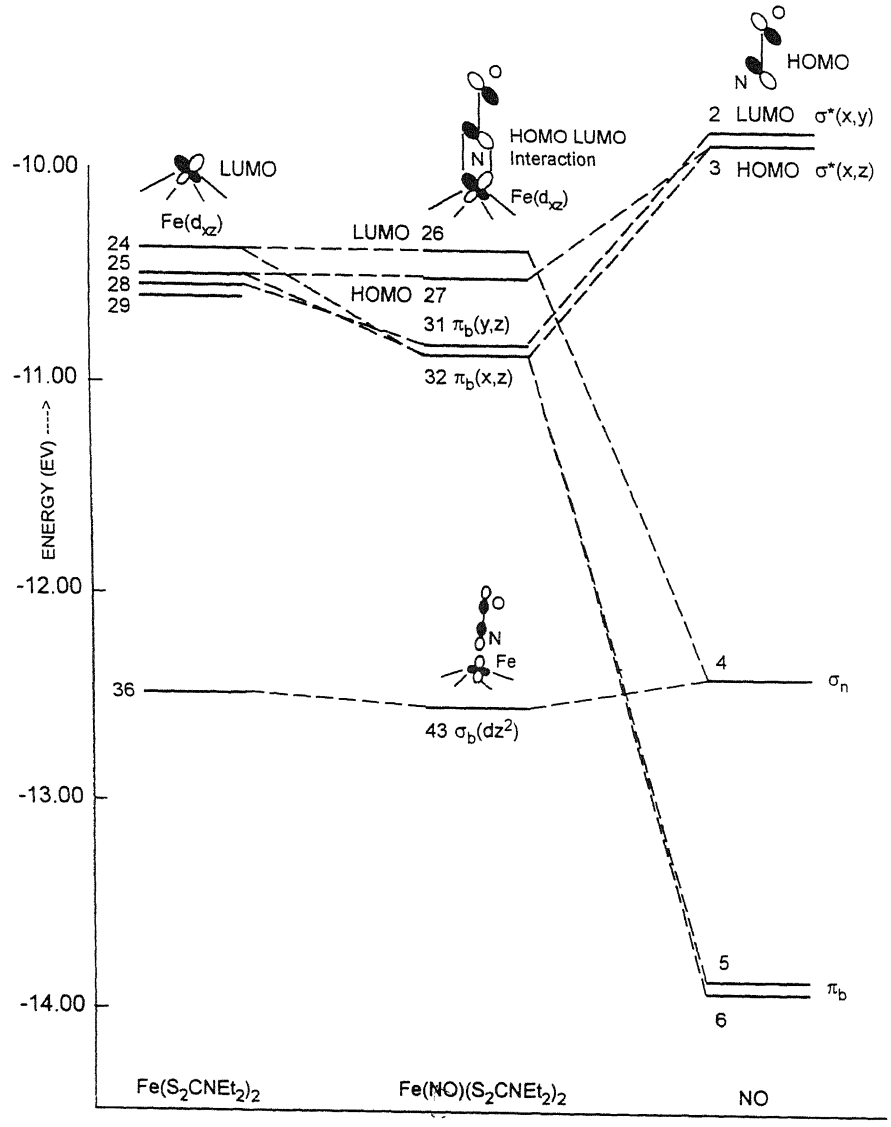

Fig. 1 – Interaction diagram of $[Fe(NO)(S_2CNEt_2)_2]$

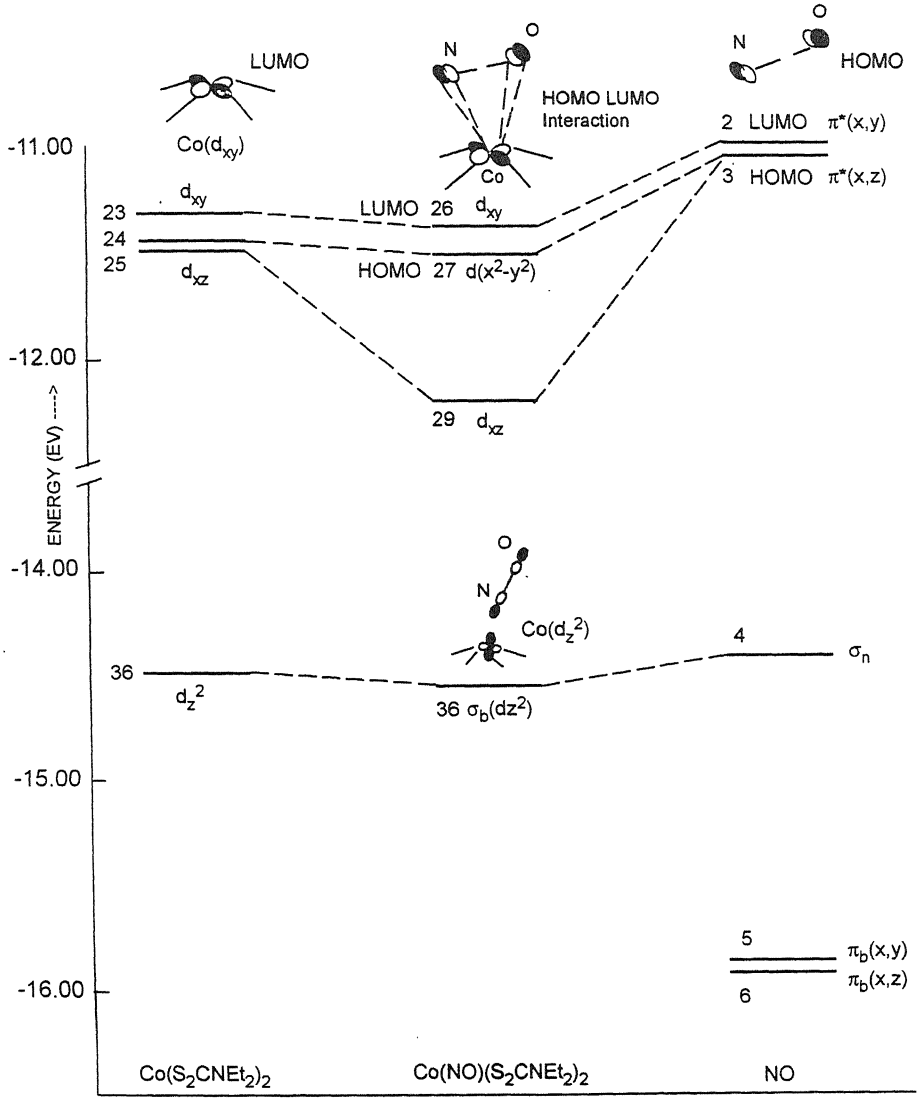

Fig. 2 – Interation diagram of [Co(NO)(S_2CNEt_2)$_2$]

$[Fe(NO)(S_2CNEt_2)_2]$ and $[Co(NO)(S_2CNEt_2)_2]$ possess net positive charges of 0.50100 and 0.36064 respectively indicating more electron donation to the metal atom in the latter complex. The fragment molecular orbital (FMO) analysis shows that the unpaired electron in the HJOMO ($\pi^*_{x,z}$) of NO flows to the LUMO (d_{xz}) of $[Fe(S_2CNEt_2)_2]$ fragment under a symmetrically and energetically favorable condition (Fig. 3a). Similar interaction is observed between the HOMO ($\pi^*_{x,y}$) of NO and the LUMO(d_{xy}) of $[Co(S_2CNEt_2)_2]$ fragment

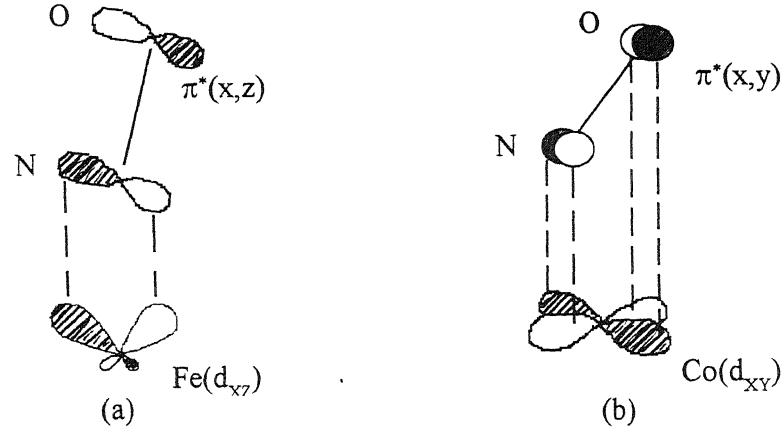

Fig. 3 – HOMO–LUMO interaction in (a) $[Fe(NO)(S_2CNEt_2)_2]$ and (b) $[Co(NO)(S_2CNEt_2)_2]$.

in the cobalt complex (Fig. 3b). It is clear from the Fig. 3 (a & b) that the iron atom forms π bond with NO through the N atom only while in the cobalt analogue both the N and O atoms of the nitrosyl group are involved in π bonding interaction with the metal d_{xy} orbital fulfilling the criteria for a bent Co-N-O system. It was suggested[9] that higher the energy of the metal d_{xz} (or d_{yz}) and d_z^2 relative to nitrosyl π^* and σ_n respectively greater is the M-N-O bending. The present work has revealed that the metal d_{xz} (or d_{yz}) and d_z^2 orbitals are more close in energy to π^* and σ_n of NO in the cobalt complex than in the iron analogue (Fig. 1 & 2) suggesting a greater Co-N-O bending than that of Fe-N-O group. Mingos[6] also reported that the bending of M-N-O group in $[Co(NO)(NH_3)_5]^{2+}$ influences substantially the energies of mainly two molecular orbitals containing metal d_{xz} and d_z^2 and nitrosyl σ_n and π^*.

Normal Coordinate Analysis : The IR spectra of $[Fe(NO)(S_2CNEt_2)_2]$ and $[Co(NO)(S_2CNEt_2)_2]$ were recorded in the range (3000-400 cm^{-1}). The bands above 2000 cm^{-1} are not assigned as there were no significant absorptions except C-H stretching[25] and because hydrogen atoms were not included in the present calculation. The bands observed

Table 1 – Refined sets of force constants (mdyn/Å) for (a) $[Fe(NO)(S_2CNEt_2)_2]$ and (b) $[Co(NO)(S_2CNEt_2)_2]$.

(a)	f_1(Fe–S) = 3.98	f_{14}(FeNO) = .68	(b)	f_1(Co–S) = 3.50	f_{14}(CoNO) = .62
	f_2(S–C) = 6.08	f_{15}(S ... S) = .80		f_2(S–C) = 6.25	f_{15}(S ... S) = .78
	f_3(C–N) = 7.92	f_{16}(Fe ... C) = .11		f_3(C–N) = 7.65	f_{16}(Co ... C) = .12
	f_4(N–R) = 7.86	f_{17}(S ... N) = .24		f_4(N–R) = 7.77	f_{17}(S ... N) = .27
	f_5(Fe–N) = 1.84	f_{18}(C ... R) = .50		f_5(Co–N) = 1.90	f_{18}(C ... R) = .43
	f_6(N–O) = 12.26	f_{19}(R ... R) = .40		f_6(N–O) = 12.2	f_{19}(R ... R) = .33
	f_7(SFeS) = .54	f_{20}(S ... N) = .03		f_7(SCoS) = .56	f_{20}(S ... N) = .05
	f_8(FeSC) = .08	f_{21}(Fe ... O) = .25		f_8(CoSC) = .08	f_{21}(Co ... O) = .23
	f_9(SCS) = .60			f_9(SCS) = .55	
	f_{10}(SCN) = .28			f_{10}(SCN) = .45	
	f_{11}(CNR) = .18			f_{11}(CNR) = .15	
	f_{12}(RNR) = .38			f_{12}(RNR) = .44	
	f_{13}(SFeN) = .72			f_{13}(SCoN) = .74	

Table 2 – Comparison of observed and calculated frequencies (cm^{-1}) and band assignments with potential energy distributions (PED).

$[Fe(NO)(S_2CNEt_2)_2]$				$[Fe(NO)(S_2CNEt_2)_2]$			
Obs	Cal	Assignment	PED (%)	Obs	Cal	Assignment	PED (%)
1687	1687	ν(N–O)	95	1682	1673	ν(N–O)	97
1550	1502	ν_{sym} (C–N)	69	1495	1497	ν_{sym} (C–N)	67
1272	1265	ν_{asym} (N–R)	94	1269	1253	ν_{asym} (N–R)	92
1067	1074	ν_{asym} (S–C)	94	1071	1083	ν_{asym} (S–C)	92
967	960	ν_{asym}(N–R)+ν_{sym}(S–C)	61,35	997	979	ν_{asym}(N–R)+ν_{sym}(S–C)	57, 37
—	686	ν_{sym} (Fe–S)	68	649	647	ν_{sym} (Co–S)	60
555	554	ν_{sym}(S–C)+ν_{sym}(Fe–S)	41, 26	551	550	ν_{sym}(S–C)+ν_{sym}(Co–S)	31, 17
—	—	————	—	504	508	δ_{sym}(CoNO)+ν_{sym}(Co–N)	30, 29
477	477	ν_{asym} (Fe–S)	99	—	437	ν_{asym} (Co–S)	99
—	379	ν_{sym} (Fe–N)	82	—	403	ν_{sym} (Co–N)	46
—	212	δ_{sym}(FeNO)+NO rock	23, 65	—	190	δ_{sym}(CoNO)+NO rock	35, 53

at 1349.6 cm^{-1} and 1197.1 cm^{-1} in the iron complex and those at 1350.2 cm^{-1} and 1210 cm^{-1} in the cobalt complex are probably due to C-C stretching of the ethyl groups and were not calculated here. The bands at 1450.2 cm^{-1} and 1376.5 cm^{-1} in the cobalt complex and at 1419.1 cm^{-1} and 1375 cm^{-1} in the iron complex are comparable to those reported[18,25,26] for $\delta_{HCH}(CH_3)$ and were excluded from calculation due to the same reason mentioned above. Similarly the bands at 848.7 cm^{-1} in the cobalt complex and that at 843.8 cm^{-1} in the iron complex might be due to the C-C-C bending coupled with the C-C and C-CH_3 stretching which were not included in the present calculation. Eleven vibrational frequencies for each complex were calculated. The agreement between the observed and the calculated frequencies are quite satisfactory (Table 2); the root mean square errors being 4.7 and 10.1 cm^{-1} for the iron and the cobalt complexes respectively. The IR assignments and the force constants for the basal ligands are consistant with those reported earlier for dithiocarbamate complexes[18,27]. The bands at 1687 cm^{-1} and 1682 cm^{-1} are assigned to ν_{NO} for $[Fe(NO)(S_2CNEt_2)_2]$ and $[Co(NO)(S_2CNEt_2)_2]$ respectively and are comparable to their corresponding methyl analogues[2]. However, these values are much less than the vibrational frequency of free NO which is about 1876 cm^{-1} [28] indicating a decrease in the N-O bond order in these two complexes. It is reasonable to expect a π-back bonding from d_{xz} and d_{yz} orbitals of the metal to the π^* (NO)[29] reducing the N-O bond order. Such a considerable π-back bonding in most nitrosyl complexes is evidenced by the relatively shorter M-N bonds in these systems[30]. The flow of electrons from σ_{nb} orbitals of NO to metal d_z^2 orbital also contributes to the decrease of N-O bond order. The combined effects of sigma mode of complexing of the NO^+ ion as a Lewis base and the π-back bonding predominate the transfer of electrons between metal and NO molecules resulting in a net decrease of N-O bond order. As the iron atom has one valence electron less than the cobalt atom so the extent of electron flow from π^* of NO to the iron *d* orbital would be more and hence the N-O bond order in the iron complex becomes slightly greater than that in the cobalt complex. It is reflected on the greater ν_{N-O} (1687 cm^{-1}) and N-O stretching force contant (f_{N-O} = 12.26 mdyn/Å) in $[Fe(NO)(S_2CNEt_2)_2]$ than the corresponding values (ν_{N-O} = 1682 cm^{-1} and f_{N-O} = 12.20 mdyn/Å) in $[Co(NO)(S_2CNEt_2)_2]$. Earnshaw *et al.*[5] reported that the electron removal from the cobalt atom by electron withdrawing substituents decreases the $d\pi$-$p\pi$ bonding between cobalt and nitric oxide and increases the N-O bond order. It suggests that with the same electron donating alkyl groups in the iron and the cobalt complexes the excess electron in cobalt will lead to a greater Co-NO $d\pi$-$p\pi$ bonding than that between Fe and NO with the expected force constant order $f_{Co-N} > f_{Fe-N}$. Present observation substantiates this with respective values of f_{Co-N} = 1.90 mdyn/Å and f_{Fe-N} = 1.84 mdyn/Å. The bands at 1495 cm^{-1} and 1500 cm^{-1} have been assigned to partially double bonded C-N

stretches and those observed at 1269 cm^{-1} and 1272 cm^{-1} are assigned to ν_{N-R} which are well within the range (1480-1550 cm^{-1} for ν_{C-N} and 1250-1350 cm–1 for ν_{N-R}) observed by Chatt *et al.*[31,32] As suggested by Cotton and McCleverty[33], the relatively higher ν_{C-N} (1500 cm^{-1}) in the iron complex than that (ν_{C-N} = 1495 cm^{-1}) in the cobalt complex might be the result of greater electron donation by the sulfur atoms to the iron atom which is ahead of cobalt in the position of the periodic table. The above explanation is substantiated by the following order of C-N and S-C stretching force constants :

F_{C-N}(Fe) = 7.92 mdyn/Å > f_{C-N}(Co) = 7.65 mdyn/Å and

f_{S-C}(Fe) = 6.08 mdyn/Å < f_{S-C}(Co) = 6.25 mdyn/Å

Conclusion

The reason for linear and bent structure for nitrosobis (diethyldithiocarbamato) iron (II) and nitrosobis (diethyldithiocarbamato) cobalt (II) has been proposed on the basis of HOMO/LUMO interaction of NO and metal dithiocarbamates, derived from EHMO calculations. The NCA of the above systems corroborate the observations obtained from EHMO analysis.

Acknowledgement

We thank University Grants Commission, New Delhi, for financial support to this work in the form of awarding a Visiting Associateship (PKG) and a Teacher Fellowship (RK).

References

1. Davies, G.R., Mais, R.H.B. & Owston, P.G. (1968) *Chem. Commun.* : 81.
2. Alderman, P.R.H., Owston, P.G. & Rowe, J.M. (1962) *J. Chem. Soc.* (A) : 668.
3. Daudel & Bucher (1952) *J. Chim. Phys.* **42** : 6.
4. Davies, G.R., Jarvis, J.A.J., Kilbourn, B.T., Mais, R.H.B. & Owston, P.G. (1970) *J. Chem. Soc. (A)* : 1275.
5. Earnshaw, A., Hewlett, P.C. & Larkworthy, L.F. (1963) *Nature* **199** : 483.
6. Mingos, D.M.P. (1973) *Inorg. Chem.* **12** : 1209.
7. Enemark, J.H. & Feltham, R.D. (1974) *J. Amer. Chem. Soc.* **96** : 5002.
8. Enemark, J.H. & Feltham, R.D. (1974) *J. Amer. Chem. Soc.* **96** : 5004.
9. Hoffmann, R., Chen, M.M.L., Elian, M., Rossi, A.R. & Mingos, D.M.P. (1974) *Inorg. Chem.* **13** : 2666.
10. Malatesta, (1940) *Gazzetta,* **70** : 734.
11. Howell, J., Rossi, A., Wallace, D., Haraki, K. & Hoffman, R. *ICON 8 Program,* Department of Chemistry, Cornell University, New York.

12. Tatsumi, K. & Hoffman, R. (1981) *Inorg. Chem.* **20** : 3771.
13. Hoffman, D.M. & Hoffman, R. (1981) *Inorg. Chem.* **20** : 3543.
14. Lowe, J.P. (1978) *Quantum Chemistry,* Academic Press, New York.
15. Wilson, E.B., Decius, J.C. & Cross, P.C. (1955) *Molecular Vibrations,* Mcgraw-Hill Book Co., Inc., New York.
16. McIntosh, D.F. & Peterson, M.R. (1988) *QCMP 067,* Department of Chemistry, University of Toronto, Canada.
17. Shimanouchi, T. (1949) *J. Chem. Phys.* **17** : 245.
18. Durgaprasad, G., Sathyanarayana, D.N. & Patel, C.C. (1969) *Can. J. Chem.* **47** : 631.
19. Nelder, J.A. & Mead, R. (1965) *Computer Jour.* **7** : 308.
20. Cambi, L. (1941) *Z. anorg.u.allgem,. Chem.* **247** : 22.
21. Jolly, W.L. (1964) *The Inorganic Chemistry of Nitrogen,* Benzamin, W.A. Inc., New York.
22. Gray, H.B., Bernal, I. & Billig, E. (1962) *J. Amer. Chem. Soc.* **84** : 3404.
23. Lewis, J. (1959) *Science Progress* : 506.
24. Alderman, P.R.H. & Owston, P.G. (1956) *Nature* **178** : 1071.
25. Behnke, G.T. & Nakamoto, K. (1967) *Inorg. Chem.* **6** : 440.
26. Periandy, S., Latha, L.R. & Mohan, S. (1998) *Proc. Nat. Acad. Sci., India.* **68(A)** : 419.
27. Nakamoto, K., Fujita, J. Candrate, R.A. & Morimoto, Y. (1963) *J. Chem. Phys.* **39** : 423.
28. Jones, L.H. (1971) *Inorganic Vibrational Spectrscopy,* Marcel Dekker, Inc., New York.
29. Scheidt, W.R. & Hoard, J.L. (1973) *J. Amer. Chem. Soc.* **95** : 8281.
30. Hodgson, D.J., Payne, N.C., McGinnety, J.A., Pearson, R.G. & Ibers, J.A. (1968) *J. Amer. Chem. Soc.* **90** : 4486.
31. Chatt, J., Duncanson, L.A. & Venanzi, L.M. (1956) *Soumen. Kemistilehti* **B29** : 75.
32. Chatt, J., Duncanson, L.A. & Venanzi, L.M. (1956) *Nature* **177** : 1042.
33. Cotton, F.A. & McCleverty, J.A. (1964) *Inorg. Chem.* **3** : 1398.

PROC. NAT. ACAD. SCI. INDIA, 73 (A), I, 2003

Equilibrium studies on metal complexes of substituted imidazoles

MOHD. ZAKEE and DEVA DAS MANWAL

Department of Chemistry, Nizam College, Osmania University, Hyderabad–500001, A.P.

E-mail : ddmanwal04@yahoo.co.in

Received December 10, 2001; Revised April 27, 2002; Accepted May 9, 2002

Abstract

Potentiometric equilibrium measurements have been made at 30°C for the formation of ternary complexes of 5-hydroxy-2-(hydroxy methyl)-4(H)pyran-4-one (known as kojic acid) or 3-hydroxy-2-methyl-4(H)-pyran-4-one (known as maltol) and Co(II), Ni(II), Cu(II) and Zn(II) with imidazole, 1-methyl imidazole, 2-methyl imidazole, 2-ethyl imidazole and benzimidazole in 1:1:1 ratio. The comparison of $\Delta \log K$ values reveals that the order of stability of ternary complexes is: 2-methyl imidazole ≥ 2-ethyl imidazole > imidazole ≥ 1-methyl imidazole > benzimidazole.

(**Keywords :** potentiometry/mixed ligand complexes/substituted imidazoles/stability constants).

Introduction

The binding of imidazole with transition metals is of interest because of this ligand's close relationship with biological systems of a more complex nature involving histidine residues. The literature contains free energy data obtained by potentiometric studies on the systems.[1-4] These data indicate that imidazole forms some of the most stable complexes of all heterocyclic –N ligands. This is corroborated by the high acid dissociation constants of imidazoles. It is also very well established that in the combination of cadmium and copper ion with serum albumin the principal binding sites are the imidazole groups of the histidine residues of the protein molecule. Several studies have been made on the imidazole ring to determine which nitrogen is involved in the binding to metals. Li *et al*[5] determined the constants of imidazole and N-methyl imidazole with Cu(II). By their similarity in formation constants the binding site was assumed to be the pyridine nitrogen.

Owing to the biological importance of imidazole, we have undertaken the study of substituted imidazoles with transition metals. In continuation of our earlier studies,[6,7] we now report the stabilities associated with the metal complexes of substituted imidazoles with bivalent metals in the presence of oxygen donors such as 5-hydroxy-

2-(hydroxy methyl)-4(H)pyran-4-one (known as kojic acid) and 3-hydroxy-2-methyl-4(H)-pyran-4-one (known as maltol).

Materials and Method

The ligands, kojic acid and maltol were obtained from Lancaster (UK). Other ligands, imidazole and substituted imidazoles were obtained from Fluka (Switzerland). The metal salts of Co(II), Ni(II), Cu(II) and Zn(II) were of Anala R grade, and the metals were standardized volumetrically by titration with the sodium salt of EDTA.[8] Potentiometric measurements were carried out at 30^0C with 0.1M KNO_3 as background electrolyte in aqueous medium using a control dynamics pH meter. The pH meter readings were plotted against *a* (moles of base added per mole of ligand) or *m* (moles of base added per mole of metal ion). Calculations were made with the help of BEST computer programme.[9]

Results and Discussion

Acid dissociation constants : The acid dissociation constants of kojic acid, maltol, imidazole 1-methyl imidazole, 2-methyl imidazole, 2-ethyl imidazole and benzimidazole were remeasured and the values obtained are in good agreement with the values found in literature.

Binary Constants : The formation constants for 1:1 [M-L] system where M = Ni(II), Co(II), Cu(II), Zn(II) and L = maltol, kojic acid, imidazole, 1-me imidazole, 2-me-imidazole, 2-ethyl imidazole and benzimidazole were measured in aqueous medium at 30^0C and μ = 0.1M KNO_3. The values obtained (Table 1) are in good agreement with literature values.[6,7]

Table 1–Acid dissociation constants of ligands and their stability constants with bivalent transition metals. [$T = 30^0$C; I = 0.1M KNO_3; aqueous medium]

Ligands	pK_a	Co(II)	Ni(II)	Cu(II)	Zn(II)
Imidazole	7.01	2.56	3.21	4.28	2.64
1-Me-imi	7.19	2.61	3.32	4.25	2.71
2-Me-imi	7.93	2.71	3.38	4.38	2.93
2-Et-imi	7.95	2.82	3.41	4.41	2.97
Bzm	5.37	2.25	2.65	3.28	2.35
Maltol	8.55	5.35	5.57	7.61	5.77
Kojic acid	7.62	4.75	4.93	6.57	5.14

Standard deviations (σ fit) are within ± 0.04 log units.

Ternary Constants : The mixed ligand titration curves of all the systems showed a feeble inflection at m = 2. Mixed ligand titration curve of Ni(II) with maltol in presence of imidazole is given in Fig. 1 along with other curves (free ligand and binary). These curves are related to the usual equilibrium.

$$HL + M + HA \rightleftharpoons [MLA] + 2H^{+} \quad (1)$$

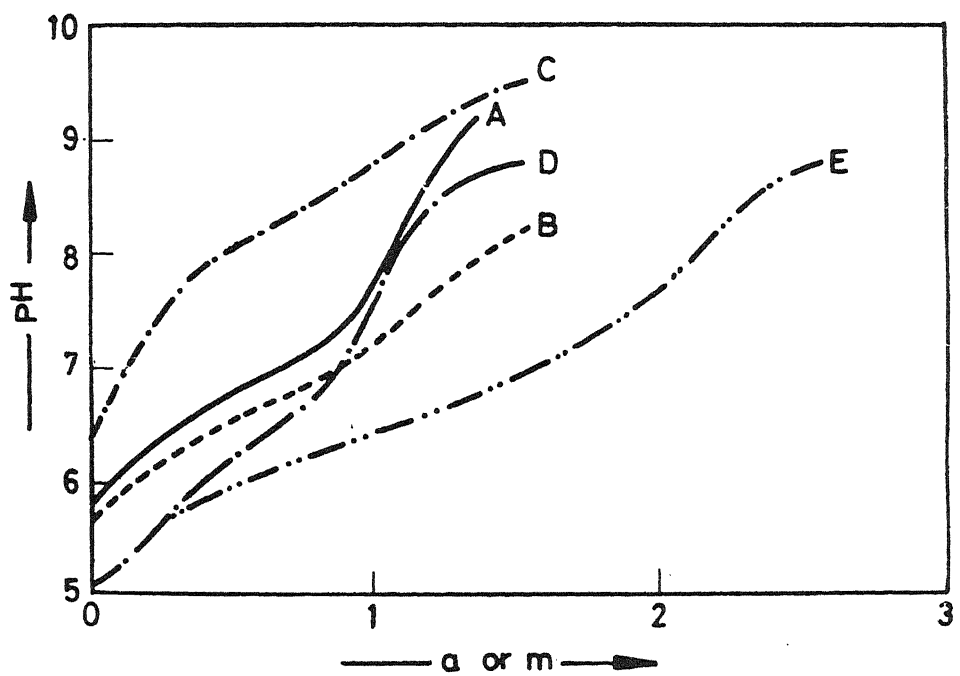

Fig. 1–Potentiometric titration curves of the ternary complexes of [maltol-Ni-imidazole] A = free ligand (imidazole), B = Ni-imidazole, C = free ligand (maltol), D = Ni-maltol, E = 1:1:1 (maltol-Ni-imidazole) ternary complexes.

Calculations were made with the help of BEST computer programme. Out of the various models, one which gave the best statistical fit was selected. The binary stability constants were used as fixed parameters for the refinement of the ternary formation constants. The values thus obtained are presented in Table 2.

The stability of the various ternary metal complexes and corresponding binary metal complexes have been quantitatively compared in terms of the parameter, $\Delta \log K$ which is expressed as

$$\Delta \log K = \log K^{ML}_{MLA} - \log K^{M}_{ML} \quad (2)$$

The $\Delta \log K$ values for the different ternary complexes have been calculated and are listed in Table 2 along with ternary constants for different systems. In order to obtain precise values of $\Delta \log K$, it is essential that the binary and ternary constants should refer to identical experimental conditions. Therefore acid dissociation constants of all the ligands under study and their binary constants have been remeasured.

Table 2– Logarithms of ternary stability constants of bivalent metals with substituted imidazoles in presence of maltol or kojic acid and their corresponding $\Delta \log K$ values.

[$T = 30^0$C; $I = 0.1$M KNO_3; aqueous medium]

	Maltol				Kojic Acid			
	Co(II)	Ni(II)	Cu(II)	Zn(II)	Co(II)	Ni(II)	Cu(II)	Zn(II)
				Ternary constants				
Imidazole	7.99	8.88	12.07	8.50	7.29	8.18	10.92	7.80
1-Me-imi	8.02	9.01	12.03	8.58	7.30	8.31	10.95	7.88
2-Me-imi	8.14	9.10	12.23	8.88	7.42	8.42	11.08	8.20
2-Et-imi	8.27	9.16	12.27	8.93	7.59	8.42	11.15	8.22
Bzm	7.57	8.28	10.93	8.14	6.92	7.54	9.90	7.43
				$\Delta \log K$				
Imidazole	+0.08	+0.10	+0.18	+0.09	-0.02	+0.04	+0.07	+0.02
1-Me-imi	+0.06	+0.12	+0.17	+0.10	-0.06	+0.06	+0.13	+0.03
2-Me-imi	+0.08	+0.15	+0.24	+0.18	-0.04	+0.11	+0.13	+0.13
2-Et-imi	+0.10	+0.18	+0.25	+0.19	+0.02	+0.08	+0.17	+0.11
Bzm	-0.03	+0.06	+0.04	+0.02	-0.08	-0.04	+0.05	-0.06

Standard deviations are within ± 0.05 log units.

Perusal of the $\Delta \log K$ values (Table 2) shows that the stability order with respect to the secondary ligands in the ternary complex is 2-methyl imidazole ≥ 2-ethyl imidazole > imidazole ≥ 1-methyl imidazole > benzimidazole. This sequence may be attributed to the decrease in the basicities of the ligands. For steric consideration, the $\Delta \log K$ values in the case of complexes with substituted imidazoles should have been smaller than that for imidazole complexes. The increase in basicity in substituted imidazoles, thus compensates for the negative contribution of the steric effect and further enhances the values of $\Delta \log K$ in all the cases.

Amongst the substituted imidazoles, there is not much difference either in the ligand basicities or in the steric effect so that both 2-methyl imidazole and 2-ethyl imidazole gave almost similar $\Delta \log K$ values. The $\Delta \log K$ values of imidazole and 1-methyl imidazole are also comparable, may be due to their similarities in the basicity. Replacement of hydrogen by CH_3 group at one position in 1-methyl imidazole has little effect. The lower stabilities of ternary complexes involving benzimidazole is in line with basicity order.

The positive $\Delta \log K$ values of these ternary systems may be attributed to the $d\pi$-$p\pi$ back bonding. Like 2-2'-bipyridyl, 1,10-phenanthroline, imidazole or substituted imidazoles are also reasonably good π acceptors. Therefore, imidazole or substituted imidazoles would prefer binding with O^--O^- donors rather than N-N donors.[6] Maltol or kojic acid being O-O^- donors prefer binding with imidazole or substituted imidazoles, hence positive or less negative $\Delta \log K$ values are obtained.

In other words, the extra stabilization of ternary complexes can be explained by considering that there is a M(II)→L, π interactions and hence the electron density on the metal ion is reduced and the effective electronegativity of $[M\text{-}L]^+$ complex is almost the same as that of $[M(H_2O)_6]^{2+}$. Thus σ bonding tendency of imidazole or substituted imidazoles to combine with $[M\text{-}L]^+$ and $[M(H_2O)_6]^{2+}$ is not significantly different. Hence ternary values are more than binary values resulted in positive $\Delta \log K$ values. The order of stability in terms of O-O^- donors is as maltol > kojic acid. This order is in line with basicity order of these two ligands. The order of stability of ternary complexes in terms of metal ions is in conformity with Irving Williams natural order of stabilities.[10]

Acknowledgements

Mohd. Zakee thanks the U.G.C. and the Principal, Mumtaz College for awarding teacher fellowship under FIP.

References:

1. Edsall, J.T., Feisenfeld, G., Goodman, D.S. & Gurd, F.R.N., (1954) *J. Am. Chem. Soc.* **76** : 3054.
2. Mickel, B.L. & Andrew, A.C. (1955) *J. Am. Chem. Soc.* 77 : 5291.
3. Andrews, A.C., Lyons, T.D. & O'Brien, T.D. (1962) *J. Chem. Soc.* : 1776.
4. Koltun, W.L., Dexter, R.N., Clark, R.E. & Gurd, F.R.N. (1958) *J. Am. Chem. Soc.* **80** : 4188.
5. Li, N.C., White, J.M. & Doody, E. (1954) *J. Am. Chem. Soc.* **76** : 6319.
6. Deva Das .P & Manwal Devadas, (1994) *Proc. Nat. Acad. Sci. India.* **64**(A)I : 135.
7. Manwal, Devadas & Aijaz Hussain Syed (1997) *Proc. Nat. Acad. Sci. India.* **67**(A)III : 301.
8. Schwarzenbech, G. (1957) *Complexometric Titrations*, Interscience, New York, p.27.
9. Motekaitis, R.J. & Martell, A.E. (1982) *Can. J. Chem.* **60** : 168 and 2403.
10. Irving, H. & Williams, R.J.P. (1953) *J. Chem. Soc.* 3192.

PROC. NAT. ACAD. SCI. INDIA, 73 (A), II, 2003

Mixed ligand complexes of inorganic phosphates - Relative stabilities of binary and ternary complexes - pH metry

SYED AIJAZ HUSSAIN, DEVA DAS MANWAL* and GOURI SHANKAR CHITEMALLA**

Department of Chemistry, Nizam College, Osmania University, Hyderbad - 500 001, India.

***Department of Chemistry, Vasavi College of Engineering, Hyderabad - 500 031, India*

e-mail: ddmanwal04@yahoo.co.in

Received Aug. 16, 2001; Revised Feb. 20, 2002; Accepted May 9, 2002

Abstract

Stability constants of ternary complexes of inorganic phosphates (viz., orthophosphate (OP), pyrophosphate (PP) and tripolyphosphate (TPP) with bivalent metal ions in presence of benzimidazole (Bzm) and substituted benzimidazoles (viz. 2-Methyl benzimidazole (Me-Bzm), 2-Propyl benzimidazole (Pro-Bzm), 5,6-Dimethyl benzimidazole (5,6-Me-Bzm), 2-Hydroxymethyl benzimidazole (HMB), 2-Hydroxethyl benzimidazole (HEB)) have been determined potentiometrically at 30°C and μ=0.1M KNO_3 in 20% methanol medium. Ternary stability constants of the various inorganic phosphates were compared. It was found that the stability of the ternary complexes in terms of inorganic phosphates decrease in order : TPP > PP > OP. The ternary complexes of TPP are more stable than PP due to more electrostatic attraction between TPP^{-5} and positive charge on coordination sphere of the metal ion. The ligand OP has comparatively less negative charges L^{2-} than PP (L^{4-}) or TPP (L^{5-}), hence it forms least stable complexes. Further, OP may act as monodentate ligand, even if it behaves as bidentate, the resultant 4-membered chelate would be less stable.

(**Key words :** pH metry/mixed ligand complexes/binary complexes/ternary complexes/stability constants).

Introduction

The interplay between nucleotides and metal ions is now well established for many enzymatic systems[1]. Consequently, metal ion-nucleotide interactions[2] have been studied in the solid state[3] and in solution[4] and our knowledge on binary metal complexes of nucleotides 5`-monophosphates or 5`-triphosphates is considerable. The

stability[5] of these complexes and their structures[4] in solution are well characterized, and the tendency for macrochelate formation in monomeric metal ion complexes of nucleoside 5`-triphosphates and the promotion of stacking by metal ions have been quantified[6,7,8]. In continuation of our earlier studies[9, 10] on stabilities of the ternary complexes involving nucleic acid constituents, we now report the stabilities associated with the ternary complexes involving benzimidazoles and inorganic phosphates and bivalent metals.

Materials and Methods

The ligands Bzm and 5,6-Me-bzm were obtained from Sigma Chemical Company(USA) and John Baker Inc., Colorado, USA respectively. The other ligands under study were prepared in this laboratory according to the procedures available[11]. The other secondary ligands, orthophosphate (OP), tetra sodium pyrophosphate (PP) and pentasodium tripolyphospyhate (TPP) were obtained from Aldrich Chemical Company Ltd., (USA).

All bivalent metal ions, EDTA, potassium hydrogen pthalate, KNO_3, NaOH were of BDH Analar grade. A stock solution of bivalent metal ions were prepared and standardized by the various methods available in literature[12, 13]. Carbonate-free sodium hydroxide was prepared and standardized by titrating with potassium hydrogen pthalate. Acid dissociation constants of the free ligands and formation constants of metal complexes were determined by potentiometric titrations of the various ligands and metal-ligands mixtures (in ratio 1:1 and 1:1:1) with standard carbonate free NaOH. The pH measurements were carried out at 30^0C with 0.1M KNO_3 as background electrolyte in 20% (v/v) methanol-water medium using a control dynamic pH meter fitted with gel filled combined electrode assembly. The pH meter readings were plotted against ***a*** (moles of base added per mole of ligand) or ***m*** (moles of base added per mole of metal ion). Calculations were carried with the help of computer programe – BEST[14].

Results and Discussion

Acid dissociation constants

(a) Benzimidazole and substituted benzimidazoles

The free ligand titration curves for the monoprotonated (added one mole of extra acid) form of all the ligands under study, show a steep inflection at a = 1 (where a =

moles of base added per mole of ligand). The dissociation constants (pK_a) were calculated in the region a = 0 to a = 1. For ligands HEB and HMB apart from pK_a, a second dissociation constants pK_{2a} were also calculated in the region a = 1 to a = 2. The dissociation constants for all the ligands were computed from the potentiometric pH profiles of their solutions in the absence of metal ions. The negative logarithms of dissociation constants are listed in Table 1.

Table 1– Acid dissociation constants of different ligands under study (T = 30°C ; μ = 0.1 M KNO_3 ; 20% methanol)

Ligands	pK_a	pK_{2a}	Ligands	pK_a	pK_{2a}
Imidazole	6.94	–	Benzimidazole	5.37	–
Me-Bzm	5.95	–	Pro-Bzm	6.02	–
5,6-Me-Bzm	6.12		HMB	5.40	11.21
HEB	5.47	12.00	OP	6.71	10.62
PP	6.32	8.50	TTP	5.61	8.10

The basicity order of ligands, listed in Table 1, increase in the order Bzm ~ HMB ≤ HEB < Me-Bzm < Pro-Bzm < 5,6-Me-Bzm < Imi. The basicities of Bzm, HMB and HEB are almost similar. The presence of hydroxyl methyl or hydroxy ethyl groups at position 2 in the benzimidazole moiety has no effect on basicity of tertiary nitrogen of benzimidazole. The pK_{2a} (dissociation of proton from hydroxyl group) of HMB, HEB is found to be above 11. The pK_a values obtained in the present investigation agree closely with those recorded in the literature[15]. Introduction of electron donating groups at position 2 (e.g. 2-Me-Bzm, 2-Et-Bzm, etc) or at positions 5 and 6 (e.g. 5,6-dimethyl benzimidazole) makes the tertiary nitrogen of benzimidazole more basic.

(b) Inorganic Phosphates

The free ligand (KH_2PO_4) titration curve of orthophosphate (OP) show an inflection at a = 1, followed by a buffer region in higher pH. The pk_a and pk_{2a} are calculated in the region a = 0 to a = 1 & a = 1 to a = 2 respectively. The free ligand curve of pyrophosphate (PP) taken in diprotonated form ($Na_2H_2P_2O_7$) shows a small inflection at a = 1 followed by a buffer region. Similarly, tripolyphosphate (TPP) in triprotonated form ($Na_3H_2P_3O_{10}$) shows two moderate inflection at a = 1 and a = 2. Acid dissociation constants are calculated using computer program PKS[14] and the values thus obtained are in good agreement with literature values[16-20].

Binary Metal Complexes

(a) Benzimidazole and substituted benzimidazoles

The potentiometric titration curves for the binary 1:1 M^{2+} ligand systems show a single steep inflection at m = 1 (where m = moles of base added per mole of metal ion). The formation constants (log K^{M}_{ML}) for the binary complexes formed were calculated and the values thus obtained are given in Table 2. The potentiometric titration curves for the binary 1:1 [M^{2+}-HMB] or [M^{2+}-HEB] systems show a single inflection at m = 1, indicating a formation of protonated complexes.

Table 2 – Logarithms of stability constants of binary complexes of substituted benzimidazoles [T = 30°C; μ = 0.1 M KNO_3; 20% methanol]

Ligands	Co^{2+}	Ni^{2+}	Cu^{2+}	Zn^{2+}
Imidazole	2.56	3.21	4.28	2.64
Bzm	2.25	2.65	3.28	2.35
Me-Bzm	2.35	2.73	3.46	2.51
5,6-Me-Bzm	2.45	2.82	3.63	2.87
Pro-Bzm	2.19	2.56	2.89	2.27
HMB	2.20	2.23	3.18	2.15
HEB	2.25	2.17	3.25	2.15

The constants are accurate to ± 0.05 logK units

The values of stability constants of HMB and HEB are log K^{M}_{MHL}

The results of the present study (Table 2) show that bzm and its alkylated derivatives form less stable coordination compounds than those of the imidazoles. This is the result of two factors (i) the pK_a of the imidazole is greater than those of the benzimidazole / substituted benzimidazoles under study. (ii) The bulky benzene ring attached to the imidazole system in the benzimidazoles probably decreases their stabilities. Freiser[21] has also suggested that the benzene portion of the benzimidazole or 2-substitued benzimidazoles interfere sterically with chelation.

(b) Benzimidazole vs. substituted benzimidazoles :

The stability constants listed in Table 2 increase in the order: Pro-Bzm < HMB ~ HEB < Bzm < Me-Bzm < 5,6-Me-Bzm < Imi for Cu^{2+} metal ion. This sequence is in

accordance with the basicity order of these ligands except 2-propyl benzimidazole, which show lower stability though it has higher basicity comparatively. This anomaly is due to the steric hinderance caused by the propyl group present at position 2 in 2-propyl benzimidazole. Generally, an alkyl group in sterically blocking positions only decreases the stability of the chelates[22]. Lane[23] showed that benzene portion of the benzimidazole does not cause any significant steric hinderance in planar chelates provided that the coordinating group in the 2-position is small e.g. $-CH_2NH_2$,-CH_2OH,-COOH etc. However, if a bulky group is coordinating, such as the methyl amino methyl, or the o-hydroxy phenyl, this group may be sufficiently large to overlap with the hydrogen in the 4-position and thus cause steric interference.

(c) Inorganic Phosphates

(i) M^{2+}-Orthophosphate: Potentiometric titration curves of M (II)-orthophosphate (diprotonated) in 1:1 ratio shows a inflection at m = 1 followed by a buffer region. The separation of ML curve from the free ligand curve is small suggesting complex formation with low stability constants. The stability constants obtained are presented in Table 3 and are in good agreement with literature values[17].

Orthophosphate can bind to the metal ion with two of its oxygen atoms to form four-member ring leaving another oxygen unbound (whose pK_a is more than 10). But the experimentally observed values (table 3), which are very low, suggest monodentate type of binding using the oxygen (whose pK_a is 6.71), leaving the oxygen (pK_a = less than 2) and another oxygen ($pK_a > 10$) unbound.

(ii) M^{2+}-Pyrophosphate: The ligand pyrophosphate has four oxygen's, which can coordinate to metal ion. Theoretically it is possible to form two four membered and one six membered rings using four oxygen's simultaneously, or with two middle oxygen atoms, it can form a single six membered ring, leaving other two oxygen's uncoordinated to metal ion.

Potentiometric titration curves of M^{2+} -pyrophosphate in 1:1 ratio shows a single inflection at m = 2. pH of metal-ligand titration curve is much lower than the free ligand curve indicating formation of strong complex with high formation constants. Potentiometric titration curves for M^{2+}-pyrophosphate in 1:2 ratio gave a feeble inflection at m = 3 and another one at m = 4. The stability constants of ML_2 are given in Table 3.

(iii) M^{2+}-Tripolyphosphate: Potentiometric titration curve of M^{2+}-tripolyphosphate (in triprotonated form) in 1:1 ratio shows an inflection at m = 3. Metal ligand titration

curve is much more lower than the free ligand curve indicating strong complex formation. The ML complexes are quite stable with large formation constants. However, it is observed that the stability constants of [M-TPP] are lower than the stability constants of [M-PP], though the fact that TPP is a tridentate and would expect to form much more stable complexes.

The stability constants for the mono binary complexes of OP, PP, TPP show that the stability decreases in the order: PP > TPP > OP.

Table 3– Logarithms of stability constants of binary complexes of inorganic phosphates [T = 30 °C, μ = 0.1 M KNO_3; 20% methanol]

Metal ions	OP	Pyrophosphate			Tripolyphosphate		
	MHL	MHL	ML	ML_2	MHL	ML	ML_2
Co^{2+}	2.31	3.50	6.45	2.50	4.92	6.05	2.71
Ni^{2+}	2.32	3.83	6.98	1.60	4.83	6.64	2.60
Cu^{2+}	2.96	5.38	8.60	4.86	5.96	7.94	2.80
Zn^{2+}	2.42	3.80	ppt	ppt	5.10	7.67	2.52

The order of stabilities of 1:1 complexes of these ligands with respect to metal ions [$Cu^{2+} > Ni^{2+} > Zn^{2+} > Co^{2+}$] is in agreement with Irving-William's order[24].

Ternary Metal Complexes

(a) $M^{2+} + PO_4^- +$ Substituted benzimidazoles: The potentiometric titration curves of the ternary complexes involving M^{2+}, PO_4^- and substituted benzimidazoles show a single inflection at m = 2 indicating the simultaneous coordination of PO_4^- and substituted benzimidazoles to the metal ion. The ternary constants are calculated in the buffer region m = 0 to m = 2 using the pKa of PO_4^- and pK_a of substituted benzimidazoles. The values thus obtained are presented in Table 4.

(b) $M^{2+} + P_2O_7^{2-} +$ Substituted benzimidazoles: The potentiometric titration curves of the ternary complexes in 1:1:1 ratio shows an inflection at m = 2 indicating the simultaneous coordination (formation of protonated complexes). The constants are calculated in the buffer region m = 0 to m = 2, using the pK_a of $P_2O_7^{2-}$ and pK_a of substituted benzimidazoles. The values then obtained are presented in Table 4.

(c) M^{2+} + $P_3O_{10}^{3-}$ + Substituted benzimidazoles: The potentiometric titration curves of the ternary complexes in 1:1:1 ratio shows an inflection at m = 3 indicating the simultaneous coordination. The constants are calculated in the buffer region m = 0 to m = 3. The values thus obtained are presented in Table 4.

Table 4– Logarithms of stability constants β^{M}_{MAL} of ternary complexes of bivalent metal ions

[T = 30°C: μ = 0.1 M KNO_3; 20% methanol medium]

Systems	Co^{2+}	Ni^{2+}	Cu^{2+}	Zn^{2+}
	L = Orthophosphate (OP)			
Bzm	4.48 ± 0.05	4.99 ± 0.03	6.26 ± 0.03	4.69 ± 0.07
Me-Bzm	4.61 ± 0.04	5.07 ± 0.04	6.43 ± 0.06	4.85 ± 0.03
5,6-Me-Bzm	4.74 ± 0.08	5.22 ± 0.06	6.64 ± 0.08	5.27 ± 0.08
Pro-Bzm	4.41 ± 0.02	4.84 ± 0.05	5.80 ± 0.06	4.57 ± 0.09
HMB	4.41 ± 0.08	4.44 ± 0.02	5.99 ± 0.05	4.44 ± 0.01
HEB	4.44 ± 0.09	4.36 ± 0.04	6.04 ± 0.06	4.45 ± 0.02
	L = Pryophosphate (PP)			
Bzm	5.77 ± 0.04	6.52 ± 0.06	8.72 ± 0.03	6.17 ± 0.08
Me-Bzm	5.91 ± 0.03	6.62 ± 0.03	8.92 ± 0.06	6.37 ± 0.06
5,6-Me-Bzm	6.03 ± 0.04	6.76 ± 0.06	9.13 ± 0.05	6.74 ± 0.05
Pro-Bzm	5.71 ± 0.08	6.40 ± 0.01	8.37 ± 0.09	6.11 ± 0.03
HMB	5.65 ± 0.01	6.09 ± 0.05	8.62 ± 0.06	5.92 ± 0.04
HEB	5.69 ± 0.06	6.02 ± 0.06	8.67 ± 0.08	5.89 ± 0.02
	L = Tripolyphosphate (TPP)			
Bzm	7.21 ± 0.05	7.54 ± 0.08	9.32 ± 0.04	7.49 ± 0.05
Me-Bzm	7.35 ± 0.04	7.64 ± 0.06	9.54 ± 0.05	7.70 ± 0.06
5,6-Me-Bzm	7.49 ± 0.03	7.80 ± 0.03	9.80 ± 0.08	8.10 ± 0.08
Pro-Bzm	7.16 ± 0.02	7.43 ± 0.02	8.93 ± 0.06	7.43 ± 0.03
HMB	7.15 ± 0.09	7.11 ± 0.08	9.21 ± 0.03	7.29 ± 0.01
HEB	7.19 ± 0.08	7.04 ± 0.06	9.27 ± 0.02	7.30 ± 0.04

The relative stability of the ternary metal complexes (MLA) as compared to that of the correspondent binary complexes have been quantitatively expressed in terms the parameter ΔlogK given by the following equation.

$$\Delta \log K = [\log K^{M}_{MLA} - (\log K^{M}_{MA} + \log K^{M}_{ML})]$$

The obtained values of ΔlogK are reported in Table - 5

Table 5– Comparison of ΔlogK values associated with ternary complexes
[T = 30^{0}C : μ = 0.1 M KNO_3; 20% methanol medium]

Systems	Co^{2+}	Ni^{2+}	Cu^{2+}	Zn^{2+}
		L = Orthophosphate (OP)		
Bzm	-0.08	+0.02	+0.02	-0.08
Me-Bzm	-0.05	+0.02	+0.01	-0.08
5,6-Me-Bzm	-0.02	+0.08	+0.05	-0.02
Pro-Bzm	-0.09	-0.04	-0.05	-0.12
HMB	-0.10	-0.11	-0.15	-0.13
HEB	-0.12	-0.13	-0.17	-0.12
		L = Pryophosphate (PP)		
Bzm	+0.02	+0.04	+0.06	+0.02
Me-Bzm	+0.06	+0.06	+0.08	+0.06
5,6-Me-Bzm	+0.08	+0.11	+0.12	+0.07
Pro-Bzm	+0.02	+0.01	+0.10	+0.04
HMB	-0.05	+0.03	+0.06	-0.03
HEB	-0.06	+0.02	+0.04	-0.06
		L = Tripolyphosphate (TPP)		
Bzm	+0.04	+0.06	+0.08	+0.04
Me-Bzm	+0.08	+0.08	+0.12	+0.09
5,6-Me-Bzm	+0.12	+0.15	+0.21	+0.13
Pro-Bzm	+0.05	+0.04	+0.08	+0.06
HMB	+0.03	+0.05	+0.07	+0.04
HEB	+0.02	+0.04	+0.06	+0.05

The ΔlogK values for ternary complexes containing benzimidazole or substituted benzimidazoles are less negative or positive than the value (-0.2) expected on the statistical grounds reflecting the extensive stabilization of these complexes. This stabilization is due to electrostatic attraction between the negatively charged oxygen's of phosphate oxygen of OP / PP / TPP in the coordination sphere of the metal and positive charge on metal ion.

The stability of the ternary complexes in terms of inorganic phosphate decrease in the order: TPP > PP > OP. The ternary complexes of TPP are more stable than PP due to more electrostatic attraction between TTP^{5-} and positive charge on coordination sphere of the metal ion. Further TPP, though, potentially tridentate may be binding to the metal ion in a tridentate fashion. This is another reason that TPP forms more stable ternary complexes than PP. The ligand, OP has comparatively less negative charges L^{2-} than PP (L^{4-}) or TPP (L^{5-}), hence, it forms least stable complexes.

The sequence of stability of ternary complexes with respect to other ligands decrease, in the order: 5,6 Me-Bzm > Me-Bzm > Bzm ~ Pro-Bzm > HMB ≥ HEB. This trend is in accordance with basicity of ligands and steric hinderance caused by substituents present in position 2.

The stability constants of ternary complexes of bivalent metal ions is in the order: $Cu^{2+} > Ni^{2+} > Co^{2+} < Zn^{2+}$. This order is in conformity with Irving - William's natural order[24] of stabilities.

Distribution Diagrams :

From a knowledge of proton-ligand and metal-ligand formation constants, the distribution of the total metal among the various metal-ligand species as a function of pH has been calculated by a computer program BEST[14]. As a representative case, the distribution diagrams for [Bzm-Cu-OP] and [PP-Ni-Bzm] systems are given in Fig.1 and 2.

[Bzm-Cu-OP]

The maximum percentage of the Cu-Bzm or ML is 61.2 at pH 6.1, as the pH increases the percentage of ML reaches minimum. The other binary species [Cu-OP] has attained maximum percentage of 5.1 at pH 6.6. After pH 5 the formation of ternary complex has started (appearance of curve LMA) and its percentage goes on increasing with increase in pH, with simultaneous decrease in percentage of both binary species (i.e. MA and ML). The ternary species is the only predominant species in higher pH.

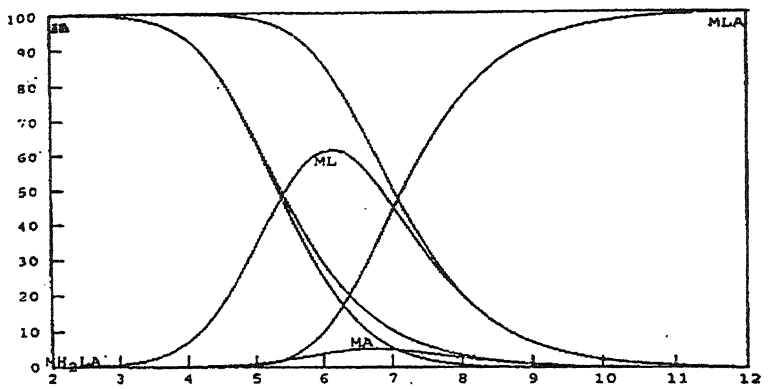

Fig. 1 : Species Distribution Diagram of Bzm-Cu-OP (1:1:1)

[PP-Ni-Bzm]

It is seen that binary complex ML or Ni-Bzm is formed to the extent of 69.5% at pH 6.9. It indicates complexation is taking place in stepwise manner. The maximum formation of binary species, MA is to the extent of 3.6% at pH 7.6 after this pH, the ternary complex is the only species present. It is concluded that up to pH 6.5 there exists only binary species MA (3.6%) and another binary species ML(69.5%). After pH 6.5 the MAL is the only species found.

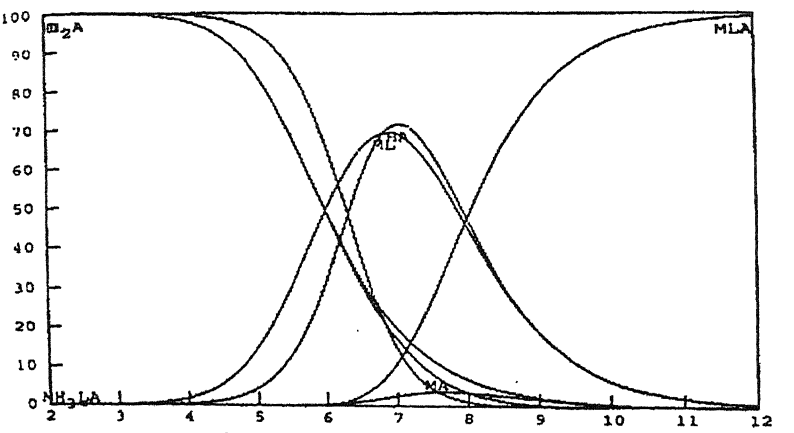

Fig. 2: Species Distribution Diagram of Bzm-Ni-PP (1:1:1)

Acknowledgment

The authors (S.A.H. & G.S.C) thanks the Head, Department of Chemistry, Nizam College for providing necessary research facilities.

References

1. Eichhorn, G.L. & Marzilli, L.G., Eds.(1981) *Adv.Inorg.Biochem*, **3.**
2. Sigel, H., Ed (1979) Met. *Ions Biol. Syst*, **8.**
3. Gellert, R. W. & Bau, R. (1979) *Met. Ions Biol. Syst*, **8** : 1.
4. Martin, R. B. & Mariam, Y.H. (1979), *Met. Ions Biol. Syst*, **8** : 57.
5. Sillen, L.G. & Martell, A.E. Spec Publ. (1964), *Chem. Soc.* No 17.
6. Sigel, H. (1987) *Eur. J. BioChem.* 165 : 65.
7. Sigel, H. (1989) *Pure Appl. Chem.* 61 : 923.
8. Sigel, H. (1990) *Coord Chem. Rev.* 100 :453.
9. Devadas Manwal & Shankaraiah, D., (2000) *Proc. Nat. Acad Sci.*, India **70(A), (II)** :173.
10. Shankaraiah, D. & Devadas Manwal, (2000) *Nat. Acad Sci., letters* **23,** (11,12) :159.
11. Philips, M.A. (1928) *J. Chem. Soc.* **172** : 2397.
12. Flaska, H.A. (1964) EDTA titration's, *Pergamon Press*, N.Y.
13. Schwarzenbach, G (1975) *Complexometric titrations,* Interscience, New York, p.77.
14. Motekaities, R.. & Martell, A.E. (1982) *Can.J.Chem.* (60): **168** :2403.
15. Lane, T.J.C.S.C. & Quinlan, K.P. (1960) *J.Am.Chem. Soc.* **82** : 2994.
16. Srinivas Yogi, D. & Venkataiah, P. (1994) *Indian.J.Chem.*: **33A** :407.
17. Sigel.H, Beker.K. & Mc.Cormick, D.B.(1967) *Bio.Chem.Bio.Phys.* Acta., **148** : 655.
18. Hammer, G.G. & Morrell, M.L. (1964) *J. Am. Chem. Soc.*, **86** : 1497.
19. Johnson, A. & Wannihen, E. (1963) *Talanta* **10** : 769.
20. Ellison, H. & Martel, E. (1964) *J. Inorg. Nucl. Chem.* **26** : 1555.
21. Johnston, W.D. & Fresier, H. (1954) *Anal. Chim. Acta.* **11** : 1.
22. Lane, T.J.C.S.C., Sam, A. & Kandathil, A.J. (1960) *J. Am. Chem. Soc.* **82** : 4462.
23. Lane, T.J.C.S.C. & Thompson, J.W. (1960) *J. Am. Chem. Soc.* **82** : 4179.
24. Irving, H. & Williams, R.J.P. (1953) *J. Chem. Soc.* 3192.

PROC. NAT. ACAD. SCI. INDIA, 73 (A), II, 2003

Mechanistic studies on D-galactose oxidation by quinolinium chlorochromate (QCC) in aqueous acetic acid medium

JAI VEER SINGH** KANCHAN MISHRA and ARCHNA PANDEY*

Department of Chemistry, Dr. H.S. Gour Vishwavidyalay, Sagar 470 003 (M.P.) India.

**For correspondence*

***Department of Chemistry, Nehru College Chhibramau–209721, Kannauj (U.P.) India.*

Received Oct. 17, 2001; Revised April 27, 2002; Accepted July 12, 2002

Abstract

The oxidation kinetics of D-galactose with quinolinium chlorochromate, $C_9H_7NHCrO_3Cl$, have been studied in aqueous acetic acid medium 50% (v/v) in the presence of perchloric acid at constant ionic strength. The reaction under pseudo-first order condition, is first order with respect to both the [oxidant] and the [substrate]. The reaction is markedly catalysed by $[H^+]$ and the effect of $[NaClO_4]$ is negligible. Increasing the dielectric constant of medium decreases the reaction rate. A 1:1 stoichiometry is observed and the reaction did not induce the polymerisation of acrylonitrile. The reaction has been carried out at different temperatures and the variation parameters have been computed. A probable mechanism of the reaction is suggested.

(Keywords : QCC/QCC-galactose intermediate/oxidation/hydride ion transfer)

Introduction

The kinetics of oxidation of reducing sugars which contain a large number of functional groups is of considerable interest from mechanistic point of view and have been fairly well studied[1-10]. Quinolinium chlorochromate[11] adds to the select list of new Cr(VI) reagents introduced recently as an oxidising agent for the effective and selective oxidation of organic substrate under mild conditions. It has been found quite useful as an oxidant synthesis[12,13] and is being increasingly used as an oxidant in kinetic investigation of many compounds[14,15]. D-Galactose plays an important role in carbohydrate chemistry. A survey of literature, however, revealed that no work has

been carried out on the kinetics of oxidation of D-galactose with quinolinium chlorochromate. The study reported in this paper deals with the oxidation kinetics of D-galactose, by quinolinium chlorochromate in aqueous acetic acid 50% (v/v) medium with a view to throw light on the mechanistic aspects of the oxidation process.

Materials and Method

Materials : Quinolinium chlorochromate was safely prepared[12] by a careful addition of quinoline (Loba-chemie) to a solution of chromium trioxide in 6M HCl followed by the filtration of yellow orange crystals. Its purity was checked by estimating Cr(VI) iodometrically. Solution of D-galactose was always freshly prepared in aqueous acetic acid 50% (v/v). The ionic strength was maintained constant with the use of concentrated solution of $NaClO_4$ (B.D.H). Perchloric acid (E-Merck) and all other chemicals were used as such without further purification.

Kinetic measurements : The reaction were performed under pseudo-first order conditions by keeping a large excess the of the [D-galactose] with respect to [QCC]. The medium of the reaction was always 1:1 (v/v) acetic acid-water in the presence of perchloric acid. Kinetic measurements were made on a Systronics 106 Spectrophotometer at 440 nm. The optical density was measured at various intervals of time. Computations of rate constants were made from the plot of log [QCC] against time.

Stoichiometry and product analysis : The stoichiometry of the reaction was performed by conducting the oxidation of D-galactose under the conditions of a known excess of quinolinium chlorochromate. A mixture of D-galactose (0.010 mol dm^{-3}) and QCC (0.10 mol dm^{-3}) was kept for several hours at 30°C for the reaction to go to completion. The unconsumed oxidant was estimated iodometrically at the end of the reaction. The stoichiometry was found to be 1 : 1 consistent with the following equation.

$$C_6H_{12}O_6+C_9H_7NHCrO_3Cl \xrightarrow{H^+} \underset{\text{Arabinose}}{C_5H_{10}O_5}+\underset{\text{Formic acid}}{HCOOH}+C_9H_7NHCl+CrO_2$$

For product analysis a reaction mixture containing D-galactose and quinolinium chlorochromate in the stoichiometric proportion of 1 : 1 was left to equilibrate at 30°C for 24 hours. The reaction mixture was neutralised with $NaHCO_3$, extracted with chloroform, washed with water and dried over anhydrous $MgSO_4$.

The formation of D-arabinose was confirmed by phenylhydrazone formation[16]. The presence of formic acid was confirmed by spot test[17].

Results and Discussion

Empirical rate law : The pseudo-first order rate constants were determined at various initial concentrations of reactants. The results obtained are given in Table 1.

Table 1– Rate constants for oxidation of D-galactose by QCC at 30° C. Solvent : acetic acid-water (50-50% v/v).

$[QCC]x10^3$ (mol dm^{-3})	[D-Galactose]$x10^2$ (mol dm^{-3})	$[H^+]x10$ (mol dm^{-3})	$k_1 \times 10^4$ (sec^{-1})	k_2 ($mol^{-1}dm^3sec^{-1}$)
0.66	1.66	6.13	6.83	–
1.33	1.66	6.13	6.82	–
2.00	1.66	6.13	6.84	–
2.66	1.66	6.13	6.82	–
3.33	1.66	6.13	6.82	–
3.33	0.33	6.13	1.36	4.12
3.33	0.66	6.13	2.70	4.09
3.33	1.00	6.13	4.12	4.12
3.33	1.33	6.13	5.43	4.09
3.33	1.66	6.13	6.82	4.11
3.33	1.66	3.1	3.38	–
3.33	1.66	6.1	6.82	–
3.33	1.66	7.7	8.47	–
3.33	1.66	9.2	10.22	–
3.33	1.66	10.7	11.92	–

Plots for different concentration QCC versus time were linear and the rate constants were independent of initial concentration of QCC, showing first order dependence of the rate on [QCC]. The reaction is first order with respect to [D-

galactose] also. A plot of log k_1 against log [D-galactose] was linear with a slope of unity thereby confirming first order dependence in [D-galactose] (Fig. 1).

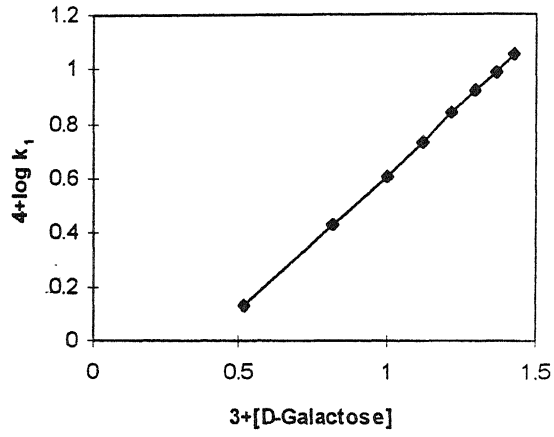

Fig. 1–Plot log k_1 versus log [D-glactose] [QCC]=3.33×10^{-3} mol dm^{-3}; [$HClO_4$]=6.13×10^{-1} mol dm^{-1}; [$NaClO_4$]=1.66×10^{-3};

Rates of oxidation were found to increase with increase in [H^+] and the slopes of the plots of log k_1 versus log [$HClO_4$] was approximately unity showing that reaction is acid catalysed and follows a first order dependence in [$HClO_4$] (Fig. 2).

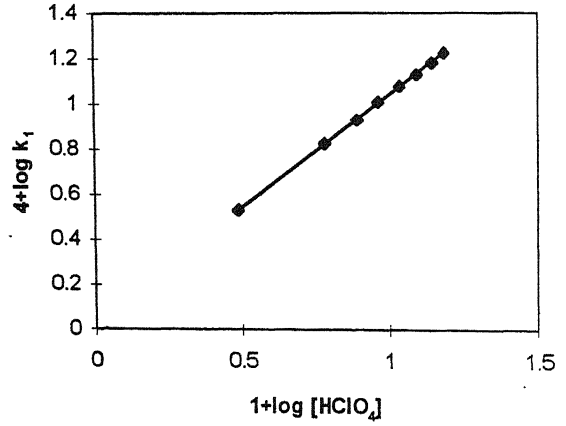

Fig. 2–Plot log k_1 versus log [H^+] [QCC]=3.33×10^{-3} mol dm^{-3}; [D-galactose]=1.66×10^{-2} mol dm^{-3} [$NaClO_4$]=1.66×10^{-1}; mol dm^{-3}; Solvent : acetic acid-water (50-50% (v/v/); temperature = 30°C.

Consequently the empirical rate law is described as follows :

$$-\frac{d[QCC]}{dt} = k_{obs}[D\text{-}Galactose][HClO_4]$$

Effect of ionic strength : The reaction rate was not influenced by ionic strength when $NaClO_4$ was initially added to the reaction mixture over the range of $0.66x10^{-1}$ to $4.00x10^{-1}$mol dm^{-3}. Similar observations were also reported in the oxidation of diols by PCC[18] and chromic acid[19].

Effect of radical-forming agent : When the reaction was initiated by adding a radical scavanger, acrylonitrile, into a solution containing D-galactose and QCC, no retardation in the rate was observed. No turbidity due to the polymerisation of acrylonitrile was observed. Thus the formation of radical intermediate is ruled out in the course of the reaction.

Effect of solvent : The reaction has been studied under varying composition of acetic acid-water mixture. It has been observed that the reaction rate increases with the increase of solvent (CH_3COOH) in acetic acid-water mixture. (Table 2 and Fig. 3).

A linear plot between log k_1 and 1/D (inverse of dielectric constant)[20] with a positive slope suggesting an interaction between an ion and a dipole[21].

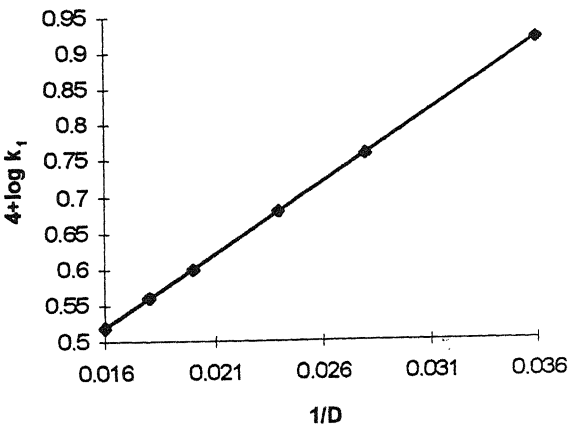

Fig. 3–Plot log k_1 versus log 1/D [QCC]=$3.33x10^{-3}$ mol dm^{-3}; [D-galactose]=$1.66x10^{-2}$ mol dm^{-3}; [$HClO_4$]=$6.13x10^{-1}$; mol dm^{-3}; [$NaClO_4$]=$1.66x10^{-1}$ mol dm^{-3}; temperature=25°C

Table 2– Dependence of rate on solvent composition

[QCC] = 3.33 x 10^{-3} mol dm^{-3}; [D-galactose] = 1.66 x 10^{-2} mol dm^{-3}; [$HClO_4$] = 6.13 x 10^{-1} mol dm^{-3}; [$NaClO_4$] = 1.66 x 10^{-1} mol dm^{-3}; [$NaClO_4$] = 1.66 x 10^{-1} mol dm^{-3}; Temperature – 25°C.

CH_3COOH :	H_2O (v/v)	1/D	k_1 x 10^4 (sec^{-1})
20	80	0.016	3.28
30	70	0.018	3.58
40	60	0.020	4.02
50	50	0.024	4.84
60	40	0.028	5.82
70	30	0.036	8.23

Effect of temperature : The reaction rates at different temperatures were determined and the values of activation parameters were calculated from the slope of linear plot of lg k_1 versus T^{-1}. The data are presented in Table 3. A perusal of data (Table 3) shows that these reactions are characterised by a high negative value of entropy of activation ($\Delta S^{\neq}$). It indicates that solvation effects are predominant in the reaction, which suggests the formation of a charged and rigid intermediate state. Further, the high positive value of energy of activation and enthalpy of activation indicate that intermediate is highly solvated.

Table 3– Temperature dependence and activation parameters of the oxidation of D-galactose by QCC.

[D-galactose] = 1.66 x 10^{-2} mol dm^{-3}; [QCC] = 3.33 x 10^{-3} mol dm^{-3}; [$HClO_4$] = 6.13 x 10^{-1}; [$NaClO_4$] = 1.66 x 10^{-1} mol dm^{-3};

Solvent : acetic acid – water (50-50% v/v)

Temperature (°C)	k_1 x 10^4 (sec^{-1})	Ea kJ mol^{-1}	$\Delta H^{\neq}$ kJ mol^{-1}	$\Delta G^{\neq}$ kJ mol^{-1}	$-\Delta S^{\neq}$ JK^{-1} mol^{-1}
20	3.28	–	53.17	91.28	130.06
25	4.84	54.26	53.13	91.31	130.14
35	9.88	58.10	53.05	93.25	130.53
40	14.29	–	53.01	93.85	130.47

Aldoses in aqueous acidic solution exist as equilibrium mixture of α – and β–pyranose (Scheme 1)[22]. The equilibrium mixture of D-galactose mainly consist of β-

anomer with equitorial orientation of the glycosidic hydroxyl group. The β-anomer is supposed to be more reactive species[23].

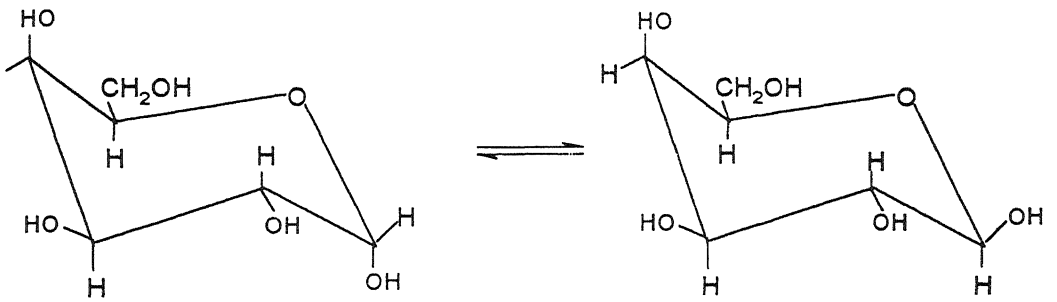

Scheme 1

An increase in the oxidation rate with acidity suggests protonation of QCC species. This protonated QCC interacts with the substrate in the rate determining step. Involvement of such species is well known in chromic acid oxidation[24].

The oxidation of D-galactose may be assumed to follow the direct hydride ion transfer of the axial anomeric proton of β-galactose as shown in Scheme 2.

However, UV spectra recorded did not show the existence of intermediate complex formation. It indicates the instability of intermediate (Fig. 4).

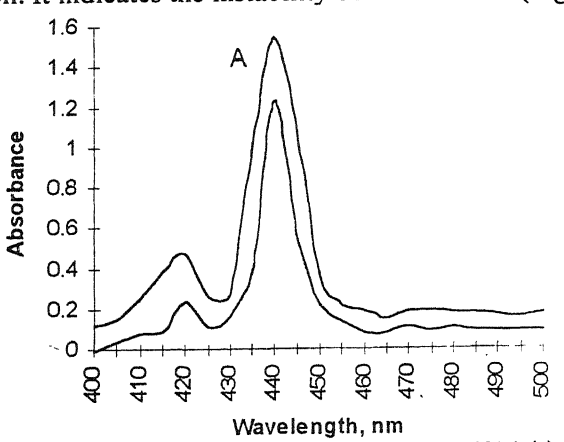

Fig. 4–Electronic spectra of QCC in aqueous acetic acid 50% (v/v) (A) and QCC in aqueous acetic acid 50% (v/v) with D-galactose.

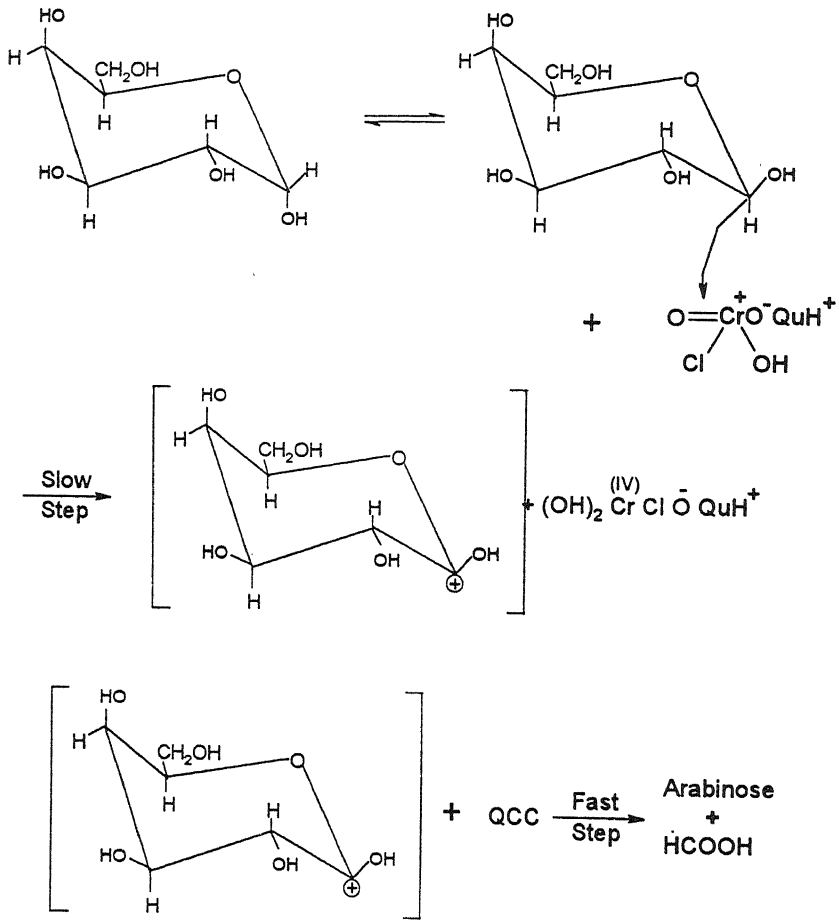

Scheme 2

Rate Law–

$$QCC + H^+ \underset{K_2}{\overset{K_1}{\rightleftharpoons}} QCCH^+ \qquad (1)$$

$$QCCH^+ + S \xrightarrow{k_1} I + Cr(IV) \quad (2)$$

$$I + QCC \xrightarrow{Fast} Products \quad (3)$$

$$Rate = -\frac{d[QCCH^+]}{dt} \alpha [QCCH^+][S] = k_1[QCCH^+][S]$$

$$Rate = k_1 [QCCH^+] [S] \quad (4)$$

Applying law of mass action to equation (1) we get,

$$K_1 = \frac{[QCC\,H^+]}{[QCC][H^+]}$$

$$[QCC\ H^+] = K_1\ [QCC]\ [H^+] \quad (5)$$

substituting the value of $[QCCH^+]$ from equation (5) into equation (4)

$$Rate = k_1K_1\ [QCC]\ [H^+]\ [S]$$

$$= kobs\ [QCC]\ [H^+]\ [S]$$

Conclusion

The oxidation of D-galactose by QCC in aqueous acetic acid medium proceeds via hydride ion transfer mechanism involving specific cleavage of C_1-C_2 bond of the substrate to give the products.

References

1. Kasper, E. (1963) *Z. Physik. Chem. (Leipzig).* **224** : 427.
2. Modi, A. P. & Ghosh, S. (1969) *J. Indian Chem. Soc.* **46** : 687.
3. Mishra, S. P. & Gupta, K. C. (1974) *J. Indian Chem. Soc.* **51** : 145.
4. Sen Gupta, K. K. & Basu, S. N. (1979) *Carbohydrate Res.* **72** : 39.
5. Anand, F. & Shrivastava, A. (1982) *Carbohydrate Res.* **102** : 23.

6. Capon, B. (1969) *Chem Rev.* **69** : 407.
7. Bhatnagar R. P. & Fandis, A. G. (1986) *J. Sci. & Ind. Res.* **45** : 90.
8. Varadarajan, R. & Dhar, R. K. (1986) *Indian J. Chem.*, **25A** : 474.
9. Virtanen, P.O.I., Lindroos-Heinanen R. (1988) *Acta Chem. Scand., Ser.* **42B** : 411.
10. Signorella, S., Daier, V., Garcia, S., Cargnello, R., Gonzalez, J. C. Rizzotto, M., Sale, L. F. (1999) *Carbohydrate Res.*, **316** : 14.
11. Singh, J., Kalsi, P. S., Jawanda, G. S., Chhabra, B. R. (1986) *Chem. & Ind.* : 751.
12. Srinivasan, R., Ramesh, C. V., Madhulatha, W., Balasubramanian, K. (1996) *Indian J. Chem.* **35B** : 480.
13. Singh, J., Kad, G. L., Shikha, V., Sharma, M., Chhabra, B. R. (1997) *Indian J. Chem* **36B** : 272.
14. Jameel, A. A. (1999) *J. Indian Chem. Soc.* **76** : 263.
15. Karthikeyan, G., Elango, K. P., Karnukaran, K., Balasubramanian, A. (1998) *Oxid. Commun.* **21(1)** : 51.
16. Honda, S., Takiura, K. (1975) *Anal Chim Acta* **77** : 125.
17. Feigl, F. (1960) : *Spot test in Organic Chemistry*, Elsevier. Amsterdam, p. 347.
18. Agrawal, G. L., Jha, S. (1989) *Revue Roumaine de Chimie* **34** : 1769.
19. Radhakrishnamurty, P.S. (1971) *Ind. J. Chem.*, **19** : 41.
20. Lange, N. A. (1956) *Hand book of Chemistry* (9^{th} Ed.) Mc Graw Hill, New York.
21. Amis, E. S. (1965) *Solvent effects on Reaction Rates and Mechanism,* Academic Press, New York, p. 42.
22. Wolfrom, M. L., Staurt, R. S. (1969) *Adv. Carbohydrate Chemistry and Biochemistry,* **24** : 13.
23. Perlen, A. S. (1964) *Can. J. Chem.*, **42** : 2365.
24. Wiberg, K. B. (1965) *Oxidation in Organic Chemistry* Part A. Academic Press London. p. 69.

PROC. NAT. ACAD. SCI. INDIA, 73 (A), I, 2003

Generalized Sobolev type spaces

R.S. PATHAK and K.K. SHRESTHA

Department of Mathematics, Banaras Hindu University, Varanasi-221 005, U.P., India.

Department of Mathematics, P.N. Campus (Tribhuvan University), Pokhara, Kaski, Nepal.

Received March 1, 2000; Accepted May 9, 2001

Abstract

The spce $G^{p,s}_{\omega,\mu}$ is defined as a generalization of space $G^{p,s}_{\mu}$. Its properties including completeness and inclusion are studied. It is shown that the space H^{μ}_{ω} is dense in $G^{p,s}_{\omega,\mu}$. The generalized Hankel Potential H^{m}_{μ} is defined and its properties are studied. The L^p-space of all such Hankel potentials, denoted by $W^{m,p}_{\omega,\mu}$, is defined. It is proved that the space $W^{m,p}_{\omega,\mu}$ is a Banach space. It is also proved that the generalized Hankel potential H^{t}_{μ} is an isometry of $W^{m,p}_{\omega,\mu}$ onto $W^{m+t,p}_{\omega,\mu}$.

(**Keywords :** Sobolev type space/generalized Hankel potential/Beurling type ultradistribution/ Pseudo-differential operator/Hankel transform).

Introduction

Let ω be a continuous real valued function defined on $I = (0, \infty)$ satisfying the following conditions :

(α) $\quad 0 \leq \omega(\xi + \eta) \leq \omega(\xi) + \omega(\eta)\ \forall\ \xi, \eta \in I$

(β) $\quad \int_0^{\infty} \omega(\xi) / (1 + \xi^2)\, d\xi < \infty$.

Sometimes we assume the following condition also :

(γ) $\omega(\xi) \geq a + b \log (1 + \xi)$, $\xi \in I$, for some real number a, and $b > 0$.

The class of all ω satisfying (α) – (γ) will be denoted by M.

Clearly, $\omega(\xi) = \log (1 + \xi)$, $\xi > 0$ and $\omega(\xi) = \xi^{\alpha}$, $\xi > 0$, $0 < \alpha < 1$,

satisfy (α) – (γ).

From (γ) it follows that

$$\xi \leq \exp(-a/b + \omega(\xi)/b), \xi > 0.$$

Let $(h_\mu u)(\xi) = \tilde{u}(\xi)$ denote the Hankel transform of $u \in L(0, \infty)$ defined by

$$\tilde{u}(\xi) = (h_\mu u)(\xi) = \int_0^\infty (x\xi)^{1/2} J_\mu(x\xi)\, u(x)\, dx$$

Then the space $H_\omega^\mu(I)$ is defined to be the set of all complex-valued infinitely differentiable functions ϕ on I such that

$$\gamma_{\lambda,\kappa}^\mu(\phi) = \sup_{x \in I} | e^{\lambda\omega(x)} (x^{-1} d/dx)^k (x^{-\mu-1/2} \phi(x)) | < \infty$$

and

$$\rho_{\lambda,k}^\mu(\tilde{\phi}) = \sup_{\xi \in I} | e^{\lambda\omega(\xi)} (\xi^{-1} d/d\xi)^k (\xi^{-\mu-1/2} \tilde{\phi}(\xi)) | < \infty.$$

Clearly, $h_\mu(H_\mu^\omega) = H_\mu^\omega$. For $\omega(x) = \log(1+x)$, $H_\omega^\mu(I) = H_\mu(I)$, the Zemanian – space[1]. The dual of H_ω^μ well be denoted by $(H_\omega^\mu)'$ which consists of all Hankel transformable Beurling type ultradistributions.

We shall make use of the function space $L_\mu^p(0, \infty)$, $1 \leq p < \infty$, which consists of all those real measurable functions on $(0, \infty)$ for which

$$\|f\|_p = \left(\int_0^\infty |f(x)|^p \, d\sigma(x) \right)^{1/p} < \infty,$$

where

$$d\sigma(x) = (2^\mu \Gamma(\mu+1))^{-1} x^{2\mu+1} dx.$$

A tempered distribution u belongs to the Sobolev space $H^s(\boldsymbol{R}^n)$, $s \in \boldsymbol{R}$, if its Fourier transform corresponds to a locally square integrable function such that

$$\| u \|_{H^s} = \left(\int_{I\!R^n} (1 + |\xi|^2)^s |\hat{u}(\xi)|^2 \right) d\xi \Big)^{1/2}$$

It has been generalized to H_ω^s by Pahk and Kang[2] using ultradistribution theory of Beurling and Bjorck. It has been further generalized to $H_\omega^{s,p}$, $1 \le p < \infty$, by Pathak[3]. The Sobolev type space $G_\mu^{p,s}$, $s \in \boldsymbol{R}$, $1 \le p < \infty$ was introduced by Pathak and Pandey[4] using Hankel transformations.

In this paper a space $G_{\omega,\mu}^{p,s}$ is defined as a generalization of the space $G_\mu^{p,s}$. It is shown that for $s \in \boldsymbol{R}$, $\mu \ge -1/2$, $1 \le p < \infty$, the space $G_{\omega,\mu}^{p,s}$ is complete. Moreover, the generalized Hankel Potential H_μ^m is defined and its properties are studied. The L^p-space of all such Hankel potentials, denoted by $W_{\omega,\mu}^{m,p}$, is defined. It is proved that the space $W_{\omega,\mu}^{m,p}$ is a Banach space. It is also shown that the generalized Hankel potential H_μ^t is an isometry of $W_{\omega,m}^{m,p}$ onto $W_{\omega,\mu}^{m+t,p}$.

The Generalized Sobolev type space $G_{\omega,\mu}^{p,s}$

Definition 1 : For $s \in \boldsymbol{R}$, $\mu \in \boldsymbol{R}$, $1 \le p < \infty$, the generalized Sobolev type space $G_{\omega,\mu}^{p,s}$ is the set of all ultradistributions $u \in (H_\omega^\mu)'$ such that its Hankel transform $h_\mu u$ corresponds to a locally integrable function over $I = (0, \infty)$ for which

$$\| u \|_{G_{\omega,\mu}^{p,s}} = \| e^{s\omega(\xi)} h_\mu u(\xi) \|_p .$$

For $\omega(\xi) = \log(1 + \xi)$, the space $G_{\omega,\mu}^{p,s}$ reduces to the space $G_\mu^{p,s}$.

Theorem 1 : The space $G_{\omega,\mu}^{p,s}$, $1 \le p < \infty$, $s > 0$, is complete.

Proof. Let $\{u_k\}$ be a Cauchy sequence in $G_{\omega,\mu}^{p,s}$. Then $\{e^{s\omega(\xi)}(h_\mu u_k)(\xi)\}$ is a Cauchy sequence in L^p. Since L^p is complete, therefore there exists a function $f \in L^p$ such that

$$e^{s\omega(\xi)} (h_\mu u_k)(\xi) \to f \text{ in } L^p \text{ as } k \to \infty. \tag{1}$$

Set
$$g(\xi) = e^{-s\omega(\xi)} f(\xi), \qquad s > 0 \tag{2}$$

Clearly, $g(\xi) \in (H_\omega^\mu)'$. Therefore its inverse Hankel transform exists. Now (2) gives

$$e^{s\omega(\xi)}\, g(\xi) \;=\; e^{s\omega(\xi)}\, h_\mu\, (h_\mu^{-1}\, g)\, (\xi) \in L^p\,.$$

Therefore, by Definition 1, $h_\mu^{-1}\, g \in G^{p,\,s}_{\omega,\,\mu}$.

Let $h_\mu^{-1}\, g = u$. Then

$$e^{s\omega(\xi)}\, (h_\mu\, u)\, (\xi) = e^{s\omega(\xi)}\, (h_\mu\, (h_\mu^{-1}\, g)\, (\xi) = e^{s\omega(\xi)}\, g(\xi) = f(\xi)$$

Now it follows from (1) that

$$u_k \;\to\; u \;\text{ in }\; G^{p,\,s}_{\omega,\,\mu}$$

This proves the theorem.

Theorem 2 : For $t > r$, $G^{p,\,t}_{\omega,\,\mu} \subseteq G^{p,\,r}_{\omega,\,\mu}$ and the inclusion map is continuous.

Proof. For $u \in G^{p,\,t}_{\omega,\,\mu}$ and $t \geq r$, we have $t = r + \varepsilon$, $\varepsilon \geq 0$.

Now,

$$\| u \|_{G^{p,\,t}_{\omega,\,\mu}} \;=\; \| e^{t\omega(\xi)}\, (h_\mu\, u)\, (\xi) \|_p \tag{3}$$

Since $$\left(\int_0^\infty | e^{r\omega(\xi)}\, (h_\mu\, u\, (\xi)\, |^p \; d\xi \right)^{\frac{1}{p}} \leq \left(\int_0^\infty | e^{(r+\varepsilon)\omega(\xi)}\, (h_\mu\, u\, (\xi)\, |^p \; d\xi \right)^{\frac{1}{p}};$$

we have

$$\| u \|_{G^{p,\,r}_{\omega,\,\mu}} \;\leq\; \| u \|_{G^{p,\,t}_{\omega,\,\mu}} \qquad \forall\; u \in G^{p,\,t}_{\omega,\,\mu}$$

Hence $G^{p,\,t}_{\omega,\mu} \subseteq G^{p,\,r}_{\omega,\,\mu}$.

Again let $\{u_k\} \to 0$ in $G^{p,\,t}_{\omega,\mu}$ then

$\{u_k\} \to 0$ in $G^{p,\,r}_{\omega,\,\mu}$.

This proves the continuity of inclusion.

Theorem 3 : The space H_{ω}^{μ} is dense in $G_{\omega,\mu}^{p,s}$.

Proof. Let $u \in G_{\omega,\mu}^{p,s}$. Then $e^{s\omega(\xi)}\,(h_{\mu}\,u)\,(\xi) \in L^{p}$. Since D is dense in L^{p}, there exists a sequence $\{\phi_j\}$ of functions belonging to D such that

$$\phi_{j(\xi)} \to e^{s\omega(\xi)}\ (h_{\mu}\,u)\,(\xi) \ \text{ in } \ L^{p}\,.$$

Define $$\psi_j\,(x) \;=\; h_{\mu}^{-1}\ (e^{-s\omega(\xi)}\,\phi_j)^{(x)}$$

Since $\phi_j \in D$, therefore $e^{-s\omega(\xi)}\,\phi_j \in D$; D being a subspace of H_{ω}^{μ}, $e^{-s\omega(\xi)}\,\phi_j$ also belongs to H_{ω}^{μ}. Hence its inverse Hankel transform exists; so that $\psi_j \in H_{\omega}^{\mu}$. Now,

$$\|\,\psi_j - u\,\|_{G_{\omega,\mu}^{p,s}} = \|\,e^{s\omega(\xi)}\,(h_{\mu}\,(\psi_j - u))\,(\xi)\,\|_{p}$$

$$= \|\,\phi_j - e^{s\omega(\xi)}\,(h_{\mu}\,u)\,(\xi)\,\|_{p} \to 0 \qquad \text{as } j \to \infty\,;$$

so that

$$\psi_j \to u \quad \text{in} \quad G_{\omega,\mu}^{p,s}$$

The following lemma will be used in the sequel.

Lemma 1 : For three real numbers s_1 , s and s_2 satisfying $s_1 < s < s_2$ and $\forall \varepsilon > 0$ there exists $C\,(\varepsilon) > 0$ such that

$$e^{s\omega(\xi)} \le \varepsilon\, e^{s_2\omega(\xi)} + C\,(\varepsilon)\, e^{s_1\omega(\xi)} \tag{4}$$

Proof. For $\rho = e^{\omega(\xi)}$ and $C\,(\varepsilon) = \varepsilon^{-\left(\frac{s-s_1}{s_2-s}\right)}$ as in Chazaran and Piriou[5], we have

$$\rho^{s} \le \varepsilon\rho^{s_2} + \varepsilon^{-\left(\frac{s-s_1}{s_2-s}\right)}\rho^{s_1}$$

i.e. $$1 \leq \varepsilon \rho^{s_2 - s} + \varepsilon^{-\left(\frac{s - s_1}{s_2 - s}\right)} \rho^{s_1 - s} \tag{5}$$

Put $k = \varepsilon^{\frac{1}{s_2 - s}}$. Then, by the inequality (5) we get

$$1 \leq (k\rho)^{s_2 - s} + (k\rho)^{s_1 - s}$$

If $k\rho \geq 1$, then we have $(k\rho)^{s_2 - s} \geq 1$. Hence the inequality is satisfied.

If $k\rho < 1$, then $k\rho^{s_1 - s} \geq 1$ so that the inequality is true in this case also

This proves the Lemma.

Theorem 4 : Let s_1, s and s_2 be three real numbers satisfying $s_1 < s < s_2$.

Then $\forall \varepsilon > 0$, there is a positive number $C(\varepsilon)$ such that

$$\| u \|_{G^{p,s}_{\omega,\mu}} \leq \varepsilon \| u \|_{G^{p,s_2}_{\omega,\mu}} + C(\varepsilon) \| u \|_{G^{p,s_1}_{\omega,\mu}} \qquad \forall u \in G^{p,s_2}_{\omega,\mu}$$

Proof. If $u \in G^{p,s_2}_{\omega,\mu}$, then by Theorem 2, we have

$$u \in G^{p,s}_{\omega,\mu} \text{ and } u \in G^{p,s_1}_{\omega,\mu}.$$

Now,

$$\| u \|_{G^{p,s}_{\omega,\mu}} = \left(\int_0^\infty | e^{s\omega(\xi)} (h_\mu u)(\xi) |^p \, d\xi \right)^{\frac{1}{p}}$$

By Lemma 1, $\forall \varepsilon > 0$, there exists a $C(\varepsilon) > 0$ such that for all $p \geq 1$ we have

$$\| u \|_{G^{p,s}_{\omega,\mu}} \leq \varepsilon \left(\int_0^\infty e^{ps_2\omega(\xi)} | (h_\mu u)(\xi) | \, d\xi \right)^{\frac{1}{p}} + C(\xi) \left(\int_0^\infty e^{ps_1\omega(\xi)} | (h_\mu u)(\xi) |^p \, d\xi \right)^{\frac{1}{p}}$$

so that

$$\| u \|_{G^{p,s}_{\omega,\mu}} \leq \varepsilon \| u \|_{G^{p,s_2}_{\omega,\mu}} + C(\varepsilon) \| u \|_{G^{p,s_1}_{\omega,\mu}}$$

Theorem 5 : For $s < 0$, $L^2(I) \subset G^{2,s}_{\omega,\mu}$.

Proof. Let $u \in L^2(I)$. Then from Macauley-Owen[6], we have

$$\| h_\mu u \|_{L^2} = \| u \|_{L^2}.$$

Now,

$$\| u \|_{G^{2,s}_{\omega,\mu}} = \| e^{s\omega(\xi)} (h_\mu u)(\xi) \|_{L^2}$$

$$= \left(\int_0^\infty | e^{s\omega(\xi)} (h_\mu u)(\xi) |^2 d\xi \right)^{1/2} \leq \| h_\mu u \|_{L^2} \leq K \| u \|_{L^2}$$

for some constant K; so that $u \in G^{2,s}_{\omega,\mu}$.

For s=0, p=2, the space $G^{2,0}_{\omega,\mu}$ is identical with L^2 (I).

Example 1 : For $a \in \boldsymbol{R}$, let δ_a be defined by

$$< \delta_a, \phi > = \phi(a) \qquad \forall \phi \in H^\mu_\omega, \omega \in M.$$

Then

$$\delta_a \in G^{p,s}_{\omega,\mu} \qquad \text{for } s < -1/(pb).$$

Indeed, we have

$$(h_\mu \delta_a)(\xi) = \sqrt{\xi a}\, J_\mu(\xi a);$$

so that

$$\| e^{s\omega(\xi)} (h_\mu \delta_a)(\xi) \|_p = \| e^{s\omega(\xi)} \sqrt{\xi a}\, J_\mu(\xi a) \|_p$$

$$= \left(\int_0^\infty e^{ps\omega(\xi)} \mid \sqrt{\xi a}\, J_\mu (\xi a) \mid^p d\xi \right)^{1/p}.$$

Since $\mid \sqrt{\xi a}\, J_\mu (\xi a) \mid$ is bounded by B_μ, the last integral is bounded by

$$B_\mu \int_0^\infty e^{sp\omega(\xi)}\, d\xi$$

$$\leq B_\mu \int_0^\infty e^{sp[a + b \log(1+\xi)]}\, d\xi, \qquad \text{by property } (\gamma)$$

$$\leq B_\mu\, e^{psa} \int_0^\infty (1+\xi)^{psb}\, d\xi$$

The ξ-integral is convergent for $s < -1/(pb)$.

The Generalized Hankel potential

Let $a(x) \neq 0$ be a multiplier in H_ω^μ such that

$$h_\mu^{-1}\ (a^{-m})\ (\xi) \in L^1\ (0, \infty)\ \forall\ m = 0, 1, 2\ \ldots\ldots \tag{6}$$

Then, for $f \in (H_\omega^\mu)'$ we define the products fa^m and $fa^{-m} \in (H_\omega^\mu)'$ by the following relations.

$$< fa^m, \phi > = < f, a^m \phi > \qquad \forall\ \phi \in H_\omega^\mu \tag{7}$$

and

$$< fa^{-m}, a^m \phi > = < f, \phi > \qquad \forall\ \phi \in H_\omega^\mu \tag{8}$$

where m is a non-negative integer.

Now, the generalized Hankel potential is defined by

$$\mathbf{H}_\mu^m = h_\mu^{-1}\ (a^{-m}\ (h_\mu\, u)) \qquad \forall\ u \in (H_\omega^\mu)' \tag{9}$$

Since the generalized Hankel transformation h_μ' is a continuous linear mapping of $(H_\omega^\mu)'$ onto $(H_\omega^\mu)'$, the same being true for $(h_\mu')^{-1}$, we conclude that the generalized Hankel potential defined by (9) is a continuous linear mapping of $(H_\omega^\mu)'$ onto $(H_\omega^\mu)'$ for all $m \in \boldsymbol{Z}$. Also

$$(\mathbf{H}_\mu^m u)(x) = \int \sqrt{x\xi}\, J_\mu(xxi)\, a^{-m}(\xi)\, (h_\mu u)(\xi)\, d\xi.$$

This shows that the generalized Hankel potential is a pseudo-differential operator with symbol a^{-m}. For $a(x) = (1 + x^2)^{h/2}$, $h \in \boldsymbol{R}$, (9) reduces to

$$(\mathbf{H}_\mu^s u)(x) = h_\mu^{-1}\left((1 + \xi^2)^{-s/2}\, (h_\mu u)(\xi)\right)(x) \qquad \text{for } s = mh$$

which is the Hankel potential investigated by Pathak and Pandey[4].

Theorem 6 : Let $u \in (H_\omega^\mu)'$. Then for $m, l \in \mathbf{Z}$ we have

(i) $\mathbf{H}_\mu^m\, \mathbf{H}_\mu^l\, u = \mathbf{H}_\mu^{m+l}\, u$

(ii) $\mathbf{H}_\mu^0\, u = u.$

Proof. For $u \in (H_\omega^\mu)'$ we have

$$\begin{aligned}
\mathbf{H}_\mu^m\, \mathbf{H}_\mu^l\, u &= h_\mu^{-1}\,(a^{-m}\, h_\mu\, (\mathbf{H}_\mu^l\, u)) \\
&= h_\mu^{-1}\,(a^{-m}\, h_\mu\, (h_\mu^{-1}\,(a^{-l}\, h_\mu\, u))) \\
&= h_\mu^{-1}\,(a^{-(m+l)}\, h_\mu\, u) \\
&= \mathbf{H}_\mu^{m+l}\, u.
\end{aligned}$$

This proves the first part. For the second part, we have

$$\mathbf{H}_\mu^0\, u = h_\mu^{-1}\,(a^0\, h_\mu\, u) = u.$$

THE SPACE $W_{\omega,\mu}^{m,p}$

For $m \in \mathbf{Z}$ and $1 < p < \infty$, the space $W_{\omega,\mu}^{m,p}(0, \infty)$ is the set of all those ultradistributions $u \in (H_\mu^m)'$ for which

$$y^{-\mu-1/2} H_\mu^{-m} u \in L_\mu^p.$$

The norm of this space is given by

$$\| u \|_{m,p,\omega,\mu} = \| y^{-\mu-1/2} H_\mu^{-m} u \|_p .$$

Theorem 7 : The space $W_{\omega,\mu}^{m,p}(0, \infty)$ is a Banach space with respect to the norm

$$\| \|_{n,p,\omega,\mu} .$$

Proof. Let $\{u_k\}$ be a Cauchy sequence in $W_{\omega,\mu}^{m,p}(0, \infty)$. Then $\left\{y^{-\mu-1/2} \mathbf{H}_\mu^{-m} u_k\right\}$ is a Cauchy sequence in L_μ^p. Since L_μ^p is complete, there exists a function $u \in L_\mu^p$ such that

$$y^{-\mu-1/2} \mathbf{H}_\mu^{-m} u_k \to u \text{ in } L_\mu^p \text{ as } k \to \infty . \tag{10}$$

Let $v = \mathbf{H}_\mu^m \; y^{\mu+1/2} u$. Then

$$\mathbf{H}_\mu^{-m} v = y^{\mu+1/2} u \text{ or } y^{-\mu-1/2} \mathbf{H}_\mu^{-m} v = u.$$

Hence $v \in W_{\omega,\mu}^{m,p}$.

From (10) it follows that $u_k \to v$ in $W_{\omega,\mu}^{m,p}$ as $k \to \infty$.

Theorem 8 : The generalized Hankel potenial $\mathbf{H}_\mu^t$ is an isometry of

$W^{m,p}_{\omega,\mu}(0,\infty)$ onto $W^{m+t,p}_{\omega,\mu}(0,\infty)$; and we have

$$\| \mathbf{H}^t_\mu \phi \|_{m+t,p,\omega,\mu} = \| \phi \|_{m,p,\omega,\mu}$$

Proof. For $\phi \in W^{m,p}_{\omega,\mu}(0,\infty)$, we have

$$\| \mathbf{H}^t_\mu \phi \|_{m+t,p,\omega,\mu} = \| y^{-\mu-1/2} \mathbf{H}^{-(m+t)}_\mu H^t_\mu \phi \|_p$$

$$= \| y^{-\mu-1/2} \mathbf{H}^{-m}_\mu \phi \|_p$$

$$= \| \phi \|_{m,p,\omega,\mu}.$$

Again let $v \in W^{m,p}_{\omega,\mu}$. Then

$$y^{-\mu-1/2} \mathbf{H}^{-(m+t)}_\mu v \in L^p_\mu,$$

$$y^{-\mu-1/2} \mathbf{H}^{-m}_\mu \mathbf{H}^{-t}_\mu v \in L^p_\mu;$$

so that $\mathbf{H}^{-t}_\mu \phi \in W^{m,p}_{\omega,\mu}$ and

$$\mathbf{H}^t_\mu \ \mathbf{H}^{-t}_\mu v = v.$$

That is, for each v in $W^{m+t,p}_{\omega,\mu}$, there exists an $\mathbf{H}^{-t}_\mu \ v \in W^{m,p}_{\omega,\mu}$ such that

$\mathbf{H}^t_\mu \ \mathbf{H}^{-t}_\mu v = v$. Hence, $\mathbf{H}^t_\mu$ is onto.

Theorem 9 : For $1 < p < \infty$, $m = 0, 1, 2, \ldots$,

$$\| y^{-\mu-1/2} \mathbf{H}^m_\mu \phi \| \le C \| t^{-\mu-1/2} \phi \|_p \ \forall \ \phi \in H^m_\omega.$$

In the sequel we shall need the following lemmas.

Lemma 2 : If $f, \ g \in L^1_\mu(0,\infty)$, then

$$(f \# g)\hat{}(x) = \hat{f}(x)\,\hat{g}(x), \qquad 0 < x < \infty, \tag{11}$$

where

$$\hat{f}(x) = \int_0^\infty j(x\,t)\,f(t)\,d\sigma(t) \tag{12}$$

and

$$j(x) = 2^\mu\,\Gamma(\mu+1)\,x^{-\mu}\,J_\mu(x).$$

The poof of this lemma is given by Haimo[7].

Lemma 3 : Let $f(x) \in L^1_\mu(0,\infty)$ and $g(x) \in L^p_\mu(0,\infty)$, $1 < p < \infty$ and let

$$f^*(x,y) = \int_0^\infty f(z)\,D(x,y,z)\,d\sigma(z). \tag{13}$$

Then the Hankel convolution

$$(f \# g)(x) = \int_0^\infty f^*(x,y)\,g(y)\,d\sigma(y) \tag{14}$$

satisfies the norm inequality

$$\|(f \# g)(x)\|_p \le \|f(x)\|_1\,\|g(x)\|_p. \tag{15}$$

The proof is given by Pathak and Pandey[4].

Proof of Theorem 9. Proceeding as in the proof of the Theorem 4.3 of Pathakand Pandey[4] we can show that

$$\left(h_\mu\,(y^{\mu+1/2} f \# g)\right)(\xi) = \xi^{-\mu-1/2}\,h_\mu\left(t^{\mu+1/2} f(t)\right)(\xi)\,.\,h_\mu\left(t^{\mu+1/2}\,g(t)\right)(\xi)\,. \tag{16}$$

Now assume that

$$\phi(t) = t^{\mu+1/2}\,g(t) \tag{17}$$

and

$$a^{-m}(\xi) = \xi^{-\mu-1/2}\left(h_\mu\left(t^{\mu+1/2} f(t)\right)\right)(\xi).$$

Then

$$f(t) = t^{-\mu-1/2}\, h_\mu^{-1}\left(\xi^{\mu+1/2}\, a^{-m}(\xi)\right)(t) \tag{18}$$

$$= t^{-\mu-1/2} \int_0^\infty \xi^{\mu+1/2} a^{-m}(\xi) \sqrt{\xi t}\; J_\mu(\xi t)\, 2^\mu\, \Gamma(\mu+1)\, \xi^{-2\mu-1}\, d\sigma(\xi)$$

Using (13) we obtain

$$f(t) = t^{-\mu-1/2} \int_0^\infty a^{-m}(\xi)\, 2^\mu\, \Gamma(\mu+1)\, (\xi t)^{-\mu} J_\mu(\xi t)\, d\sigma(\xi)$$

$$= \int_0^\infty a^{-m}(\xi)\, j(\xi t)\, d\sigma(\xi) = h_\mu^{-1}(a^{-m})(\xi) \in L^1(0,\infty) \text{ by (6).}$$

Now, using (16), (17) and (18) we obtain

$$h_\mu\left(y^{\mu+1/2}(f \# g)\right)(\xi) = \xi^{-\mu-1/2}\, h_\mu\left[t^{+\mu+1/2}\, t^{-\mu-1/2}\, h_\mu^{-1}\left(\xi^{\mu+1/2}\, a^{-m}(\xi)\right)\right] h_\mu\left[t^{\mu+1/2}\, t^{-\mu-1/2}\, \phi(t)\right]$$

$$= \xi^{-\mu-1/2}\; \xi^{\mu+1/2}\, a^{-m}(\xi)\, h_\mu \phi(\xi)$$

$$= a^{-m}(\xi)\, (h_\mu \phi)(\xi);$$

so that

$$y^{\mu+1/2}(f \# g) = h_\mu^{-1}(a^{-m} h_\mu \phi) = \mathbf{H}_\mu^m \phi.$$

Therefore,

$$f \# g = y^{-\mu-1/2}\; \mathbf{H}_\mu^m\; \phi.$$

Hence,

$$\| y^{-\mu-1/2} \mathbf{H}_{\mu}^{m} \phi \|_p = \| f \# g \|_p .$$

Using Lemma 3 we get

$$\| y^{-\mu-1/2} \mathbf{H}_{\mu}^{m} \phi \|_p \leq \| f \|_1 \| t^{-\mu-1/2} \phi \|_p ;$$

so that

$$\| y^{-\mu-1/2} \mathbf{H}_{\mu}^{m} \phi \|_p \leq C \| t^{-\mu-1/2} \phi \|_p .$$

This completes the proof of the theorem.

Theorem 10 : For $1 < p < \infty$ and $m \leq l$,

$$W_{\omega,\mu}^{l,p} \subseteq W_{\omega,\mu}^{m,p}$$

and we have

$$\| \phi \|_{m,p,\omega,\mu} \leq C \| \phi \|_{l,p,\omega,\mu}$$

Proof. Let $\phi \in W_{\omega,\mu}^{l,p}$. Then

$$y^{-\mu-1/2} \mathbf{H}_{\mu}^{-l} \phi \in L_p^{\mu} .$$

Also $$\mathbf{H}_{\mu}^{-m} \phi = \mathbf{H}_{\mu}^{l-m} \mathbf{H}_{\mu}^{-l} \phi .$$

Now,
$$\| \phi \|_{m,p,\omega,\mu} = \| y^{-\mu-1/2} \mathbf{H}_{\mu}^{-m} \phi \|_p$$

$$= \| y^{-\mu-1/2} \mathbf{H}_{\mu}^{l-m} \mathbf{H}_{\mu}^{-l} \phi \|_p$$

$$\leq C \| y^{-\mu-1/2} \mathbf{H}_{\mu}^{-l} \phi \|_p$$

$$= C \| \phi \|_{l,p,\omega,\mu}$$

Theorem 11 : For $1 < p < \infty$ and any symbol a^m, $m \in Z$, define the pseudo-differential operator :

$$(A(D)\, u)(x) = h_\mu^{-1} [a^m h_\mu u](x) .$$

Then

$$A(D) : W^{m,p}_{\omega,\mu} \to W^{0,p}_{\omega,\mu} \text{ is a bounded linear operator.}$$

Proof. Consider the following operators :

$$\mathbf{H}_\mu^{-l} : W^{l,p}_{\omega,\mu} \to W^{0,p}_{\omega,\mu}$$

$$A(D)\, \mathbf{H}_\mu^{m} : W^{0,p}_{\omega,\mu} \to W^{o,p}_{\omega,\mu}$$

$$\mathbf{H}_\mu^{l-m} : W^{o,p}_{\omega,\mu} \to W^{l-m,\,p}_{\omega,\mu}$$

The operator $\mathbf{H}_\mu^{-l}$ is bounded. Indeed, for $\phi \in W^{l,p}_{\omega,\mu}$ we have

$$\| \phi \|_{l,p,\omega,\mu} = \| y^{-\mu-1/2}\, \mathbf{H}_\mu^{-l} \phi \|_p < \infty$$

and

$$\| \mathbf{H}_\mu^{-l} \phi \|_{0,p,\omega,\mu} = \| y^{-\mu-1/2}\, \mathbf{H}_\mu^{-l} \phi \|_p < \infty .$$

The second operator is also bounded. For, let $\phi \in W^{0,p}_{\omega,\mu}$. Then

$$\| \phi \|_{0,p,\omega,\mu} = \| y^{-\mu-1/2}\, \phi \|_p < \infty.$$

Now,

$$\| A(D)\, \mathbf{H}_\mu^{m} \phi \|_{0,p,\omega,\mu} = \| y^{-\mu-1/2}\, A(D)\, \mathbf{H}_\mu^{m} \phi \|_p$$

$$= \| y^{-\mu-1/2} h_\mu^{-1} a^m h_\mu \mathbf{H}_\mu^m \phi \|_p$$

$$= \| y^{-\mu-1/2} \mathbf{H}_\mu^{-m} \mathbf{H}_\mu^m \phi \|_p = \| y^{-\mu-1/2} \phi \|_p < \infty.$$

For the third operator we see that

$$\| \mathbf{H}_\mu^{l-m} \phi \|_{l-m,p,\omega,\mu} = \| y^{-\mu-1/2} \mathbf{H}_\mu^{-l+\mu} \mathbf{H}_\mu^{l-m} \phi \|_p$$

$$= \| y^{-\mu-1/2} \phi \|_p < \infty ;$$

so that third operator is also bounded. Hence the product $\mathbf{H}_\mu^{m-l} A(D) \mathbf{H}_\mu^{l-m}$ is a bounded linear operator form $W_{\omega,\mu}^{l,p}$ into $W_{\omega,\mu}^{l-m,p}$.

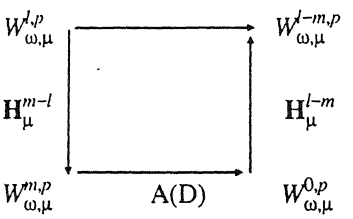

Moreover, by Theorem 8, the operators $\mathbf{H}_\mu^{m-l}$ and $\mathbf{H}_\mu^{l-m}$ in Fig. 1 are isometric and onto. A generalization of the above theorem is given below.

Theorem 12 : For $m \in \mathbf{Z}$ and symbol a^m, the pseudo-differential operator

$$A(D) = h_\mu^{-1} a^m h_\mu : W_{\omega,\mu}^{lp} \to W_{\omega,\mu}^{l-m,p}$$

is a bounded linear operator.

Proof. Let $u \in W_{\omega,\mu}^{l,p}$. Then

$$\| u \|_{l,p,\omega,\mu} = \| y^{-\mu-1/2} \mathbf{H}_\mu^{-l} \| < \infty .$$

Now,

$$\| A(D)\, u \|_{l-m,p,\omega,\mu} = \| y^{-\mu-1/2}\, \mathbf{H}_{\mu}^{m-l}\, A(D)\, u \|_p . \tag{19}$$

Here h_{μ}^{m-l} A(D) is a pseudo-differential operator with symbol a^l. For,

$$\begin{aligned} \mathbf{H}_{\mu}^{m-l}\, A(D)\, u &= h_{\mu}^{-1}\left[a^{-m+l}\, h_{\mu}[A(D)\, u] \right] \\ &= h_{\mu}^{-1}\left[a^{-m+l}\, h_{\mu}\left[h_{\mu}^{-1}\, (a^m\, h_{\mu}\, u) \right] \right] \\ &= h_{\mu}^{-1}\left[a^l\, h_{\mu}\, u \right]. \end{aligned}$$

Then (19) gives

$$\begin{aligned} \| A(D)\, u \|_{l-m,p,\omega,\mu} &= \| y^{-\mu-1/2}\, h_{\mu}^{-1}\, (a^l\, h_{\mu}\, u \|_p \\ &= \| y^{-\mu-1/2}\, \mathbf{H}_{\mu}^{-l} \|_p < \infty . \end{aligned}$$

This completes the proof of the theorem.

References

1. Zemanian, A.H. (1968) *Generalized Integral Transformations,* Interscience Publishers, New York, p. 129.
2. Pahk, D.H. & Kang, B.H. (1991) *Tsukuba J. Math.* **15**(2) : 325.
3. Pathak, R.S. 1996) in *Structure of Solutions of Differential Equations* (Ed.), Morimoto, M. and Kawai, T., World Scientific, Singapore, p. 343.
4. Pathak, .S. & Pandey, P.K. (1997) *J. Math. Anal. Appl.* **215 :** 95.
5. Chazarain, J. & Piriou, A. (1982), *Introduction to the Theory of Linear Partial Differential Equations,* North-Holland Publishing Co., Amsterdam, p. 97.
6. Macauley-Owen, P. (1939) *Proc. London Math. Soc.,* **45** (2), 458.
7. Haimo, D.T. (1965) *Trans. Amer. Math. Soc.,* **116,** 330.

PROC. NAT. ACAD. SCI. INDIA, Vol. 73, A(I), 2003

Thermosolutal instability of Rivlin-Ericksen rotating fluid in the presence of magnetic field and variable gravity field in porous medium

VEENA SHARMA and GIAN CHAND RANA*

Department of Mathematics, Himachal Pradesh University, Summer Hill, Shimla-171005, India.

**Department of Mathematics, Government Post Graduate College, Sarkaghat-175 024, Himachal Pradesh, India.*

Received Aug. 16, 2000; Accepted May 9, 2001

Abstract

In this paper, the thermosolutal instability of Rivlin-Ericksen visco-elastic fluid in the presence of rotation in porous medium has been considered to include the effects of magnetic filed and variable gravity field. For the stationary convection, the stable solute gradient has a stabilizing effect, whereas rotation has stabilizing/destabilizing effects when gravity increases/decreases upwards. The magnetic field has stabilizing effect in the absence of rotation, whereas in the presence of rotation, magnetic field has stabilizing effect when $T_{A_1} < \left(1 + x + \frac{PQ_1}{\in}\right)^2 \left[(1+x)P^2\right]^{-1}$ The medium permeability has destabilizing effect in the absence of rotation, where as in the presence of rotation medium permeability has stabilizing effect when $T_{A_1} < \in^2 \left(1 + x + \frac{PQ_1}{\in}\right)^2 \left[(1+x)P^2\right]^{-1}$ increases upwards (i.e. $\lambda > 0$). The case of overstability is also considered wherein the sufficient conditions for the existence of overstability are derived. The effect of stable solute gradient, rotation, magnetic field and medium permeability have also been shown graphically.

(**Keywords** : thermosolutal instability/Rivlin-Ericksen elastico-viscous fluid/rotation/magnetic field/variable gravity.)

Introduction

The theoretical and experimental results of the onset of thermal instability (Benard convection) in a fluid layer under varying assumptions of hydrodynamics and hydromagnetics has been treated in detail by Chandrasekhar[1]. Veronis[2] has investigated the problem of thermohaline convection in a layer of fluid heated from

below and subject to a stable solute gradient whereas the problem of thermohaline convection in a horizontal layer of viscous fluid heated from below and salted from above has been studied by Nield[3].

With the growing importance of non-Newtonian fluids in modern technology and industries, the investigations on such fluids are desirable. There are many viscoelastic fluids that cannot be characterized by Maxwell's constitutive relations or Oldroyd's constitutive relations. One such class of viscoelastic fluids is the Rivlin-Ericksen fluid. Rivlin and Ericksen[4] have proposed a theoretical model for such viscoelastic fluid. This and other class of polymers is used in the manufacture of parts of space-crafts, aeroplanes, tyres, belt conveyers, ropes cushions, seats, foams, plastic, engineering equipments etc. Recently, polymers are also used in agriculture, communication appliances and in biomedical applications. When fluid permeates a porous material, the gross effect is represented by the Darcy's law. As a result of this macroscopic law, the usual viscous terms in the equations of Rivlin-Ericksen viscoelastic fluid motion is replaced by $\left[-\frac{1}{k_1}(\mu+\mu')\frac{\partial}{\partial t}\vec{q}\right]$, where μ and μ' are the viscosity and viscoelasticity of the thermosolutal instability of Rivlin-Ericksen fluid, k_1 is the medium permeability and $\vec{q}$ is the Darcian (filer) velocity of the fluid.

The problem of thermosolutal convection of rotating fluid in a porous medium is of importance in geophysics, soil sciences, ground-water hydrology and astrophysics. The development of geothermal power resources hold increased general interest in the study of the properties of convection in porous media. The scientific importance of the field has also increased because hydrothermal circulation is the dominant heat transfer mechanism in the development of young oceanic crust Lister[5]. Srivastava and Singh[6] have studied the unsteady flow of a dusty elastico-viscous Rivlin-Ericksen fluid in the presence of time-dependent pressure gradient. Recently, Sharma and Rana[7] have studied the instability of streaming Rivlin-Ericksen fluid in porous medium in hydromagnetics.

Keeping in mind the importance in ground-water hydrology, soil sciences, geophysics and astrophysics, the effect of magnetic field on thermosolutal convection in Rivlin-Ericksen viscoelastic rotating fluid in porous medium in the presence of variable gravity field has been considered in this paper.

Formulation of the problem and perturbation equations :

Consider an infinite, horizontal, incompressible Rivlin-Ericksen viscoelastic fluid of thickness d, bounded by the planes $z = 0$ and $z = d$ in an isotropic and homogenous

porous medium of porosity ϵ and medium permeability k_1, which is acted upon by a uniform rotation $\vec{\Omega}(0,0,\Omega)$, magnetic field $\vec{H}(0,0,H)$ and variable gravity $\vec{g}(0,0,-g)$. The layer is heated and soluted from below such that a uniform temperature gradient $\beta\left(=\frac{dT}{dz}\right)$ and uniform solute gradient $\beta'\left(=\frac{dT}{dz}\right)$ are maintained.

Let p, ρ, T, C, α, α', $\vec{q}(u, v, w)$ υ, υ' and μ_e denote, respectively, pressure, density, temperature, solute concentration, thermal coefficient of expansion, an analogous solvent coefficient of expansion, fluid velocity (initially zero), kinematic viscosity, kinematic viscoelasticity and magnetic permeability. Then equations of motion, continuity, heat conduction, solute concentration through porous medium and equation of state of Rivlin-Ericksen fluid are

$$\frac{1}{\epsilon}\left[\frac{\partial\vec{q}}{\partial t}+\frac{1}{\epsilon}(\vec{q}.\nabla)\vec{q}\right]=-\left(\frac{1}{\rho_0}\right)\nabla p+\vec{g}\left(1+\frac{\delta\rho}{\rho_0}\right)-\frac{1}{k_1}\left(\upsilon+\upsilon'\frac{\partial}{\partial t}\right)\vec{q}+\frac{\mu_e}{4\pi\rho_0}(\nabla\times\vec{H})\times\vec{H}+\frac{2}{\epsilon}(\vec{q}\times\vec{\Omega}) \tag{1}$$

$$\nabla.\vec{q}=0, \tag{2}$$

$$E\frac{\partial T}{\partial t}+(\vec{q}.\nabla)T=\kappa\nabla^2T, \tag{3}$$

$$E'\frac{\partial C}{\partial t}+(\vec{q}.\nabla)C=\kappa'\nabla^2C, \tag{4}$$

$$\text{and } \rho=\rho_0\,[1-\alpha(T-T_0)+\alpha'(C-C_0)] \tag{5}$$

where the suffix zero refers to values at the reference level z = 0. The kinematic viscosity υ, kinematic viscoelasticity υ', the thermal diffusivity κ and solute diffusivity κ' are all assumed to be constant $E=\epsilon+(1-\epsilon)(\rho_s c_s/\rho_0 c_f)$ is constant and E is a constant analogous to E, but corresponding to solute rather than heat, ρ_s, c_s; ρ_0 and c_f denote the density and heat capacity of solid (porous) matrix and fluid respectively.

Maxwell's equations and the modified Ohm's law yields

$$\in \frac{\partial \vec{H}}{\partial t} = \nabla \times \left(\vec{q} \times \vec{H}\right) + \in \eta \nabla^2 \vec{H} \tag{6}$$

$$\nabla . \vec{H} = 0, \tag{7}$$

where η is the electrical resistivity.

The steady state solution is

$$\vec{q} = (0,0,0),\ T = -\beta z + T_0,\ C = -\beta' z + C_0,\ \rho = \rho_0 (1 + \alpha\beta z - \alpha'\beta' z). \tag{8}$$

Consider a small perturbation on the steady state solution and let $\delta\rho$, δp, θ , γ $\vec{q}(u, v, w)$ and $\vec{h}(h_x, h_y, h_z)$ denote, respectively, the perturbations in density ρ pressure p, temperature T, solute concentration C, velocity $\vec{q} = (0,0,0)$ and magnetic field $\vec{H} = (0,0,H)$.

The change in density $\delta\rho$ caused by perturbation θ and γ in temperature and solute concentration, is given by

$$\delta\rho = -\rho_0(\alpha\theta - \alpha'\gamma). \tag{9}$$

Then the linearized perturbation equations relevant to the problem are

$$\frac{1}{\in}\frac{\partial \vec{q}}{\partial t} = -\left(\frac{1}{\rho_0}\right)\nabla \delta p - \vec{g}(\alpha\theta - \alpha'\gamma) - \frac{1}{k_1}\left(\upsilon + \upsilon' \frac{\partial}{\partial t}\right)\vec{q} + \frac{\mu_e}{4\pi\rho_0}\left(\nabla \times \vec{h}\right) \times \vec{H} + \frac{2}{\in}\left(\vec{q} \times \vec{\Omega}\right), \tag{10}$$

$$\nabla . \vec{q} = 0, \tag{11}$$

$$E\frac{\partial \theta}{\partial t} = \beta w + \kappa \nabla^2 \theta, \tag{12}$$

$$E'\frac{\partial \gamma}{\partial t} = \beta' w + \kappa' \nabla^2 \gamma, \tag{13}$$

$$\in \frac{\partial \vec{h}}{\partial t} = \nabla \times \left(\vec{q} \times \vec{H}\right) + \in \eta \nabla^2 \vec{h}\,, \tag{14}$$

$$\nabla . \vec{h} = 0, \tag{15}$$

In the Cartesian form, equations (10) - (15) with the help of equation (9) can be expressed as

$$\frac{1}{\in}\frac{\partial u}{\partial t} = -\frac{1}{\rho_0}\frac{\partial \delta p}{\partial x} - \frac{1}{k_1}\left(\upsilon + \upsilon'\frac{\partial}{\partial t}\right)u + \frac{\mu_e H}{4\pi\rho_0}\left(\frac{\partial h_x}{\partial z} - \frac{\partial h_z}{\partial x}\right) + \frac{2}{\in}\Omega v, \tag{16}$$

$$\frac{1}{\in}\frac{\partial \upsilon}{\partial t} = -\frac{1}{\rho_0}\frac{\partial \delta p}{\partial y} - \frac{1}{k_1}\left(\upsilon + \upsilon'\frac{\partial}{\partial t}\right)v + \frac{\mu_e H}{4\pi\rho_0}\left(\frac{\partial h_y}{\partial z} - \frac{\partial h_z}{\partial y}\right) - \frac{2}{\in}\Omega u\,, \tag{17}$$

$$\frac{1}{\in}\frac{\partial w}{\partial t} = -\frac{1}{\rho_0}\frac{\partial \delta p}{\partial z} - \frac{1}{k_1}\left(\upsilon + \upsilon'\frac{\partial}{\partial t}\right)w + g(\alpha\theta - \alpha'\gamma), \tag{18}$$

$$\frac{\partial u}{\partial x} + \frac{\partial v}{\partial y} + \frac{\partial w}{\partial z} = 0, \tag{19}$$

$$\in \frac{\partial h_x}{\partial t} = H\frac{\partial u}{\partial z} + \in \eta \nabla^2 h_x, \tag{20}$$

$$\in \frac{\partial h_y}{\partial t} = H\frac{\partial v}{\partial z} + \in \eta \nabla^2 h_y, \tag{21}$$

$$\in \frac{\partial h_z}{\partial t} = H\frac{\partial w}{\partial z} + \in \eta \nabla^2 h_z \tag{22}$$

$$\frac{\partial}{\partial x}h_x + \frac{\partial}{\partial y}h_y + \frac{\partial}{\partial z}h_z = 0 \tag{23}$$

$$E\frac{\partial \theta}{\partial t} = \beta w + \kappa \nabla^2 \theta, \tag{24}$$

$$E'\frac{\partial \gamma}{\partial t} = \beta' w + \kappa' \nabla^2 \gamma, \tag{25}$$

Operating equations (16) and (17) by $\frac{\partial}{\partial x}$ and $\frac{\partial}{\partial y}$, respectively, adding and using equation (19), we get

$$\frac{1}{\epsilon}\frac{\partial}{\partial t}\left(\frac{\partial w}{\partial z}\right) = \frac{1}{\rho_0}\left(\nabla^2 - \frac{\partial}{\partial z^2}\right)\delta p - \frac{1}{k_1}\left(\upsilon + \upsilon'\frac{\partial}{\partial t}\right)w + \frac{\mu_e H}{4\pi\rho_0}\nabla^2 h_z - 2\Omega\zeta \tag{26}$$

where $\nabla^2 = \frac{\partial}{\partial x} + \frac{\partial}{\partial y} + \frac{\partial}{\partial z}$,

and $\zeta = \frac{\partial v}{\partial x} - \frac{\partial u}{\partial y}$ is the z-component of vorticity.

Operating equations (18) and (26) by

$\left(\nabla^2 - \frac{\partial}{\partial z^2}\right)$ and $\frac{\partial}{\partial z}$ respectively and adding, to eliminate δp between equations (18) and (26), we get

$$\frac{1}{\epsilon}\frac{\partial}{\partial t}\left(\nabla^2 w\right) = g\left(\frac{\partial^2}{\partial x^2} + \frac{\partial^2}{\partial y^2}\right)\left(\alpha\theta - \alpha'\gamma\right) - \frac{1}{k_1}\left(\upsilon + \upsilon'\frac{\partial}{\partial t}\right)\nabla^2 w + \frac{\mu_e H}{4\pi\rho_0}\frac{\partial}{\partial t}\left(\nabla^2 h_z\right) - 2\Omega\frac{\partial \zeta}{\partial z} \tag{27}$$

Operating equations (16) and (17) by

$-\frac{\partial}{\partial y}$ and $\frac{\partial}{\partial x}$ respectively and adding and using equations (19), we get

$$\frac{1}{\epsilon}\frac{\partial \zeta}{\partial t} = -\frac{1}{k_1}\left(\upsilon + \upsilon'\frac{\partial}{\partial t}\right)\zeta + \frac{\mu_e H}{4\pi\rho_0}\frac{\partial \xi}{\partial t} + 2\Omega\frac{\partial w}{\partial z}, \tag{27}$$

where $\xi = \frac{\partial h_y}{\partial x} - \frac{\partial h_x}{\partial y}$ is the z-component of current density.

Operating equations (20) and (21) by

$-\frac{\partial}{\partial y}$ and $\frac{\partial}{\partial x}$ respectively and adding, we get

$$\frac{1}{\epsilon}\frac{\partial \xi}{\partial t} = H\frac{\partial \zeta}{\partial t} + \epsilon \eta \nabla^2 \xi, \tag{29}$$

The dispersion relation :

Analyzing the disturbances into normal modes, we assume that the perturbation quantities are of the form

$$[w, \theta, \gamma, h_z, \zeta, \xi] = [W(z), \Theta(z), \Gamma(z), Z(z), X(z)] \exp[ik_x x + ik_y y + nt] \tag{30}$$

where k_x, k_y are the wave numbers along the x and y directions respectively,

$$k = (k_x^2 + k_y^2)^{1/2}$$

is the resultant wave number and n is the growth rate.

Using equation (30), equations (27) - (29), (22), (24) and (25) become

$$\frac{n}{\epsilon}Z = \left(\frac{d^2}{dz^2} - k^2\right)W = -gk^2(\alpha\theta - \alpha'\Gamma) - \frac{1}{k_1}(\upsilon + \upsilon' n)\left(\frac{d^2}{dz^2} - k^2\right)W + \frac{\mu_e}{4\pi\rho_0}\frac{d}{dz}\left(\frac{d^2}{dz^2} - k^2\right)K - 2\Omega\frac{dZ}{dz} \tag{31}$$

$$\frac{n}{\epsilon}Z = -\frac{1}{k_1}\left(\upsilon + \upsilon'\frac{\partial}{\partial t}\right)Z + \frac{\mu_e H}{4\pi\rho_0}DX + 2\Omega\frac{dW}{dz} \tag{32}$$

$$\epsilon nX = H\frac{dZ}{dz} + \epsilon n\left(\frac{d^2}{dz^2} - k^2\right)X \tag{33}$$

$$\epsilon nK = H\frac{dW}{dz} + \epsilon n\left(\frac{d^2}{dz^2} - k^2\right)K \tag{34}$$

$$\epsilon n\Theta = \beta W + \kappa\left(\frac{d^2}{dz^2} - k^2\right)\Theta \tag{35}$$

$$\epsilon n\Gamma = \beta' W + \kappa'\left(\frac{d^2}{dz^2} - k^2\right)\Gamma \tag{36}$$

Expressing the coordinates (x,y,z) in the new unit of length d and letting $a = kd$,

$\sigma = \frac{nd^2}{\upsilon}$, $F = \frac{\upsilon'}{d^2}$ and $D^* = d\frac{d}{dz}$ and the superscripts * is suppressed.

Equations (31) - (36), in non-dimensional form, become

$$\left[\frac{\sigma}{\epsilon} + \frac{1}{p_t}(1+\sigma F)\right](D^2 - a^2)W - \frac{\mu_e Hd}{4\pi\rho_0\upsilon}(D^2 - a^2)DK + \frac{g\alpha a^2 d^2}{\upsilon}\Theta - \frac{g\alpha' a^2 d^2}{\upsilon}\Gamma + \frac{2\Omega d^3}{\epsilon\upsilon}DZ = 0, \tag{37}$$

$$\left[\frac{\sigma}{\epsilon} + \frac{1}{p_t}(1+\sigma F)\right]Z = \frac{\mu_e Hd}{4\pi\rho_0\upsilon}DX + \frac{2\Omega d}{\epsilon\upsilon}DW, \tag{38}$$

$$[D^2 - a^2 - Ep_1\sigma]\Theta = -\left(\frac{\beta d^2}{\kappa}\right)W \tag{39}$$

$$[D^2 - a^2 - E'q_1\sigma]\Gamma = -\left(\frac{\beta' d^2}{\kappa'}\right)W \tag{40}$$

$$[D^2 - a^2 - p_2\sigma]X = -\left(\frac{Hd}{\epsilon\eta}\right)DZ, \tag{41}$$

$$\left[D^2 - a^2 - p_2\sigma\right] K = -\left(\frac{Hd}{\epsilon\eta}\right) DW, \tag{42}$$

where $p_1 = \frac{\upsilon}{\kappa}$, is the thermal Prandtl number, $p_2 = \frac{\upsilon}{\eta}$ is the magnetic Prandtl number, $q = \frac{\upsilon}{\kappa'}$ is the Schmidt number, and $p_t = \frac{k_1}{d^2}$ is the dimensionless medium permeability.

Applying the operator $(D^2 - a^2 - p_2\sigma)$ to equation (38), to eliminate X between equations (38) and (41), we get

$$\left[\left\{\frac{\sigma}{\epsilon} + \frac{1}{p_t}(1+\sigma F)\right\}(D^2 - a^2 p_2\sigma) + \frac{Q}{\epsilon} D^2\right] Z = \frac{2\Omega d}{\epsilon\upsilon}(D^2 - a^2 - p_2\sigma) DW. \tag{43}$$

Eliminating K, Θ, Γ and Z between equations (37) - (43), we obtain

$$\left[\left\{\frac{\sigma}{\epsilon} + \frac{1}{p_t}(1+\sigma F)\right\}(D^2 - a^2 - p_2\sigma) + \frac{Q}{\epsilon} D^2\right] \times \left\{\frac{\sigma}{\epsilon} + \frac{1}{p_t}(1+\sigma F)\right\}$$

$$(D^2 - a^2 - Ep_1\sigma)(D^2 - a^2 - E'q\sigma)(D^2 - a^2 - p_2\sigma)(D^2 - a^2) + \frac{Q}{\epsilon} D^2$$

$$(D^2 - a^2 - p_2\sigma) + Sa^2\lambda (D^2 - a^2 - Ep_1\sigma)(D^2 - a^2 - p_2\sigma)]W$$

$$\frac{T_A}{\epsilon^2} D^2 (D^2 - a^2 - p_2\sigma)(D^2 - a^2 - E'q\,\sigma)(D^2 - a^2 - E'q\sigma)]W = 0 \tag{44}$$

where $Q = \left(\frac{\mu_e H^2 d^2}{4\pi\rho_0\upsilon\eta}\right)$, is the Chandrasekhar number,

$R = \left(\frac{g_0\alpha\beta d^4}{\upsilon\kappa}\right)$, is the thermal Rayleigh number,

$S = \left(\frac{g_0 \alpha' \beta' d^4}{\upsilon \kappa'} \right)$, is the analogous solute Rayleigh number,

$T_A = \left(\frac{2\Omega d^2}{\upsilon} \right)$, is the Taylor number.

Here we assume that the temperatures and concentrations at the boundaries are kept fixed, the fluid layer is confined between two boundaries and the adjoining medium is electrically non-conducting. The boundary conditions appropriate to the problem, using equation (16) are

$$W = D^2W = X = DZ = \Theta = \Gamma = 0 \qquad \text{at } z = 0 \text{ and } 1, \tag{45}$$

and the components of $\vec{h}$ are continuous. Since the components of the magnetic field are continuous and the tangential components are zero outside the fluid, we have

$$DK = 0,$$

on the boundaries. Using the boundary conditions (45) and (46), we can show that all the even order derivatives of W must vanish on the boundaries and hence, the proper solutions of equation (44) characterizing the lowest mode is

$$W = W_0 \sin \pi z, \tag{47}$$

where W_0 is a constant. Substituting (47) in (44) and letting $x = \frac{a^2}{\pi^2}$, $R_1 = \frac{R}{\pi^4}$ $S_1 = \frac{S}{\pi^4}$, $Q_1 = \frac{Q}{\pi^4}$, $i\sigma_1 = \frac{\sigma}{\pi^2}$, $P = \pi^2 P_r$ and $T_{A_1} = \frac{T_A}{\pi^4}$ and keeping in mind that σ can be complex, we obtain the dispersion relation

$$R_1 = \frac{(1+x)}{\lambda x}\left\{\frac{i\sigma_1}{\epsilon} + \frac{1+i\sigma_1\pi^2 F}{P}\right\}(1+x+iEp_1\sigma_1) + \frac{Q_1}{\epsilon}\frac{(1+x)}{\lambda x}\left(\frac{(1+x+Ep_1 i\sigma_1)}{(1+x+p_2 i\sigma_1)}\right)$$
$$+ S_1 \frac{(1+x+Ep_1 i\sigma_1)}{(1+x+E'q i\sigma_1)} + \frac{T_{A_1}}{\lambda \epsilon^2} \frac{(1+x+p_2 i\sigma_1)(1+x+Ep_1 i\sigma_1)}{x\left[\left\{\frac{i\sigma_1}{\epsilon} + \frac{(1+i\sigma_1\pi^2 F)}{P}\right\}(1+x+p_2 i\sigma_1) + \frac{Q_1}{\epsilon}\right]} x + iEp_1\sigma_1. \tag{48}$$

Equation (48) is the required dispersion relation studying the effects of magnetic field, stable solute gradient and rotation on the thermosolutal instability of Rivlin-Ericksen fluid in porous medium.

The stationary convection :

When the instability sets in as stationary convection, the marginal state will be characterized by $\sigma = 0$, the dispersion relation (48) reduces to

$$R_1 = \frac{1+x}{\lambda x}\left[\frac{1+x}{P} + \frac{T_{A_1}(1+x)}{\epsilon^2\left(1+x+\frac{PQ_1}{\epsilon}\right)} + \frac{Q_1}{\epsilon}\right] + S_1, \tag{49}$$

which expresses the modified Rayleigh number R_1 as a function of the dimensionless wave number x and the parameters S_1, Q_1, T_{A_1} and P. Rivlin-Ericksen viscoelastic fluid behave like an ordinary Newtonian fluid since viscoelastic parameter F. vanishes with σ.

To study the effects of stable solute gradient, rotation, magnetic filed and medium permeability, we examine the behaviour of $\frac{dR_1}{dS_1}, \frac{dR_1}{dT_{A_1}}, \frac{dR_1}{dQ_1}$ and $\frac{dR_1}{dP}$ analytically. Equation (49) yields,

$$\frac{dR_1}{dS_1} = 1, \tag{50}$$

which implies that the stable solute gradient has a stabilizing effect on the thermosolutal convection. The adverse solute gradient has destabilizing effect on the system since $\frac{dR_1}{dS_1}$ then becomes negative.

Also from equation (49), we have

$$\frac{dR_1}{dT_{A_1}} = \frac{(1+x)^2 P}{\lambda x \epsilon^2 \left(1+x+\frac{PQ_1}{\epsilon}\right)}, \tag{51}$$

which implies that rotation stabilizes the system when gravity is increasing upwards (*i.e.*, $\lambda > 0$).

$$\frac{dR_1}{dQ_1} = \frac{1+x}{\lambda x}\left[\frac{1}{\epsilon} - \frac{T_{A_1}}{\epsilon^3}\frac{(1+x)P^2}{\left(1+x+\frac{PQ_1}{\epsilon}\right)^2}\right], \tag{52}$$

which implies that magnetic field stabilizes/destabilizes the system and gravity increases upwards (i.e., $\lambda > 0$) when

$$T_{A_1} < \frac{\epsilon^2\left(1+x+\frac{PQ_1}{\epsilon}\right)^2}{(1+x)P^2} \Big/ T_{A_1} > \frac{\epsilon^2\left(1+x+\frac{PQ_1}{\epsilon}\right)^2}{(1+x)P^2}$$

Also from (49), we have

$$\frac{dR_1}{dP} = -\frac{(1+x)^2}{\lambda x}\left[\frac{1}{P^2} - \frac{T_{A_1}}{\epsilon^2}\frac{(1+x)}{\left(1+x+\frac{PQ_1}{\epsilon}\right)^2}\right]. \tag{53}$$

The medium permeability stabilizes/destabilizes the system when $\frac{1}{P^2} < \frac{T_{A_1}}{\epsilon^2}\frac{(1+x)}{\epsilon^2\left(1+x+\frac{PQ_1}{\epsilon}\right)^2} \Big/ \frac{1}{P^2} > \frac{T_{A_1}}{\epsilon^2}\frac{(1+x)}{\epsilon^2\left(1+x+\frac{PQ_1}{\epsilon}\right)^2}$ and $\lambda > 0$. In the absence

of rotation and for constant gravity field $\frac{dR_1}{dP}$ is always negative implying thereby the destabilizing effect of medium permeability.

The dispersion relation (49) is analyzed numerically. Graphs have been plotted by giving some numerical values to the parameters, to depict the stability characteristics.

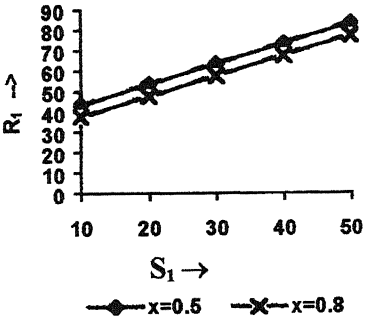

Fig. 1 – Variation of Rayleigh Number (R_1) with stable solute gradient (S_1) for $\lambda = 2$, $\epsilon = 0.5$, $P = 0.2$, $Q_1 = 3$, $T_{A_1} = 20$ for fixed wave numbers x = 0.5 and $x = 0.8$.

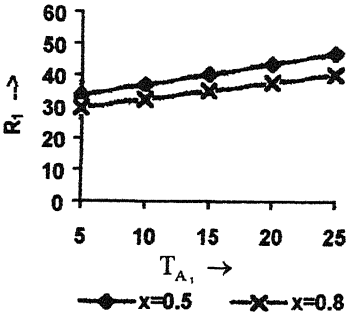

Fig. 2 – Variation of Rayleigh Number (R_1) with rotation $\left(T_{A_1}\right)$ for $\lambda = 2$, $\epsilon = 0.5$, $P = 0.2$, $Q_1 = 3$, $S_1 = 10$ for fixed wave numbers x = 0.5 and $x = 0.8$.

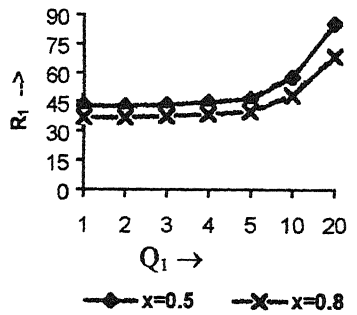

Fig. 3 – Variation of Rayleigh Number (R_1) with magnetic field (Q_1) for $\lambda = 2$, $\epsilon = 0.5$, $P = 0.2$, T_{A_1} =20, $S_1 = 10$ for fixed wave numbers x = 0.5 and $x = 0.8$.

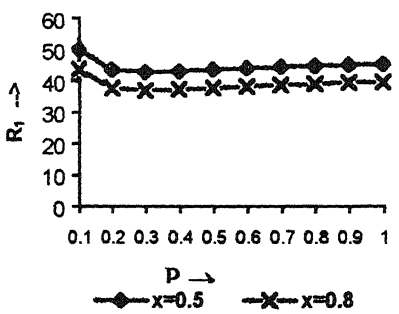

Fig. 4 – Variation of Rayleigh Number (R_1) with medium permeability (P) for $\lambda = 2$, $\epsilon = 0.5$, $P = 0.2$, $Q_1 = 3$, T_{A_1} =20, $S_1 = 10$ for fixed wave numbers x = 0.5 and $x = 0.8$.

In Figure, 1, R_1 is plotted against S_1 for $\lambda = 2$, $\epsilon = 0.5$, $P = 0.2$, T_{A_1} =20, $Q_1 = 3$ for fixed wave numbers x = 0.5 and $x = 0.8$. This shows that stable solute gradient has stabilizing effect. In figure 2, R_1 is plotted against T_{A_1} for $\lambda = 2$, $\epsilon = 0.5$, $P = 0.2$, $Q_1 = 3$, $S_1 = 10$ for fixed wave numbers x = 0.5 and $x = 0.8$. This shows that the rotation has stabilizing effect. In figure 3, R_1 is plotted against Q_1 for $\lambda = 2$, $\epsilon = 0.5$, $P = 0.2$, T_{A_1} =20, $S_1 = 10$ for fixed wave numbers x = 0.5 and $x = 0.8$. This shows that magnetic field has destabilizing effect. for $Q_1 = 1$ to 2 and has stabilizing effect for $Q_1 = 2$ to 20.

In Figure 4, R_1 is plotted against P for $\lambda = 2$, $\epsilon = 0.5$, $S_1 = 10$ T_{A_1} =20, $Q_1 = 3$ for fixed wave numbers x = 0.5 and $x = 0.8$, which shows that medium permeability has destabilizing effect. for $P = 0.1$ to 0.3 and has stabilizing effect for $P = 0.3$ to 1.

Stability of the system and oscillatory modes :

We discuss oscillatory modes, if any, on the onset of stability problem due to the presence of magnetic field and rotation. Multiplying equation (37) by W^*, the complex conjugate of W, integrating over the range of z and making use of (38) - (42) together with the boundary conditions (45), we obtain

$$\left[\frac{\sigma}{\epsilon}+\frac{1}{P_\ell}(1+\sigma F)\right]I_1-\frac{\mu_e \epsilon \eta}{4\pi\rho_0\upsilon}\left[I_2+\sigma^* p_2 I_3\right]-\frac{\lambda g\alpha\kappa a^2}{\upsilon\beta}\left[I_4+\sigma^* E p_1 I_5\right]$$
$$+\frac{\lambda g\alpha'\kappa' a^2}{\upsilon\beta'}\left[I_6+E'q\sigma^* I_7\right]-d^2\left[\frac{\sigma^*}{\epsilon}+\frac{1}{P_\ell}\left(1+\sigma^* F\right)\right]I_8 \qquad (54)$$
$$+\frac{\mu_e d^2\eta\epsilon}{4\pi\rho_0\upsilon}\left[I_9+p_2\sigma I_{10}\right]=0,$$

where $I_1=\int_0^1\left(|DW|^2+a^2|W|^2\right)dz,$

$$I_2=\int_0^1\left(|D^2K|^2+a^4|K|^2+2a^2|DK|^2\right)dz,$$

$$I_3=\int_0^1\left(|DK|^2+a^2|K|^2\right)dz,$$

$$I_4=\int_0^1\left(|D\Theta|^2+a^2|\Theta|^2\right)dz,$$

$$I_5=\int_0^1|\Theta|^2\,dz,$$

$$I_6=\int_0^1\left(|D\Gamma|^2+a^2|\Gamma|^2\right)dz,$$

$$I_7 = \int_0^1 \left(|\Gamma|^2\right) dz,$$

$$I_8 = \int_0^1 \left(|Z|^2\right) dz,$$

$$I_9 = \int_0^1 \left(|DX|^2 + a^2|X|^2\right) dz,$$

$$I_{10} = \int_0^1 \left(|X|^2\right) dz,$$

which are all positive definite. Substituting $\sigma = \sigma_r + i\sigma_i$, in equation (54) then equating the real and imaginary parts, we obtain

$$\sigma_r \left[\begin{array}{l} \left(\frac{1}{\epsilon} + \frac{F}{P_t}\right) I_7 - \frac{\mu_e \in \eta}{4\pi\rho_0 \upsilon} p_2 I_3 - \frac{g\alpha\kappa a^2}{\upsilon\beta} E p_1 I_5 + \frac{g\alpha'\kappa' a^2}{\upsilon\beta'} E' q I_7 \\ d^2 I_8 \left(\frac{1}{\epsilon} + \frac{F}{P_\ell}\right) + \frac{\mu_e d^2 \in \eta}{4\pi\rho_0 \upsilon} p_2 I_{10} \end{array} \right] = \\ - \left[\frac{1}{P_\ell} - \frac{\mu_e \in \eta}{4\pi\rho_0 \upsilon} I_2 \frac{g\alpha\kappa a^2}{\upsilon\beta} I_4 + \frac{g\alpha'\kappa' a^2}{\upsilon\beta'} I_6 + \frac{\mu_e d^2 \in \eta}{4\pi\rho_0 \upsilon} p_2 I_9 \right] \tag{56}$$

$$\text{and } \sigma_i \left[\begin{array}{l} \left(\frac{1}{\epsilon} + \frac{F}{P_t}\right) I_1 - \frac{\mu_e \in \eta}{4\pi\rho_0 \upsilon} p_2 I_3 + \frac{g\alpha\kappa a^2}{\upsilon\beta} E p_1 I_5 - \frac{g\alpha'\kappa' a^2}{\upsilon\beta'} E' q I_7 \\ -d^2 I_8 \left(\frac{1}{\epsilon} + \frac{F}{P_t}\right) + \frac{\mu_e d^2 \in \eta}{4\pi\rho_0 \upsilon} p_2 I_{10} \end{array} \right] = 0 \tag{57}$$

Equation (38) yields that σ_r may be positive or negative. The system is, therefore, stable or unstable. It is clear from equation (57) that σ_i may be zero or non-zero, meaning thereby the modes may be non-oscillatory. The oscillatory modes are introduced due to the presence of a magnetic field, rotation, viscoelasticity and stable solute gradient, which were non-existent in their absence.

The case of overstability :

Here we discuss the possibility of whether instability may occur as overstability. Since for overstability we wish to determine the critical Rayleigh number for the onset of instability via a state of pure oscillations, it suffices to find conditions for which (48) will admit solutions with σ_1 real.

Equating real and imaginary parts of (48) and eliminating R_1 between them, we obtain

$$A_4 c_1^4 + A_3 c_1^3 + A_2 c_1^2 + A_1 c_1 + A_0 = 0 \tag{58}$$

where we have put $c_1 = \sigma_1^2$ and

$$A_4 = p_2^4 (1+x)^2 \left(\frac{1}{\epsilon} + \frac{F\pi^2}{P}\right)^3 E'^2 q^2 + \frac{(1+x)p_2^4}{P}\left(\frac{1}{\epsilon} + \frac{F\pi^2}{P}\right)^2 Ep_1 E'^2 q^2,$$

$$A_0 = \frac{(1+x)^8}{P^2}\left(\frac{1}{\epsilon} + \frac{F\pi^2}{P}\right) + (1+x)^7 \left\{\frac{Ep_1}{P^3} + \frac{Q_1}{\epsilon P}\left(\frac{1}{\epsilon} + \frac{F\pi^2}{P}\right) + \left(\frac{1}{\epsilon} + \frac{F\pi^2}{P}\right)\left(\frac{Q_1}{\epsilon P} - \frac{T_{A_1}}{\epsilon^2}\right)\right\}$$

$$+ (1+x)^6 \left\{\left(\frac{1}{\epsilon} + \frac{F\pi^2}{P}\right)\frac{Q_1^2}{\epsilon^2} + \frac{Ep_1}{P^3}\left(\frac{2Q_1}{\epsilon P} + \frac{T_{A_1}}{\epsilon^2}\right) + \frac{Q_1}{\epsilon P^2}(Ep_1 - p_2)\right\}$$

$$+ (1+x)^5 \left\{\frac{Ep_1 Q_1^2}{P\epsilon^2} + \frac{2Q_1^2}{P\epsilon^2}(Ep_1 - p_2) + \lambda S_1 x \frac{(Ep_1 - E'q)}{\epsilon P}\right\}$$

$$+ (1+x)\left\{S_1 \lambda x \frac{Q_1^2}{\epsilon^2}(Ep_1 - E'q)\right\}. \tag{63}$$

Since σ_1 is real for overstability, the four values of c_1 are positive. The product of the roots of equation (58) is $\frac{A_0}{A_4}$, and if this is to be positive then $A_0 > 0$ since from equation from equation (59) $A_4 > 0$.

Equation (59) shows that this is clearly possible *i.e.* A_0 is always positive if

$$Ep_1 > E'q, \quad Ep_1 > p_2 \text{ and } \frac{Q_1}{P} > \frac{T_{A_1}}{\epsilon} \tag{60}$$

which implies that

$$E'\kappa > E\kappa', \qquad \kappa < E\eta \text{ and } \upsilon > \left(\frac{4\Omega}{H}\right)^2\left(\frac{\pi k_1\rho_0}{\mu_e \in}\right)\mu$$

Therefore,

$$E'\kappa > E\kappa', \qquad \kappa < E\eta \text{ and } \upsilon > \left(\frac{4\Omega}{H}\right)^2\left(\frac{\pi k_1\rho_0}{\mu_e \in}\right)\eta$$

- - - - - - -

$$+ \frac{T_{A_1}}{\in^2}Q_1(Ep_1 - p_2)\Big\} + (1+x)^4\left\{\frac{Q_1^3}{\in^3}(Ep_1 - p_2) + \lambda S_1 x\frac{2Q_1}{\in P}(Ep_1 - E'q)\right\}$$

are the sufficient conditions for the existence of overstability and the principle of exchange of stability is not valid.

Conclusion

The stable solute gradient is found to have stabilizing effect whereas rotation has stabilizing effect for $\lambda > 0$ and destabilizing effect for $\lambda < 0$ which is in contrast to the Newtonian fluids. The magnetic field has a stabilizing effect for $T_{A_1} < \dfrac{\in^2\left[1+x+\dfrac{PQ_1}{\in}\right]^2}{(1+x)P^2}$ and as gravity increase upwards (i.e., $\lambda > 0$) and has destabilizing effect when $T_{A_1} < \dfrac{\in^2\left[1+x+\dfrac{PQ_1}{\in}\right]^2}{(1+x)P^2}$ and as gravity increase upwards (i.e., $\lambda > 0$) whereas medium permeability has stabilizing/destabilizing effect on the system for $\dfrac{1}{P^2} < \dfrac{T_{A_1}(1+x)}{\in^2\left[1+x+\dfrac{PQ_1}{\in}\right]^2} \Big/ \dfrac{1}{P^2} > \dfrac{T_{A_1}(1+x)}{\in^2\left[1+x+\dfrac{PQ_1}{\in}\right]^2}$ for $\lambda > 0$ and the same behaviour have also been shown graphically. The case of overstability is also

considered and it is found that $E'\kappa < E\kappa'$, $\kappa < E\eta$ and $\upsilon > \left(\frac{4\Omega}{H}\right)^2 \left(\frac{\pi k_1 \rho_0}{\mu_e \in}\right) \eta$ are the sufficient conditions for the existence of overstability.

References

1. Chandrasekhar S., (1981) *Hydrodynamic and Hydromagnetic Stability*, Dover Publications, New York.
2. Veronis, G. (1965) *J. Marine Res.* **23** : 1.
3. Nield, D. A. (1967) *J. Fluid Mech.* **29** : 545.
4. Rivlin, R. S. & Ericksen, J. L. (1955) *J. Rational Mech. Anal.* **4** : 323.
5. Lister, C. R. b. (1972) *J. Roy, Astr. Soc.* **26** : 515.
6. Srivastava, R. K. & Singh, K. K. (1988) *Bull. Cal. Math. Soc.* **80** : 286.
7. Sharma, V. & Rana, G. C. (1999) *J. Indian Acad. Math.* **21(2)** : 121.

PROC. NAT. ACAD. SCI. INDIA, 73 (A), I, 2003

Microstretch thermoelastic interactions without energy dissipation due to mechanical and thermal sources

RAJNEESH KUMAR and SUNITA DESWAL

Department of Mathematics, Kurukshetra University, Kurukshetra

e-mail : rajneesh-kuk@rediffmail.com

Received Jan. 10, 2000; Revised Dec. 27, 2000; Accepted June 28, 2001

Abstract

The linear theory of generalized thermoelasticity without energy dissipation for homogeneous and isotropic microstretch elastic materials is employed to study the disturbance due to mechanical and thermal sources in a half-space by the use of Laplace-Hankel transform techniques. The integral transforms have been inverted by using a numerical technique. The analytical expressions of the displacement components, force stress, couple stress, microstress and temperature field are obtained. Normal force stress and tangential couple stress for instantaneous and continuous mechanical and thermal sources have been computed numerically and illustrated graphically. Stretch effect on various expressions has also been obtained analytically and depicted graphically.

(Keywords : Microstretch, Thermoelasticity, Sources, Integral transforms)

Introduction

Thermoelasticity theories which admit a finite speed for thermal signals (second sound) have aroused much interest in the last three decades. Recently, relevant theoretical developments on the subject of finite velocity of heat propagation are due to Green and Naghdi[1-3] which provide sufficient basic modifications in the constitutive equations that permit treatment of a much wider class of heat flow problems. An important feature of this theory, which is not present in other thermoelasticity theories, is that this theory does not accommodate dissipation of thermal energy.

"Micropolar elasticity" termed by Eringen[4] is used to describe deformation of elastic media with oriented particles. A micropolar continuum is a collection of interconnected particles in the form of small rigid bodies undergoing both translational and rotational motions. The linear theory of micropolar thermoelasticity was developed by extending the theory of micropolar continua to include thermal

effects by Eringen[5] and Nowacki.[6] The theory of microstretch elastic solids is a generalization of the micropolar theory and was introduced by Eringen.[7,8] The theory of thermo-microstretch elastic solids was developed by Eringen.[9] Recently many authors[10-18] discussed different type of problems in microstretch and thermo-microstretch solids. Following[9,3] we study the disturbance due to mechanical and thermal sources acting at a point on the surface $z = 0$ in the generalized thermo-microstretch elastic half space by applying integral transform techniques.

Formulation of the problem and solution

A homogeneous, isotropic microstretch generalized thermo elastic solid occupying the semi-infinite region $z > 0$, is considered in an undisturbed state and initially at uniform temperature T_o. We take the origin of the cylindrical co-ordinate system (r, θ, z) on the surface $z = 0$ and z-axis pointing vertically into the medium. Let $T(r, z, t)$ be the change in temperature of the medium at any time. A mechanical source or thermal source is assumed to be acting at the origin of the cylindrical co-ordinate system having isothermal boundary.

For two dimensional problem, we assume

$$\vec{u}=(u_r,0,u_z), \qquad \vec{\phi}=(0,\phi_\theta,0) \tag{1}$$

and introducing dimensionless quantities defined by the expressions

$$r'=\frac{\omega^*}{c_2}r, \quad z'=\frac{\omega^*}{c_2}z, \quad t'=\omega^* t, \quad u_r'=\frac{\rho\omega^* c_2}{\nu T_o}u_r, \quad u_z'=\frac{\rho\omega^* c_2}{\nu T_o}u_z,$$

$$T'=\frac{T}{T_0}, \quad \phi_\theta'=\frac{\rho c_2^2}{\nu T_o}\phi_\theta, \quad \phi^{*'}=\frac{\rho c_2^2}{\nu T_o}\phi^*, \quad t_{ij}'=\frac{1}{\nu T_o}t_{ij}, \quad m_{ij}'=\frac{\omega^*}{c_2\nu T_o}m_{ij},$$

$$\lambda_z'=\frac{\omega^*}{c_2\nu T_o}\lambda_z, \tag{2}$$

where

$$\omega^*=\frac{\rho C^* c_2^3}{lK^*}, \quad c_2^2=\frac{\mu}{\rho} \text{ and l is a standard length,}$$

in the field equations derived by Eringen[9] and Green and Naghdi[3] and then inserting the potentials Φ, ψ and Γ defined by the relations

$$u_r=\frac{\partial\Phi}{\partial r}+\frac{\partial^2\psi}{\partial r\partial z},\qquad u_z=\frac{\partial\Phi}{\partial z}-\left(\nabla^2-\frac{\partial^2}{\partial z^2}\right)\psi,\qquad \phi_\theta=\frac{-\partial\Gamma}{\partial r},\tag{3}$$

in the resulting equations, we obtain

$$\left(\nabla^2-a_o\frac{\partial^2}{\partial t^2}\right)\Phi-a_oT+a_5\phi^*=0\ ,\tag{4}$$

$$\left(\nabla^2-a_3\frac{\partial^2}{\partial t}\right)\psi+a_4\Gamma=0\ ,\tag{5}$$

$$\left(\nabla^2-2a_1-a_2\frac{\partial^2}{\partial t^2}\right)\Gamma-a_1\nabla^2\psi=0\ ,\tag{6}$$

$$\left(\nabla^2-\frac{\partial^2}{\partial t^2}\right)T-\epsilon\frac{\partial^2}{\partial t^2}\nabla^2\Phi=0\ ,\tag{7}$$

$$a_9T-a_8\nabla^2\Phi+\left(a_6\nabla^2-a_7-\frac{\partial^2}{\partial t^2}\right)\phi^*=0\ ,\tag{8}$$

where

$$a_1=\frac{Kc_2^2}{\gamma\omega^{*2}},\quad a_2=\frac{\rho jc_2^2}{\gamma},\quad a_3=\frac{\rho c_2^2}{\mu+K},\quad a_4=\frac{K}{\mu+K},\quad a_5=\frac{\lambda_0}{\lambda+2\mu+K},$$

$$a_6=\frac{c_6^2}{c_2^2},\quad a_7=\frac{c_7^2}{\omega^{*2}},\quad a_8=\frac{c_8^2}{\omega^{*2}},\quad a_9=\frac{2\nu_1c_2^2}{9\nu\omega^{*2}j},\quad a_0=\frac{c_2^2}{c_1^2},$$

$$c_1^2=\frac{\lambda+2\mu+K}{\rho},\qquad \epsilon=\frac{\nu^2T_o}{\rho K^*}\ ,\quad \nabla^2=\frac{\partial^2}{\partial r^2}+\frac{1}{r}\frac{\partial}{\partial r}+\frac{\partial^2}{\partial z^2}\ .\tag{9}$$

Applying Laplace and Hankel transforms defined by

$$\bar{f}(p)=\int_0^\infty e^{-pt} f(t)dt$$

and

$$\hat{f}(q,z,p)=\int_0^\infty \bar{f}(r,z,p)\ rJ_n(rq)dr\ , \tag{10}$$

on equations (4)-(8) and then eliminating $\hat{T},\hat{\phi}^*$ and $\hat{\Gamma}$ from the resulting expressions, we obtain

$$\left[\nabla'^6 + A\nabla'^4 + B\nabla'^2 + C\right]\left[\hat{\Phi}\right] = 0 \tag{11}$$

and

$$\left[\frac{d^4}{dz^4}+E\frac{d^2}{dz^2}+F\right]\left[\hat{\psi}\right]= 0 \tag{12}$$

where

$$A = -p^2(a_0 + d_6 + \in a_0) - d_7 + a_5 d_8\ ,$$

$$B = p^2\left[d_6 d_7 + a_o\left(d_6 p^2 + d_7\right) - \in a_5 d_9 + \in a_o d_7 - a_5 d_8 d_6\right],$$

$$C = -a_o p^4 d_6 d_7\ , \qquad E = -2q^2 - 2a_1 - p^2(a_2 + a_3) + a_1 a_4\ ,$$

$$F = q^4 + q^2\left[2a_1 + p^2(a_2 + a_3) - a_1 a_4\right] + a_3 p^2\left(2a_1 + a_2 p^2\right),$$

$$d_6 = \frac{\rho C^* c_2^2}{K^*}\ ,\quad d_7 = \frac{a_7 + p^2}{a_6}\ ,\quad d_8 = \frac{a_8}{a_6}\ ,\qquad d_9 = \frac{a_9}{a_6}\ . \tag{13}$$

The solutions of equations (11) and (12), satisfying the radiation conditions at infinity are

$$\hat{\Phi} = A_1 \exp(-\xi_1 z) + A_2 \exp(-\xi_2 z) + A_3 \exp(-\xi_3 z), \tag{14}$$

$$\hat{T} = b_1^* A_1 \exp(-\xi_1 z) + b_2^* A_2 \exp(-\xi_2 z) + b_3^* A_3 (-\xi_3 z), \tag{15}$$

$$\hat{\phi}^* = a_1^* A_1 \exp(-\xi_1 z) + a_2^* A_2 \exp(-\xi_2 z) + a_3^* A_3 \exp(-\xi_3 z), \tag{16}$$

$$\hat{\psi} = A_4 \exp(-\xi_4 z) + A_5 \exp(-\xi_5 z), \tag{17}$$

$$\hat{\Gamma} = a_4^* A_4 \exp(-\xi_4 z) + a_5^* A_5 \exp(-\xi_5 z), \tag{18}$$

where

$$\xi_n^2 = q^2 + s_n - \frac{A}{3}, \qquad s_n = 2\sqrt{-H}\cos\left(\frac{\phi + 2\pi(n-1)}{3}\right), \qquad (n=1,2,3)$$

$$\xi_{4,5}^2 = \left[-E \pm \sqrt{E^2 - 4F}\right]/2, \qquad \phi = \tan^{-1}\left(\sqrt{|\Delta|}/-G\right), \qquad \Delta = G^2 + 4H^3,$$

$$G = \frac{2A^3}{27} - \frac{AB}{3} + C, \qquad H = \frac{B}{3} - \frac{A^2}{9}, \qquad a_i^* = \left(\xi_i^2 - q^2 - p^2 a_o\right)/\left(a_o N_i - a_5\right)$$

$$b_i^* = \frac{1}{a_o}\left[a_5 a_i^* + \xi_i^2 - q^2 - p^2 a_o\right],$$

$$N_i = \left[\frac{\epsilon p^2 \left(\xi_i^2 - q^2 - d_7\right)}{d_8\left(\xi_i^2 - q^2 - p^2\right) - \epsilon p^2 d_9}\right], \qquad (i=1,2,3)$$

$$a_{4,5}^* = -\frac{1}{a_4}\left[\xi_{4,5}^2 - q^2 - a_3 p^2\right]$$

and $\xi_i (i = 1,.....5)$ are supposed to have positive real parts. (19)

Case I : Instantaneous Mechanical Source acting on the Surface

The boundary conditions in this case are

$$t_{zz} = \frac{-P\delta(r)\delta(t)}{2\pi r}, \qquad t_{zr} = m_{z\theta} = T = \lambda_z = 0 \qquad at\, z = 0, \qquad (20)$$

where t_{zz}, t_{zr}, $m_{z\theta}$ and λ_z have been borrowed from the constitutive relations derived by Eringen[9] and Green and Naghdi[3], $\delta(\ )$ denotes the Dirac delta function and P is the magnitude of the force. Making use of equations (2) and (3) in the boundary conditions (20); applying the transforms defined by equation (10) and then substituting the equations (14) – (18) in the resulting expressions, we obtain the expressions for displacement components, stresses, temperature field and microstress as

$$\hat{u}_r = \frac{1}{\Delta_o}\left[-q\left(\Delta_1 e^{-\xi_1 z} + \Delta_2 e^{-\xi_2 z} + \Delta_3 e^{-\xi_3 z}\right) + q\left(\xi_4\Delta_4 e^{-\xi_4 z} + \xi_5\Delta_5 e^{-\xi_5 z}\right)\right], \qquad (21)$$

$$\hat{u}_z = \frac{1}{\Delta_o}\left[-\xi_1\Delta_1 e^{-\xi_1 z} - \xi_2\Delta_2 e^{-\xi_2 z} - \xi_3\Delta_3 e^{-\xi_3 z} + q^2\left(\Delta_4 e^{-\xi_4 z} + \Delta_5 e^{-\xi_5 z}\right)\right], \qquad (22)$$

$$\hat{t}_{zz} = \frac{1}{\Delta_o}\left[f_1\Delta_1 e^{-\xi_1 z} + f_2\Delta_2 e^{-\xi_2 z} + f_3\Delta_3 e^{-\xi_3 z} - b_2 q^2\left(\xi_4\Delta_4 e^{-\xi_4 z} + \xi_5\Delta_5 e^{-\xi_5 z}\right)\right], \qquad (23)$$

$$\hat{t}_{zr} = \frac{q}{\Delta_o}\left[b_2\xi_1\Delta_1 e^{-\xi_1 z} + b_2\xi_2\Delta_2 e^{-\xi_2 z} + b_2\xi_3\Delta_3 e^{-\xi_3 z} + f_4\Delta_4 e^{-\xi_4 z} + f_5\Delta_5 e^{-\xi_5 z}\right], \qquad (24)$$

$$\hat{m}_{z\theta} = \frac{-b_6 q}{\Delta_o}\left[\xi_4 a_4^*\Delta_4 e^{-\xi_4 z} + \xi_5 a_5^*\Delta_5 e^{-\xi_5 z}\right], \qquad (25)$$

$$\hat{T} = \frac{1}{\Delta_o}\left[b_1^*\Delta_1 e^{-\xi_1 z} + b_2^*\Delta_2 e^{-\xi_2 z} + b_3^*\Delta_3 e^{-\xi_3 z}\right], \qquad (26)$$

$$\hat{\lambda}_z = \frac{-b_7}{\Delta_o}\left[\xi_1 a_1^*\Delta_1 e^{-\xi_1 z} + \xi_2 a_2^*\Delta_2 e^{-\xi_2 z} + \xi_3 a_3^*\Delta_3 e^{-\xi_3 z}\right], \qquad (27)$$

where

$$\Delta_o = b_1^*\left[\xi_2 a_2^*\left(\xi_5 a_5^* e_2 - \xi_4 a_4^* e_1\right) + \xi_3 a_3^*\left(\xi_4 a_4^* e_3 - \xi_5 a_5^* e_4\right)\right] +$$

$$b_2^*\left[\xi_1 a_1^*\left(\xi_4 a_4^* e_1 - \xi_5 a_5^* e_2\right) + \xi_3 a_3^*\left(\xi_5 a_5^* e_6 - \xi_4 a_4^* e_5\right)\right] +$$

$$b_3^*\left[\xi_1 a_1^*\left(\xi_5 a_5^* e_4 - \xi_4 a_4^* e_3\right) + \xi_2 a_2^*\left(\xi_4 a_4^* e_5 - \xi_5 a_5^* e_6\right)\right],$$

$$\Delta_1 = P_o e_7\left(\xi_3 b_2^* a_3^* - \xi_2 b_3^* a_2^*\right), \qquad \Delta_2 = P_o e_7\left(\xi_1 a_1^* b_3^* - \xi_3 b_1^* a_3^*\right),$$

$$\Delta_3 = P_o e_7\left(\xi_2 b_1^* a_2^* - \xi_1 b_2^* a_1^*\right), \qquad \Delta_4 = P_o \xi_5 a_5^* b_2 \Delta_6 ,$$

$$\Delta_5 = -P_o \xi_4 a_4^* b_2 \Delta_6 , \; \Delta_6 = -b_1^* \xi_2 \xi_3\left(a_3^* - a_2^*\right) + b_2^* \xi_1 \xi_3\left(a_3^* - a_1^*\right) - b_3^* \xi_1 \xi_2\left(a_2^* - a_1^*\right),$$

$$f_i = \left(b_1 + b_2\right)\xi_i^2 - b_1 q^2 - b_i^* a_o + b_o a_i^* \quad , \qquad i = 1,2,3 \;\; ;$$

$$f_j = -b_2 \xi_j^2 + b_4\left(\xi_j^2 - q^2\right) - b_5 a_j^* \quad , \qquad j = 4,5 \;\; ; \qquad P_o = P/2\pi ,$$

$$e_1 = f_3 f_5 + q^2 b_2^2 \xi_3 \xi_5 \; , \quad e_2 = f_3 f_4 + q^2 b_2^2 \xi_3 \xi_4 \; , \quad e_3 = f_2 f_5 + b_2^2 q^2 \xi_2 \xi_5 \; ,$$

$$e_4 = f_2 f_4 + q^2 b_2^2 \xi_2 \xi_4 \; , \quad e_5 = f_1 f_5 + q^2 b_2^2 \xi_1 \xi_5 \; , \quad e_6 = f_1 f_4 + q^2 b_2^2 \xi_1 \xi_4 \; ,$$

$$e_7 = f_5 \xi_4 a_4^* - f_4 \xi_5 a_5^* \; , \quad b_o = \frac{\lambda_o}{\rho c_2^2} \; , \qquad b_1 = \frac{\lambda}{\rho c_2^2} \; , \qquad b_2 = \frac{2\mu + K}{\rho c_2^2} \; ,$$

$$b_4 = \frac{\mu}{\rho c_2^2} \quad ,$$

$$b_5 = \frac{K}{\rho c_2^2} \; , \quad b_3 = b_4 + b_5 \; , \quad b_6 = \frac{\gamma}{\rho c_2^2}\left(\frac{\omega^*}{c_2}\right)^2 \; , \quad b_7 = \frac{\alpha_o}{\rho c_2^2}\left(\frac{\omega^*}{c_2}\right)^2 . \qquad (28)$$

Particular Case I :

By taking $\alpha_o = \lambda_o = \lambda_1 = 0$ in equations (21) – (27), we obtain the expressions for displacement components, stresses and temperature field in a micropolar generalized thermoelastic medium as

$$\hat{u}_r = \frac{1}{\Delta_o'}\left[-q\left(\Delta_1' e^{-\xi_1' z} + \Delta_2' e^{-\xi_2' z}\right) + q\left(\xi_4 \Delta_4' e^{-\xi_4 z} + \xi_5 \Delta_5' e^{-\xi_5 z}\right)\right], \tag{29}$$

$$\hat{u}_z = \frac{1}{\Delta_o'}\left[-\xi_1' \Delta_1' e^{-\xi_1' z} - \xi_2' \Delta_2' e^{-\xi_2' z} + q^2\left(\Delta_4' e^{-\xi_4 z} + \Delta_5' e^{-\xi_5 z}\right)\right], \tag{30}$$

$$\hat{t}_{zz} = \frac{1}{\Delta_o'}\left[f_1' \Delta_1' e^{-\xi_1' z} + f_2' \Delta_2' e^{-\xi_2' z} - b_2 q^2\left(\xi_4 \Delta_4' e^{-\xi_4 z} + \xi_5 \Delta_5' e^{-\xi_5 z}\right)\right], \tag{31}$$

$$\hat{t}_{zr} = \frac{q}{\Delta_o'}\left[b_2\left(\xi_1' \Delta_1' e^{-\xi_1' z} + \xi_2' \Delta_2' e^{-\xi_2' z}\right) + f_4 \Delta_4' e^{-\xi_4 z} + f_5 \Delta_5' e^{-\xi_5 z}\right], \tag{32}$$

$$\hat{m}_{z\theta} = \left(\frac{-b_6 q}{\Delta_o'}\right)\left[\xi_4 a_4^* \Delta_4' e^{-\xi_4 z} + \xi_5 a_5^* \Delta_5' e^{-\xi_5 z}\right], \tag{33}$$

$$\hat{T} = \frac{1}{\Delta_o'}\left[q_1 \Delta_1' e^{-\xi_1' z} + q_2 \Delta_2' e^{-\xi_2' z}\right], \tag{34}$$

where

$$\Delta_o' = \xi_4 a_4^*(q_1 S_1 - q_2 S_3) - \xi_5 a_5^*(q_1 S_2 - q_2 S_4),$$

$$\Delta_1' = -P_o q_2\left(f_4 \xi_5 a_5^* - f_5 \xi_4 a_4^*\right), \qquad \Delta_2' = P_o q_1\left(f_4 \xi_5 a_5^* - f_5 \xi_4 a_4^*\right),$$

$$\Delta_4' = P_o \xi_5 a_5^* b_2\left(\xi_1' q_2 - \xi_2' q_1\right), \qquad \Delta_5' = P_o \xi_4 a_4^* b_2\left(\xi_2' q_1 - \xi_1' q_2\right),$$

$$S_1 = f_2' f_5 + b_2^2 q^2 \xi_2' \xi_5, \qquad S_2 = f_2' f_4 + b_2^2 q^2 \xi_2' \xi_4,$$

$$S_3 = f_1' f_5 + b_2^2 q^2 \xi_1' \xi_5 , \qquad S_4 = f_1' f_4 + b_2^2 q^2 \xi_1' \xi_4 ,$$

$$\xi_{1,2}'^2 = \left[-A' \pm \sqrt{A'^2 - 4B'} \right] \Big/ 2 , \quad A' = -p^2 (d_6 + a_o + \in a_o) - 2q^2 ,$$

$$B' = q^4 + q^2 p^2 (d_6 + a_o + \in a_o) + p^4 a_o d_6 , \; q_{1,2} = \frac{1}{a_o} \left[\xi_{1,2}'^2 - q^2 - p^2 a_o \right],$$

$$f_i' = (b_1 + b_2) \xi_i'^2 - b_1 q^2 - q_i , \qquad i = 1, 2 . \tag{35}$$

Case II : Continuous Mechanical Source acting on the Surface

The boundary conditions, now take the form

$$t_{zz} = \frac{-P\delta(r)H(t)}{2\pi r} , \qquad t_{zr} = m_{z\theta} = T = \lambda_z = 0 \quad at\, z = 0 , \tag{36}$$

where $H(t)$ is Heaviside unit step function. The expressions for displacement components, stresses, temperature field and microstress in this case are again given by equations (21) – (27), with P_o in right hand side of $\Delta_i (i=1,....5)$ be replaced by $P_o^* = \left(\frac{P_o}{p} \right)$.

Particular Case II :

Neglecting stretch effect, the expressions for displacement components, stresses and temperature field are given by equations (29)-(34) with P_o in right hand side of $\Delta_i' (i = 1,2,4,5)$ be replaced by P_o^*.

Case III : Instantaneous Thermal Source acting on the Surface

The boundary conditions in this case are

$$t_{zz} = t_{zr} = m_{z\theta} = \lambda_z = 0 , \; T = \frac{P\delta(r)\delta(t)}{2\pi r} \qquad at\, z = 0 , \tag{37}$$

where P is the constant temperature applied on the boundary and the boundary is kept stress free. With the help of these boundary conditions (37) and following the procedure adopted in Case I, the expressions for displacement components, force stresses, couple stress, microstress and temperature field are again given by equations (21)-(27) with $\Delta_i (i=1,....6)$ replaced by Δ_i^* ,

where

$$\Delta_1^* = -P_o\left[\xi_2 a_2^*\left(\xi_4 a_4^* e_1 - \xi_5 a_5^* e_2\right) + \xi_3 a_3^*\left(\xi_5 a_5^* e_4 - \xi_4 a_4^* e_3\right)\right],$$

$$\Delta_2^* = P_o\left[\xi_1 a_1^*\left(\xi_4 a_4^* e_1 - \xi_5 a_5^* e_2\right) + \xi_3 a_3^*\left(\xi_5 a_5^* e_6 - \xi_4 a_4^* e_5\right)\right],$$

$$\Delta_3^* = -P_o\left[\xi_1 a_1^*\left(\xi_4 a_4^* e_3 - \xi_5 a_5^* e_4\right) + \xi_2 a_2^*\left(\xi_5 a_5^* e_6 - \xi_4 a_4^* e_5\right)\right],$$

$$\Delta_4^* = -P_o \xi_5 a_5^* b_2 \Delta_6^* , \qquad \Delta_5^* = P_o \xi_4 a_4^* b_2 \Delta_6^* ,$$

$$\Delta_6^* = \xi_1 a_1^*\left(f_2\xi_3 - f_3\xi_2\right) - \xi_2 a_2^*\left(f_1\xi_3 - f_3\xi_1\right) + \xi_3 a_3^*\left(f_1\xi_2 - f_2\xi_1\right). \tag{38}$$

Particular Case III :

Neglecting stretch effect $\left(\alpha_o = \lambda_o = \lambda_1 = 0\right)$, we obtain the expressions for displacement components, stresses and temperature field in a micropolar generalized thermoelastic medium as given by equations (29)-(34), only with $\Delta_i' \left(i = 1,2,4,5\right)$ replaced by Δ_i^o,

where

$$\Delta_1^o = -P_o\left[\xi_5 a_5^* S_2 - \xi_4 a_4^* S_1\right], \qquad \Delta_2^o = -P_o\left[\xi_4 a_4^* S_3 - \xi_5 a_5^* S_4\right],$$

$$\Delta_4^o = -P_o \xi_5 a_5^* b_2\left(f_1\xi_2 - f_2\xi_1\right), \quad \Delta_5^o = P_o \xi_4 a_4^* b_2\left(f_1\xi_2 - f_2\xi_1\right). \tag{39}$$

Case IV : Continuous Thermal Source acting on the Surface :

The boundary conditions in this case, take the form

$$t_{zz} = t_{zr} = m_{z\theta} = \lambda_z = 0\,,\ T = \frac{P\delta(r)H(t)}{2\pi r} \qquad at\ z = 0\,, \qquad (40)$$

The expressions for displacement components, stresses, temperature field and microstress are obtained in the similar manner as obtained in case II and again are given by equations (21) – (27) with $\Delta_i\,(i = 1,.....,6)$ replaced by Δ_i^* given by equations (38) and P_0 in right hand side of $\Delta_i^*(i = 1,.....5)$ be replaced by P_o^*.

Particular Case IV

If we neglect stretch effect, the expressions for displacement components, stresses and temperature field are given by equations (29)-(34) with the replacement of $\Delta_i'\,(i = 1,2,4,5)$ by Δ_i^o given by equation (39) and with P_0 in right hand side of $\Delta_i^o\,(i = 1,2,4,5)$ be replaced by P_o^*.

Following Honig and Hirdes[19] and Press et al.[20], the transforms in equations (21)-(27) and (29) – (34) are inverted for all the four cases to obtain the solution of the problem.

Discussion of Numerical Results

We take the case of magnesium crystal[21] like material subject to thermal disturbance for numerical calculations. The physical constants used by us are

ρ=1.74gm/cm^3, j=0.2x10^{-15}cm^2, λ=9.4x10^{11}dyne/cm^2,

μ=4.0x10^{11}dyne/cm^2, K=1.0x10^{11}dyne/cm^2, γ=0.779x10^{-4}dyne,

λ_o=0.5x10^{11}dyne/cm^2, λ_1=0.5x10^{11}dyne/cm^2, α_o=0.779x10^{-4}dyne,

K^*=1.0005x10^{11}cal dyne/gm°C cm^2, C*=0.23cal/gm°C, t_o=6.131x10^{-13}sec.,

t_1=8.765x10^{-13}sec., ϵ=0.073, ϵ_1=0.069, T_o=23°C, l = 1 cm.

The variations of normal force stress $T_{zz}(= t_{zz}/P)$ and tangential couple stress $M_{z\theta}(= m_{z\theta}/P)$ with radial distance 'r' at time t = .1 sec. have been shown by (a) solid line for cases I and III, and dashed line for cases II and IV in microstretch generalized thermoelastic (MSGTE) medium and by (b) solid line with centered symbols for cases I and III and dashed line with centered symbols for cases II and IV in

micropolar generalized thermo-elastic (MGTE) medium. The variations for the above said cases (I-IV) are shown in Figs. 1-4.

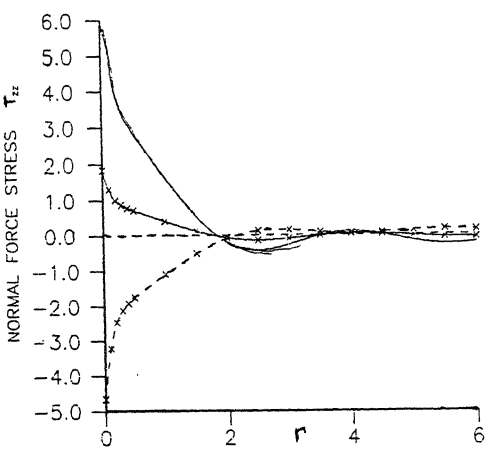

Fig. 1–Variations of normal force stress $T_{zz}\left(=t_{zz}/P\right)$ with radial distance r (Case I, II).

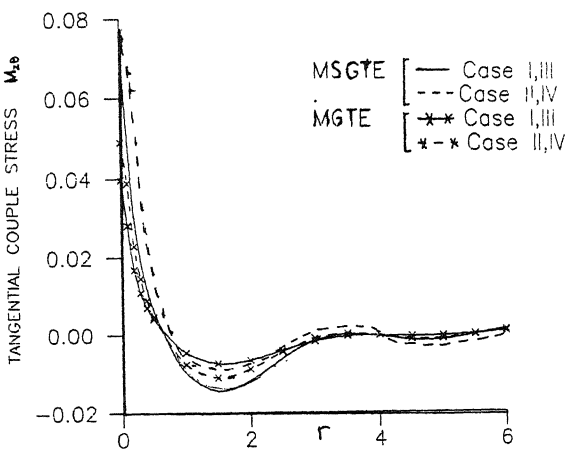

Fig. 2–Variations of tangential couple stress $M_{z\theta}\left(=m_{z\theta}/P\right)$ with radial distance r (Case I, II).

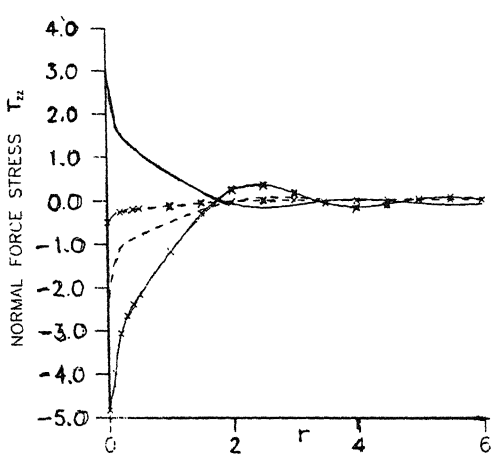

Fig. 3–Variations of normal force stress $T_{zz}\left(=t_{zz}/P\right)$ with radial distance r (Case III, IV).

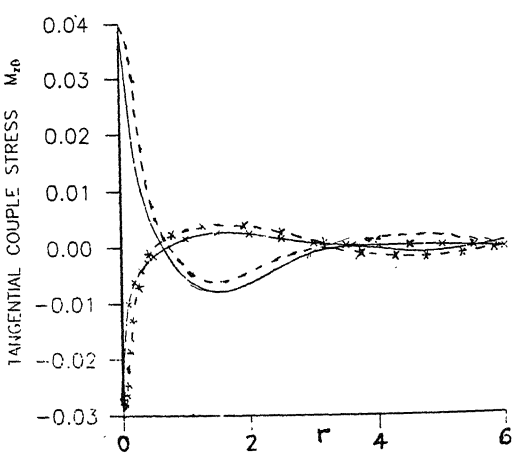

Fig. 4–Variations of tangential couple stress $M_{z\theta}\left(=m_{z\theta}/P\right)$ with radial distance r (Case III, IV).

The values of normal force stress T_{zz} in case I, vary in a similar manner in two media (MSGTE and MGTE) and in case II, values of T_{zz} are large in MSGTE medium in comparison to MGTE medium in the range $0 \leq r \leq 2.0$ but are small in the further range ($2.0 \leq r \leq 6.0$) as shown in Fig. 1. The variations of tangential couple stress ($M_{z\theta}$) lie in the range $-0.02 \leq M_{z\theta} \leq 0.08$ in both the media and for both cases I and II and the variations have oscillatory behaviour as depicted in Fig. 2. Fig. 3 illustrates the variations of T_{zz} for the cases III and IV in both the media. Due to stretch effect the values of T_{zz} in MSGTE medium are large in the range $0 \leq r \leq 1.8$ and $3.5 \leq r \leq 5.0$, small in the range $1.8 \leq r \leq 3.5$ and $5.0 \leq r \leq 6.0$ in comparison to MGTE medium for case III, whereas for Case IV, values of T_{zz} in MSGTE medium are small in the range $0 \leq r \leq 2.55$, in comparison to MGTE medium and thereafter attains almost same values for both the media. The slight oscillatory behaviour of $M_{z\theta}$ is shown in Fig. 4 for the cases III and IV and for both the media. Thus, from the above numerical results, we conclude that stretch has a significant effect on normal force stress and tangential couple stress in all the four cases.

References

1. Green, A. E. & Naghdi, P.M. (1991) *Proc. Roy Soc. London Ser.* **32A** : 171.
2. Green, A. E. & Naghdi, P.M. (1992) *J. of Thermal stresses*, **15** : 253.
3. Green, A. E. & Naghdi, P.M. (1993) J. Elasticity, **31** : 189.
4. Eringen, A.C. (1996) *J. Math. Mech.*, **15** : 909.
5. Eringen, A.C. (1970) Foundation of Micropolar Thermoelasticity, course of 6. lectures no. 23, CISM Udine, Springer.
6. Nowacki, W. (1966) *Couple Stresses in the theory of thermoelasticity*, Proc. IUTAM Symposia, Vienna, Springer-Verlag, p.259.
7. Eringen, A. C. (1971), *Ari Kitabevi Matbassi,* **24** : 1.
8. Eringen, A. C. (1990) *Int. J. Engng. Sci*, **28** : 133.
9. Eringen, A. C. (1990) *Int. J. Engng. Sci.*, **28** : 1291.
10. Bofill, F. & Quintanilla, R. (1995) *Int. J. Engng. Sci.*, **33** : 2115.
11. Cicco, S. De & Nappa, L. (1997) *Int. J. Engng. Sci.*, 35 :573.
12. Ciarletta, M. (1999) *Int. J. Engng. Sci.*, 37 : 1309.
13. Iesan, D. & Quintanilla, R.(1994) *Int. J. Engng. Sci.*, **32** : 991.
14. Iesan, D. & Nappa, L. (1995) Int. J. Engng. Sci., **33** : 1139.
15. Iesan, D. & Pompei, A.(1995) Int. J. Engng. Sci., **33** : 399.

16. Iesan, D., (1997) *Int. J. Engng. Sci.*, 35 :669.

17. Singh, B. & Kumar, R. (1998) *Int. J. Engng. Sci.* **36** : 891.

18. Singh, B. & Kumar, R.(1998) *Int. J. Engng. Sci.* **36** : 865.

19. Honig, G. & Hirdes, U.(1984) *J. Comp. Appl. Math.*, **10** : 113.

20. Press, W. H., Teukolsky, S. A., Vellerling, W.T. & Flannery, B.P. (1986) *Numerical Recipes*, Cambridge University Press, Cambridge, p. 134.

21. Eringen, A. C. (1984) *Int. J. Engng. Sci.* **22** : 1113.

PROC. NAT. ACAD. SCI. INDIA, 73 (A), I, 2003

An analytical approach to the problem of dispersion of a pollutant from multiple sources having constant removal rate

M. AGARWAL and B. PAUL

Department of Mathematics and Astronomy, Lucknow University, Lucknow-226 007, India.

Received December 6, 1999; Revised October 16, 2001; Accepted January 1, 2001

Abstract

An analytical solution to the steady state three dimensional atmospheric diffusion equation with multiple sources has been developed. The modelling is done using Non-Gaussian model, where the wind speed and eddy diffusivities are assumed to vary with the power of vertical height which is uniformly assumed to be 1/2. The removal mechanism is also incorporated in the model and Green's function concept has been applied for the solution of the problem. This model is useful in the prediction of pollution concentration not only from a single point source, but also from multiple point soruces. It also helps in studying the effect of sink mechanism in decreasing the concentration of pollutants from the atmosphere.

(**Keywords** : Multiple sources/variable wind velocity/variable diffusivities/removal rate/Green's function)

Introduction

In past, many steps have been raised to understand the dispersion of air pollutant in the atmosphere under various meteorological conditions. An atmospheric dispersion model is needed in order to calculate the spatial distribution of pollution concentration due to the emission source. Many investigators[1,2] have tried to develop such models considering different meteorological conditions, and adopting different methods of solution. Generally, the Gaussian[3] and the non-Gaussian type models are in practice. When compared to Gaussian models, the non-Gaussian models have wider applicability.

Analytical solutions of the atmospheric diffusion equation using non-Gaussian type models have been found in literature since the 1950s. Earlier, the solutions of the non-Gaussian type models were found out, considering only the two dimensional cases, or neglecting the inversion effect. By applying the Green's function method, solutions for three dimensional diffusion equation under both bounded and unbounded boundary conditions have been obtained[4–6]. But in the above models, the presence of several removal mechanisms in the atmosphere have been not taken ito account. In the environment various mechanisms such as rain out, wash out, deposition on vegetative canopies[7] etc. are known to exist which are effective in removal of pollutants from the atmosphere.

In the light of above, we have analysed the problem of steady state transport of a contaminant, emitted from multiple sources, under Dirichlet's boundary conditions, considering the effect of removal mechanism present in the atmosphere and using the non-Gaussian plume equation, to describe dispersion.

In order to simplify the problem, we have considered the case of equal power profiles of wind speed and diffusivities which is assumed to be 1/2. The solution of this problem is obtained utilizing the Green's function concept.

Diffusion Equation

The partial differential equation describing the steady state dispersion of a non-reactive contaminant released continuously from 'n' point sources located at (x_s^1, y_s^1, z_s^1), (x_s^2, y_s^2, z_s^2) — (x_s^n, y_s^n, z_s^n) in a Cartesian co-ordinate system, where the removal of the contaminant which is assumed by some removal mechanism in the region of interest is given by

$$U(z)\frac{\partial C(x,y,z)}{\partial x} = \frac{\partial}{\partial y}\left(K_y(x,z)\frac{\partial C(x,y,z)}{\partial y}\right) + \frac{\partial}{\partial z}\left(K_z(z)\frac{\partial C(x,y,z)}{\partial z}\right)$$

$$+ \sum_{j=1}^{n} Q^j \delta(x - x_s^j)\,\delta(y - y_s^j)\,\delta(z - z_s^j) - K_1 C(x,y,z) \qquad (1)$$

where $C(x, y, z)$ is the ambient concentration of the contaminant. Q is the emission strength of j^{th} source located at (x_s^j, y_s^j, z_s^j), δ is the Dirac delta function[8] with the property $\int_R \delta(x - x_0)\,dx = 1$ and K_1 is the removal rate of the contaminant.

Here the wind is assumed to be blowing in the x-direction, the turbulent fluxes are approximated by gradient transport (K-theory) and the turbulent diffusion is neglected compared to advection (Slender plume approximation) since the scale of the turbulent transport is smaller than plume dimensions[9].

The wind speed $U(z)$ and eddy diffusivities $K_y(x, z)$ and $K_z(z)$ are assumed to vary with height and are taken as the following power law profiles.

$$U(z) = \frac{U_H z^{\alpha}}{H^{\alpha}}$$

$$K_y = \frac{K_H f(x) z^{\gamma}}{H^{\gamma}}$$

$$K_z = \frac{K_H z^{\beta}}{H^{\beta}}$$

where $f(x)$ is an integrable function of x and U_H and K_H are the wind speed and eddy diffusivity respectively at reference height. H. For simplicity in our paper, we have assumed $\alpha = \beta = \gamma = 1/2$.

Equation (1) is reduced to

$$U_H z^{1/2} \frac{\partial C}{\partial x} = \frac{\partial}{\partial y}\left\{K_H f(x)\left(\frac{z}{H}\right)^{1/2} \cdot \frac{\partial C}{\partial y}\right\} + \frac{\partial}{\partial z}\left\{K_H\left(\frac{z}{H}\right)^{1/2} \cdot \frac{\partial C}{\partial z}\right\} - K_1 C$$

$$+ \sum_{j=1}^{n} Q^j \delta(x - x_s^j)\, \delta(y - y_s^j)\, \delta(z - z_s^j) \qquad (2a)$$

Boundary Conditions

It is assumed here that the pollutant is immediately removed on touching the boundaries (Dirichlet's condition)

$$C(x, y, z) = 0 \ , \ x \to \infty \qquad 2(b)$$

$$C(x, y, z) = 0 \ , \ y \to \pm\infty \qquad 2(c)$$

$$C(x, y, z) = 0 \ , \ z = 0 \qquad 2(d)$$

$$C(x, y, z) = 0 \ , \ z = H \qquad 2(e)$$

where H is the height of inversion layer. The dispersion equation and it's boundary conditions are made dimensionless by considering the following dimensionless quantities :

$$\bar{z} = \frac{z}{H},\ \bar{x} = \frac{xK_H}{U_H H^2},\ \bar{y} = \frac{y}{H},\ \bar{C} = \frac{U_H H^2 C}{Q},\ \bar{K} = \frac{-K_1 H^2}{K_H}$$

$$\delta(\bar{x} - \bar{x}_s^j) = \delta(x - x_s^j)\frac{U_H H^2}{K_H},\ \delta(\bar{y} - \bar{y}_s^j) = \delta(y - y_s^j)\ H,$$

$$\delta(\bar{z} - \bar{z}_s^j) = \delta(z - z_s^j)\ H,\ \bar{f}(\bar{x}) = f(x),\ \bar{Q}^j = \frac{Q^j}{Q}.$$

On removing bars, dispersion equation (2) and its boundary conditions are changed to the form :

$$z^{1/2}\frac{\partial C}{\partial x} = -\frac{\partial}{\partial y}\left[f(x)\, z^{1/2}\frac{\partial C}{\partial y}\right] + \frac{\partial}{\partial z}\left[z^{1/2}\frac{\partial C}{\partial z}\right] + KC + \sum_{j=1}^{n} Q^j \delta(x - x_s^j)\,\delta(y - y_s^j)\,\delta(z - z_s^j), \tag{3}$$

$$C(x, y, z) = 0,\ x \to \infty \tag{4(a)}$$

$$C(x, y, z) = 0,\ y \to \pm\infty \tag{4(b)}$$

$$\left.\begin{aligned} C(x, y, z) &= 0,\ z = 0 \\ C(x, y, z) &= 1,\ z = 1 \end{aligned}\right\} \tag{5}$$

Analytical Solution

This boundary value problem is solved following the procedures of Yeh and Huang[6] and Yeh[5] for a single isolated source. The solution is comprised of three components, a source strength Q^j, a vertical dispersion factor, the vertical sub-Green's function $G_z^j(x, z, x_s^j, z_s^j)$ and a cross wind dispersion factor – the cross wind sub-Green's function $G_y^j(x, y, x_s^j, y_s^j)$.

Thus solution of equation (3) is

$$C(x, y, z) = \sum_{j=1}^{n} Q^j\, G_z^j(x, z, x_s^j, z_s^j)\ G_y^j(x, y, x_s^j, y_s^j) \tag{6}$$

where the two dispersion factors G_z^j and G_y^j are both equal to zero if $x > x_s^j$. The product of these two factors (or sub Green's functions) constitutes a Green's function[10,11] which can be interpreted as the concentration response due to unit disturbance (source) at (x_s^j, y_s^j, z_s^j).

The total concentration at (x, y, z) is, therefore, the sum of the responses from 'n' various sources.

Method of Solution

For the concentration response due to a single source, equation (6) can be written for $j = 1$ as –

$$C(x, y, z) = \int_0^\infty \int_{-\infty}^{\infty} \int_0^1 G_z(x_0, z_0; x, z) \cdot G_y(x_0, y_0; x, y)$$

$$\cdot \delta(x_0 - x_s)\, \delta(y_0 - y_s)\, \delta(z_0 - z_s)\, dx_0\, dy_0\, dz_0,$$

$$C(x, y, z) = QG_z(x, z; x_s, z_s)\, G_y(x, y; x_s, y_s)$$

where $G_z(x_0, z_0;\ x, z)$. $G_y(x_0, y_0; x, y)$ is the Green's function that satisfies the following pairs of adjoint partial differential equations[12,13].

$$z_0^{1/2} \frac{\partial G_z}{\partial z_0} + z_0^{1/2} \frac{\partial G_z}{\partial x_0} + KG_z = -\delta(x_0 - x)\, \delta(z_0 - z),\ x_0 < x \qquad (7)$$

and $$G_z(x_0, z_0; x, z) = 0 \text{ for } x_0 > x$$

and $$f(x_0) \frac{\partial^2 G_y}{\partial y_0^2} + \frac{\partial G_y}{\partial x_0} = -\delta(x_0 - x)\, \delta(y_0 - y),\ x_0 < x \qquad (8)$$

and $$G_y(x_0, z_0; x, z) = 0 \text{ for } x_0 > x$$

x_0, y_0, z_0 are used as independent variables instead of x, y, z so that finally we get $C(x, y, z)$ after integration. For any location x_0, equation (7) can be expressed as

$$\frac{\partial}{\partial z_0}\left(z_0^{1/2}\frac{\partial G_z}{\partial z_0}\right) + z_0^{1/2}\frac{\partial G_z}{\partial x_0} + KG_z = 0\,. \tag{9}$$

$$\lim_{x_0 \to x} z_0^{1/2}\, G_z = \delta(z_0 - z)\,. \tag{10}$$

The method of separation of variables is used and on setting

$G_z(x_0, z_0) = M(z_0)\,.\,N(x_0)$, we have

$$\frac{d^2 M}{d z_0^2} + \frac{1}{2z_0}\frac{dM}{dz_0} + (Kz_0^{-1/2} + \eta^2)\,M = 0 \tag{11}$$

and

$$\frac{1}{N}\frac{dN}{dx_0} = \eta^2 \tag{12}$$

where η^2 is the separation constant. The method of power series is employed to solve equation (11).

$$\begin{aligned} M(z_0) = a_0^1 \{1 &- 0.6667\,Kz_0^{3/2} - 0.333\eta^2 z_0^2 + 0.0899\,K^2 z_0^3 + 0.0952\,K\eta^2 z_0^{7/2} \\ &- 0.0952\,\eta^2 z_0 - 4.938\times 10^{-3}\,K^3 z_0^{9/2} - 8.1834\times 10^{-3}\,K^2 z_0^{10} - 4.329\times 10^{-3}\,K\eta^4\} \\ &+ a_1^1 \{2z_0^{1/2} - 0.6667Kz_0^2 - 0.4\,\eta^2 z_0^{5/2} + 0.0635K^2 z_0^{7/2} + 0.0762K\eta^2 z_0^4 \\ &+ 0.0222\eta^4 - 2.822\times 10^{-3}\,K^3 z_0^5 - 5.0794\times 10^{-3}\,K^2\eta^2 z_0^{11/2}\} \\ &+ 0\,(z^6) \end{aligned} \tag{13}$$

The solution of equation (12) has been found as

$$N(x_0) = C_1\, e^{-\eta^2 (x - x_0)} \tag{14}$$

Thus,

$$G_z(x_0, z_0) = \exp\{-\eta^2 (x - x_0)\} [a_0 (1 - 0.6667 K z_0^{3/2} .....)$$

$$+ a_1 (2 z_0^{1/2} - 0.6667 K z_0^2 .....)] \tag{15}$$

We have applied the conditions (5) and (10) to equation (15) and replacing variables to get the vertical dispersion factor due to the j^{th} source at (x_s^j, y_s^j, z_s^j) as

$$G_z(x, z; x_s^j, z_s^j) = \sum_{i=1}^{\infty} \left\{ \frac{M_i(z) M_i(z_s^j) \exp\{-\eta_1^2 (x - x_s^j)\}}{\int_0^1 z^{1/2} \{M_i(z)\}^2 dz} \right\} \tag{16}$$

where η_i is given by the eigenvalue equation

$$2 - 0.6667 K - 0.4 \eta^2 + 0.0635 K^2 + 0.0762 K\eta^2 + 0.0222 \eta^4$$

$$- 2.822 \times 10^{-3} K^3 - 5.0794 \times 10^{-3} K^2 \eta^2 ..... \infty = 0 \tag{17}$$

and

$$M_i(z) = 2 z^{1/2} - 0.6667 K z^2 - 0.4 \eta_i^2 z^{5/2}$$

$$+ 0.0635 K^2 z^{7/2} + 0.0762 K \eta_i z^4 + 0.0222 \eta_i^4 z^{9/2}$$

$$- 2.822 \times 10^{-3} K^3 z^5 - 5.0794 \times 10^{-3} K^2 \eta_i^2 z^{11/2}$$

$$+ 0(z^6) \tag{18}$$

Now, equation (8) can be written as

$$f(x_0) \frac{\partial^2}{\partial y_0^2} G_y + \frac{\partial}{\partial x_0} G_y = 0, \tag{19}$$

$$\lim_{x_0 \to x} G_y(x_0, y_0; x, y) = \delta(y_0 - y) \tag{20}$$

The Fourier transform is employed to solve equation (19) and (20), to get

$$G_y(x_0, y_0; x, y) = \frac{\exp\left[\dfrac{-(y-y_0)^2}{4\left\{\int_{x_c}^{x} f(\phi_0)\, d\phi_0 - \int_{x_c}^{x_0} f(\phi_0)\, d\phi_0\right\}}\right]}{\sqrt{4\pi}\left\{\int_{x_c}^{x} f(\phi_0)\, d(\phi_0) - \int_{x_c}^{x_0} f(\phi_0)\, d\phi_0\right\}} \tag{21}$$

where x_c is some reference location in Cartesian co-ordinates. To find an explicit $f(x)$, we have used the relation (as is frequently done in dispersion modelling) as

i.e. $$K_y = \frac{1}{2} U \frac{d\sigma_y^2}{dx}$$

$$\Rightarrow \qquad f(x) = \frac{1}{2} \frac{d\sigma_y^2}{dx} \tag{22}$$

where σ_y^2 is the mean square particle displacement.

For multiple source modelling, we have assumed that $f(x)$ depends on the relative distance between source and the location of interest.

We have put (22) in (21) and replaced variables to get the cross wind dispersion factor due to the j^{th} source at (x_s^j, y_s^j, z_s^j) as

$$G_y(x, y; x_s^j, y_s^j) = \frac{1}{\sqrt{2\pi\sigma_y^2 (x - x_s^j)}} \cdot \exp\left[\frac{-(y - y_s^j)^2}{2\sigma_y^2 (x - x_s^j)}\right] \tag{23}$$

where σ_y is standard deviation.

We have finally obtained the total concentration response at (x, y, z) due to n sources located in the region of interest as –

$$C(x, y, z) = \sum_{j=1}^{n} \left[Q^j \left\{ \sum_{i=1}^{\infty} \frac{M_i(z_s^j) \exp\{-\eta_i^2 (x - x_s^j)\}}{\int_0^1 \{M_i(z)\}^2 dz} \right\} \left\{ \exp \left(\frac{-\frac{(y - y_s^j)^2}{2\sigma_y^2 (x - x_s^j)}}{\sqrt{2\pi\sigma_y^2 (x - x_s^j)}} \right) \right\} \right] \tag{24}$$

Discussion

The case of a single elevated point source at dimensionless parameters (0, 0, 0.2) is discussed here. The dimensionless removal rate constant $K = -2.77$, standard deviation $\sigma_y = 1.878\, x^{2/3}$, and $Q^1 = 1$.

To illustrate the behaviour of this three-dimensional atmospheric dispersion model, concentration profiles have been calculated for a variety of conditions using equation (24).

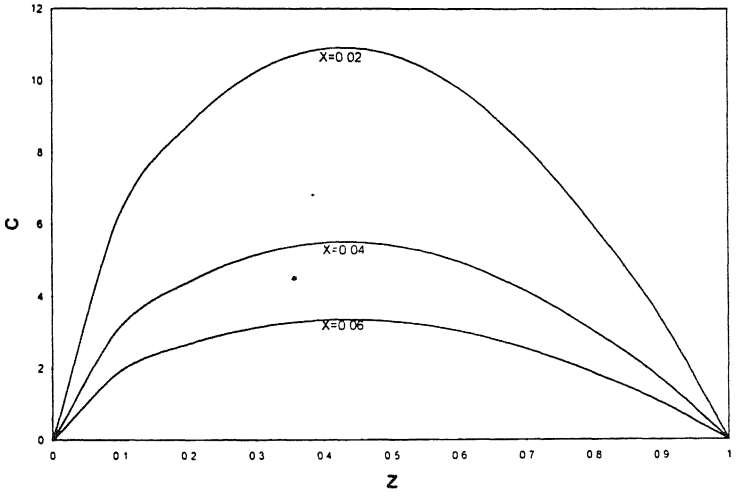

Fig. 1 – Dimensionless concentration $C(X, 0, Z)$ plotted against dimensionless vertical height Z.

In Fig. 1, the concentration of pollutants is plotted with respect to vertical distance ($0 \leq z \leq 1$) for different down wind distances ($x = 0.02, 0.04, 0.06$), keeping the crosswind distance constant. It is seen that for a particular downwind distance ($x = 0.02$), the concentration profile attains it's peak at $z = 0.45$. But with increasing down wind distance ($x = 0.04, 0.06$), concentration decreases, and the concentration profiles approach uniform distribution. This results primarily from horizontal spreading. As a consequence, the concentration level of pollutant near the ground becomes high, which may prove dangerous.

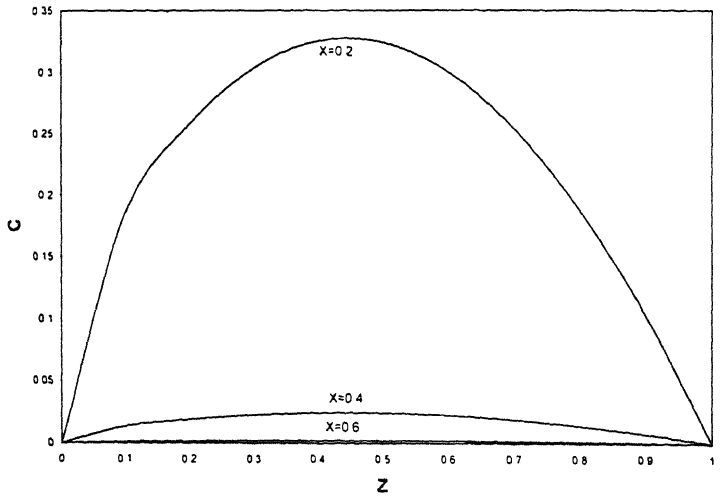

Fig. 2 – Dimensionless concentration $C(X, 0, Z)$ plotted against dimensionless vertical height Z.

In Fig. 2, the concentration is plotted with respect to vertical distance for different down wind distances (x = 0.2, 0.4, 0.6). It is seen here that at low down wind distance (x = 0.2), the plume attains it's peak, while for higher down wind distances (x = 0.4, 0.6), there is a uniform distribution.

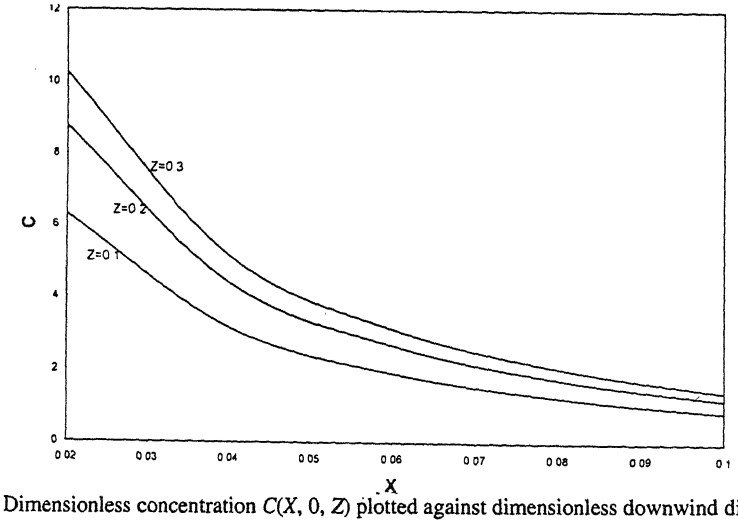

Fig. 3 – Dimensionless concentration $C(X, 0, Z)$ plotted against dimensionless downwind distance X.

In Fig. 3, concentration is plotted against the down wind distance ($0.02 \leq x \leq 1$) for different vertical distances (z = 0.1, 0.2, 0.3). The extensive horizontal spreading shown in this graph confirms the deductions made in (1) and (2).

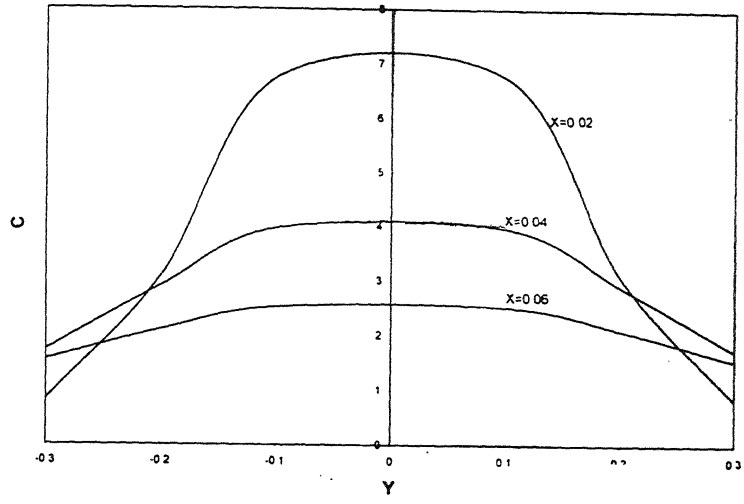

Fig. 4 – Dimensionless concentration $C(X, 0, Z)$ plotted against dimensionless downwind distance X.

In Fig. 4, concentration is plotted agaisnt the cross wind distance ($-0.3 \leq y \leq 0.3$) for different values of down wind distances ($x = 0.02, 0.04, 0.06$). It is seen here that in the cross-wind direction, the concentration profiles are symmetric with peak concentrations along the centre line of the plume. It is also seen that concentration levels decrease and there is marked lateral spreading with increasing down wind distance ($x \geq 0.4$) from the source.

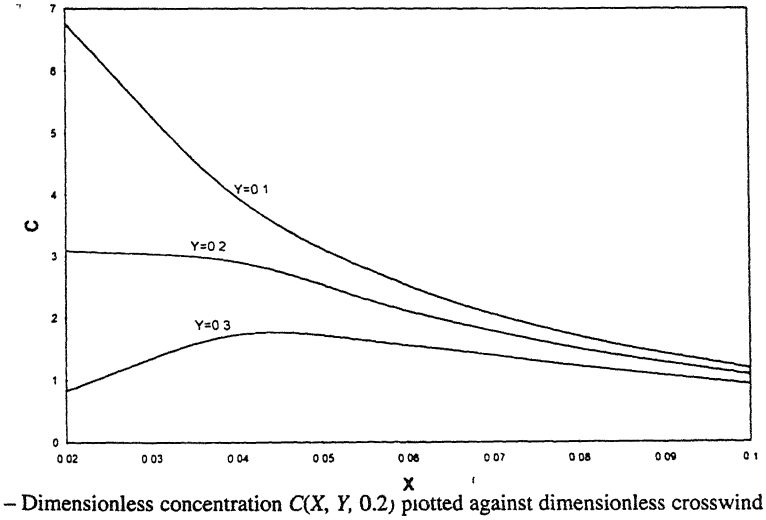

Fig. 5 – Dimensionless concentration $C(X, Y, 0.2)$ plotted against dimensionless crosswind distance Y.

In Fig. 5, concentration is plotted with respect to down wind distance ($0.02 \leq x \leq 0.1$) for different cross wind distances ($y = 0.1, 0.2, 0.3$). For a particular cross wind distance

(y = 0.1), concentration is seen to decrease regularly with the down wind distance. For the cross wind distance (y = 0.2), concentration profile is almost uniform for down wind distance ($0.02 \leq x < 0.04$) and then decreases regularly for $x \geq 0.04$.

For the cross wind distance ($y = 0.3$), it is seen that the concentration profile is a curve which attains it's peak at ($x \sim 0.045$) with extended horizontal spreading in the increasing down wind direction.

Summary

A steady state three dimensionless non-Gaussian model with multiple sources is developed, taking into account the various sink mechanisms present in the atmospheric which are effective in the removal of the pollutants. An analytical solution to this problem is obtained using the concept of Green's function. he diffusion equation is broken into three components – a source strength, a cross-wind dispersion factor and a vertical dispersion factor.

The model is useful in the prediction of the harmful effects of pollutant from multiple sources and its removal by the natural or artificial sinks present in the atmosphere.

References

1. Tirabassi, . (1989) *Water, Air, Soil Pollution* **47** : 19.
2. Sturm, Peter (2000) *Atmospheric Environment* **34(27)** : 4579.
3. Bindu G. Babu C.A., Anil Kumar K.G. (1997) *Indian Environ. Prot.* **17(11)** : 801.
4. Yeh, G.T. (1975) *Geophysics Res. Lett.* **2** : 293.
5. Yeh, G.T. & Huang, C.H. (1975) *Boundary Layer Met.* **9** : 381.
6. Huang, C.H. (1979) *Atmospheric Environment* **13** : 141.
7. Shukla, J.B. (1996) *Research Report,* Project No. 19/58/86-RE, Department of Environment and Forests, New Delhi, India.
8. Carslaw, H.S. & Jaeger, J.C. (1941) *Operational Methods in Applied Mathematics,* Dover Publication Inc., New York.
9. Seinfield, J.H. (1986) *Atmospheric Chemistry and Physics of Air Pollution,* Wiley, New York, Chapter 13, p. 564-569.
10. Greenberg, M.D. (1971) *Application of Green's Functions in Science and Engineering,* Prentice Hall, Englewood Cliffs, New Jersey, p. 69.
11. Sta Kgold, I. (1979) *Green's Functions and Boundary Value Problems,* Wiley, New York.
12. Morse, P.M. & Feshback, H. (1953) *Methods of theoretical physics Part I and Part II,* McGraw Hill, New York.
13. Friedman, B. (1990) *Principles and Techniques of Applied Mathematics,* Dover Publications, New York, p. 148.

PROC. NAT. ACAD. SCI. INDIA, 73 (A), I, 2003

Even- and odd-mode analysis of interdigital line

A. K. AGRAWAL and HEM RAJ*

**Punjab Engineering College, Chandigarh.*

Present Address : B2G, Ganga Vatika, Muni Ki Reti, Tehri Garhwal, Uttranchal, India.

***Department of Electronics and Communication, Lala Lajpat Rai Institute of Engineering and Technology, Moga-Ferozepur Road, Moga (Punjab), India.*

Received December 27, 2000; Accepted January 30, 2002

Abstract

An interdigital microstrip line has been analysed and its image impedance Z_{it}, and phase constant θ determined as a function of frequency, for the given microstrip dimensions and substrate dielectric constant, for both even and odd numbers of strips. An open circuit Z-matrix was obtained between the voltages and currents of the input and output ports in terms of the coupled microstrip even-and odd-mode characteristic impedances Z_{0e}, Z_{00}, and velocities v_e, v_0, Z_{it}, and θ were then determined from the matrix in each case. The results were compared with those obtained for meander lines, complementary to the corresponding interdigital lines. The curves of Z_{it}, and θ as a function of frequency were also plotted and compared.

(**Keywords** : MICs/microstrips/interdigital line/periodic structures).

Introduction

In a previous paper by Agrawal[1] the analysis of n-coupled microstrips was carried out taking all the couplings into account. This was in contrast with the 'unit cell' approximation used by other authors[2-9] wherein the coupling between the unit cell and other adjacent strips were not considered, thus giving erroneous results.

In this paper, the 'interdigital' line (which is complementary to 'meander' line) has been analysed for n = 3, 4 and 5 coupled microstrips. The iterative impedance Z_{it} and phase shift θ of the interdigital line as a function of the even-and-odd-mode characteristic impedances Z_{0e} and Z_{00}, phase velocities of propagation v_e and v_0, and frequency f have been derived for each value of n. The Z_{it} and θ of the interdigital line have been compared with those of the 'corresponding' complementary meanders previously obtained by Agrawal[1].

Open Circuit Impedance Z-Matrix for a Coupled Line Section

Fig. 1 shows a coupled line section. Assumed fictitious current sources drive the line in the even-and odd-modes, and are denoted by small letters. The port voltages and currents are also defined in the figure. By superposition, the total port currents, I_i can be expressed in terms of the even-and odd-mode currents as

$$I_1 = i_{1e} - i_{30} \qquad I_2 = i_{2e} - i_{40}$$
$$I_3 = i_{1e} + i_{30} \qquad I_4 = i_{2e} + i_{40} \tag{1}$$

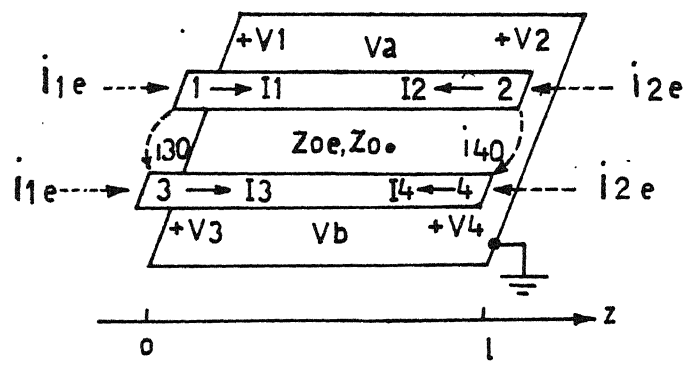

Fig. 1–A parallel coupled line section with even and odd-mode fictitious current sources. The terminal voltages and currents on the strips are shown by capital letters.

First we consider the line as being driven in the even-mode by the i_{1e} current sources. If the other ports are open circuited, the impedance seen at ports 1 or 2 is

$$Z_{in}^{e} = -jZ_{0e}\,\mathrm{Cot}\,\beta_e l \tag{2}$$

where β_e is the phase constant in the even-mode.

The voltage on either conductor can be expressed as

$$V_a^1(z) = V_b^1(z) = V_e^+\left[e^{-j\beta(z-1)} + e^{j\beta(z-1)}\right] = 2V_e^+\mathrm{Cos}\beta_e(1-z) \tag{3}$$

so the voltage at port 1 or 3 is

$$V_a^1(0) = V_b^1(0) = 2V_e^+\mathrm{Cos}\,\beta_e 1 = i_{1e}Z_{in}^{e} \tag{4}$$

Using (2) and (4), V_a^+ is substituted in (3) to get

$$V_a^1(z) = V_b^1(z) = \frac{i_{1e} Z_{in}^e}{\text{Cos}\,\beta_e 1} \text{Cos}\,\beta_e(1-z)$$

$$\frac{-jZ_{0e}\,\text{Cos}\,\beta_e(1-z)}{\text{Sin}\,\beta_e 1}\, i_{1e} \tag{5}$$

Similarly the voltages due to the current sources i_{2e} are

$$V_a^2(z) = V_b^2(z) = -jZ_{0c}\frac{\text{Cos}\,\beta_e z}{\text{Sin}\,\beta_e 1} i_{2e} \tag{6}$$

And the odd-mode voltages due to the current sources i_{30} and i_{40} are

$$V_a^3(z) = V_b^3(z) = -jZ_{00}\frac{\text{Cos}\,\beta_0(1-z)}{\text{Sin}\,\beta_0 1} i_{30} \tag{7}$$

$$V_a^4(z) = V_b^4(z) = -jZ_{00}\frac{\text{Cos}\,\beta_0 z}{\text{Sin}\,\beta_0 1} i_{40} \tag{8}$$

The total voltage on a strip a or b is equal to the sum of voltages due to all the current sources on that strip.

From (1), he fictitious current sources can now be replaced by the terminal currents as

$$i_1 = (I_t + I_3)/2 \qquad i_{2e} = (I_2 + I_4)/2$$

$$i_{30} = (I_3 - I_1)/2 \qquad i_{40} = (I_4 - I_2)/2 \tag{9}$$

The total voltage at port 1 is

$$V_1 = V_a^1(0) + V_a^2(0) + V_a^3(0) + V_a^4(0)$$

$$= - jZ_{0e}\left(i_{1e}\text{Cot}\,\beta_e 1 + i_{2e}\text{Csc}\,\beta_e 1\right) + jZ_{00}\left(i_{30}\text{Cot}\,\beta_0 1 + i_{40}\text{Csc}\,\beta_0 1\right)$$

Using (9) we get

$$2V_1 = -jZ_{0e}\,[(I_1 + I_3)\,\text{Cot}\beta_e 1 + (I_2 + I_4)\,\text{Csc}\beta_e 1] +$$

$$jZ_{00}\,[(I_3 - I_1)\,\text{Cot}\beta_0 1 - (I_4 - I_2)\,\text{Csc}\beta_0 1]$$

or $$V_1 = -j/2[I_1\{Z_{0e}\,\text{Cot}\beta_e 1 + Z_{00}\,\text{Cot}\beta_0 1\} + I_2\{Z_{0e}\,\text{Csc}\beta_e 1 + Z_{00}\,\text{Cot}\beta_0 1\} + I_3\{Z_{0e}\,\text{Cot}\beta_e 1 - Z_{00}\,\text{Cot}\beta_0 1\} + I_4\{Z_{0e}\,\text{Csc}\beta_e 1 - Z_{00}\,\text{Cot}\beta_0 1\} \quad (10)$$

This result yields the top row of the open-circuit impedance matrix [Z] that describes the coupled line section. From symmetry all other matrix elements can be found once the first row s known. The matrix elements are then

$$Z_{11} = Z_{22} = Z_{33} = Z_{44} = -j/2\,(Z_{0e}\text{Cot}\beta_e 1 + Z_{00}\text{Cot}\beta_0 1) \quad (11a)$$

$$Z_{12} = Z_{21} = Z_{34} = Z_{43} = -j/2\,(Z_{0e}\text{Csc}\beta_e 1 + Z_{00}\text{Csc}\beta_0 1) \quad (11b)$$

$$Z_{13} = Z_{31} = Z_{24} = Z_{42} = -j/2\,(Z_{0e}\text{Cot}\beta_e 1 - Z_{00}\text{Cot}\beta_0 1) \quad (11c)$$

$$Z_{14} = Z_{41} = Z_{23} = Z_{32} = -j/2\,(Z_{0e}\text{Csc}\beta_e 1 - Z_{00}\text{Csc}\beta_0 1) \quad (11d)$$

A two port network can be formed from the coupled line section by terminating two of the four ports in either open or short circuits depending on the boundary conditions. The image impedance Z_{it} and dispersion θ of the two port network can then be found out.

A. Coupled Microstrip Interdigital Lines

3-Coupled Microstrip Interdigital Line

The current source excitations of 3-coupled microstrips a, b and c of an interdigital line are shown in Fig. 2. Proceeding as in the case of a pair of coupled microstrips, the terminal voltages can be written as—

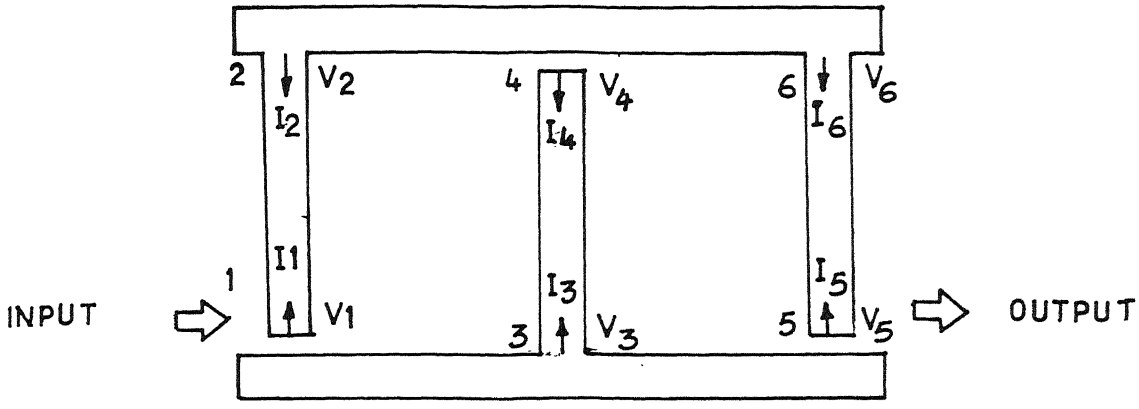

Fig. 2–Interdigital line structure for 3-coupled microstrips.

$$V_1 = -jZ_{0e}\,\mathrm{Csc}\beta_e l\,(i_{1e}\mathrm{Cos}\beta_e l + i_{2e}) + jZ_{00}\mathrm{Csc}\beta_0 l(i_{30}\mathrm{Cos}\beta_0 l + i_{40}) \quad (12a)$$

$$V_2 = -jZ_{0e}\,\mathrm{Csc}\beta_e l\,(i_{1e} + i_{2e}\mathrm{Cos}\beta_e l) - jZ_{00}\,\mathrm{Csc}\beta_e l(i_{30} + i_{40}\mathrm{Cos}\beta_e l) \quad (12b)$$

$$V_3 = -jZ_{0e}\,\mathrm{Csc}\beta_e l\,(i_{1e}\mathrm{Cos}\beta_e l + i_{2e})$$

$$-jZ_{00}\,\mathrm{Csc}\beta_0 l\,[(i_{30} - i_{50})\mathrm{Cos}\beta_e l + (i_{40} - i_{60})] \quad (12c)$$

$$V_4 = -jZ_{0e}\,\mathrm{Csc}\beta_e l\,(i_{1e} + i_{2e}\,\mathrm{Cos}\beta_e l)$$

$$-jZ_{00}\,\mathrm{Csc}\beta_0 l\,[(i_{30} - i_{50}) + (i_{40} - i_{60})\,\mathrm{Cos}\beta_0 l] \quad (12d)$$

$$V_5 = -jZ_{0e}\,\mathrm{Csc}\beta_e l\,(i_{1e}\mathrm{Cos}\beta_e l + i_{2e}) - jZ_{00}\mathrm{Csc}\beta_0 l(i_{50}\mathrm{Cos}\beta_0 l + i_{60}) \quad (12e)$$

$$V_6 = -jZ_{0e}\,\mathrm{Csc}\beta_e l\,(i_{1e} + i_{2e}\mathrm{Cos}\beta_e l) - jZ_{00}\mathrm{Csc}\beta_0 l(i_{50} + i_{60}\mathrm{Cos}\beta_0 l) \quad (12f)$$

where

$$i_{1e} = 1/3\,(I_1 + I_3 + I_5) \qquad i_{2e} = 1/3(I_2 + I_4 + I_6)$$
$$i_{30} = 1/3\,(I_3 + I_5 - 2I_1) \qquad i_{40} = 1/3(I_4 + I_6 - 2I_2)$$
$$i_{50} = 1/3\,(2I_5 - I_1 - I_3) \qquad i_{60} = 1/3(2I_6 - I_2 - I_4) \quad (13)$$

The boundary conditions for the itnerdigital line of Fig. 2 are

$$I_3 = 0 = I_4; \qquad V_2 = V_6$$

$$I_2 = -I_6 \tag{14}$$

Applying the boundary conditions in (12) and (13) and simplifying we obtain a [z] matrix between the input and output quantities as :

$$\begin{bmatrix} V_1 \\ V_5 \end{bmatrix} = \begin{bmatrix} Z_{11} & Z_{15} \\ Z_{51} & Z_{55} \end{bmatrix} \begin{bmatrix} I_1 \\ I_5 \end{bmatrix} \tag{15a}$$

where

$$Z_{11} = Z_{55} = -j/3Z_{0e}\text{Cot}\beta_e 1 + jZ_{00}\{\text{Csc}(2\beta_0 1) - 2/3\text{Cot}\beta_0 1\} \tag{15b}$$

$$Z_{15} = Z_{51} = -j/3Z_{0e}\text{Cot}\beta_e 1 - jZ_{00}\{\text{Csc}(2\beta_0 1) - 1/3\text{Cot}\beta_0 1\} \tag{15c}$$

The iterative impedance of the 3 strip interdigital line is

$$Z_{it(3I)} = \sqrt{Z_{55}^2 - Z_{15}^2} \tag{16a}$$

and dispersion

$$\theta_{(3I)} = \text{Cos}^{-1}\left(\frac{Z_{55}}{Z_{15}}\right) \tag{16b}$$

4-Coupled Microstrip Interdigital Line

The 4-coupled microstrip interdigital line with current source excitations is shown in Fig. 3

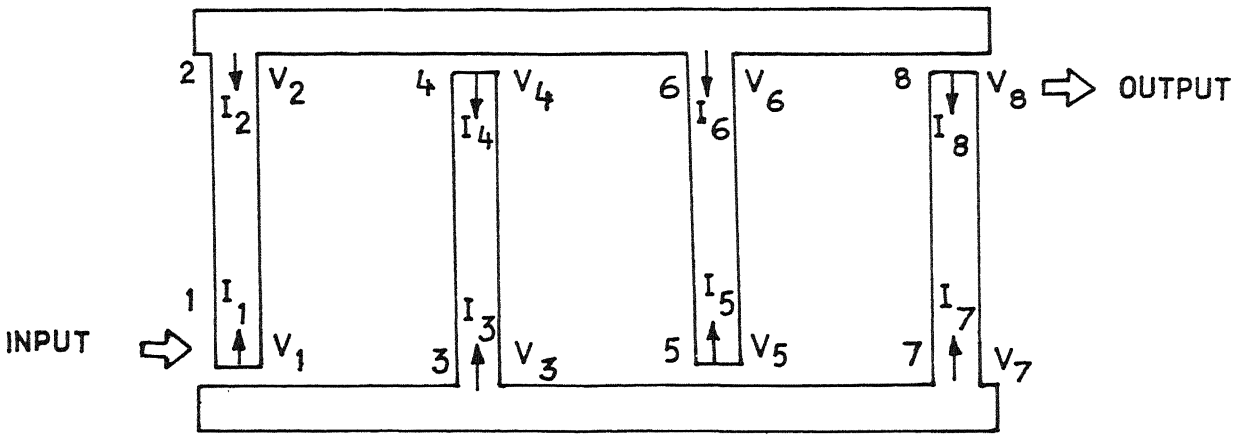

Fig. 3–Interdigital line structure for 4-coupled microstrips

The terminal voltages are given below :

$$V_1 = -jZ_{0e}\,(i_{1e}\mathrm{Cot}\beta_e l + i_{2e}\mathrm{Csc}\beta_e l) + jZ_{00}(i_{30}\mathrm{Cot}\beta_0 l + i_{40}\mathrm{Csc}\beta_0 l) \quad (17a)$$

$$V_2 = -jZ_{0e}\,(i_{1e}\mathrm{Csc}\beta_e l + i_{2e}\mathrm{Cot}\beta_e l) + jZ_{00}(i_{30}\mathrm{Csc}\beta_0 l + i_{40}\mathrm{Cot}\beta_0 l) \quad (17b)$$

$$V_3 = -jZ_{0e}\,(i_{1e}\mathrm{Cot}\beta_e l + i_{2e}\mathrm{Csc}\beta_e l)$$
$$-jZ_{00}\,[(i_{30} - i_{50})\mathrm{Cot}\beta_0 l + (i_{40} - i_{60})]\ \mathrm{Csc}\ \beta_0 l \quad (17c)$$

$$V_4 = -jZ_{0e}\,(i_{1e}\mathrm{Csc}\beta_e l + i_{2e}\mathrm{Cot}\beta_e l)$$
$$-jZ_{00}\,[(i_{30} - i_{50})\mathrm{Csc}\beta_0 l + (i_{40} - i_{60})]\ \mathrm{Cot}\ \beta_0 l \quad (17d)$$

$$V_5 = -jZ_{0e}\,(i_{1e}\mathrm{Cot}\beta_e l + i_{2e}\mathrm{Csc}\beta_e l)$$
$$-jZ_{00}\,[(i_{50} - i_{70})\mathrm{Cot}\beta_0 l + (i_{60} - i_{80})\mathrm{Csc}\ \beta_0 l] \quad (17e)$$

$$V_6 = -jZ_{0e}\,(i_{1e}\mathrm{Csc}\beta_e l + i_{2e}\mathrm{Cot}\beta_e l)$$
$$-jZ_{00}\,[(i_{50} - i_{70})\mathrm{Csc}\beta_0 l + (i_{60} - i_{80})\mathrm{Cot}\ \beta_0 l \quad (17f)$$

$$V_7 = -jZ_{0e}\,(i_{1e}\mathrm{Cot}\beta_e l + i_{2e}\mathrm{Csc}\beta_e l) - jZ_{00}\,(i_{10}\mathrm{Cot}\beta_0 l + i_{80}\mathrm{Csc}\beta_0 l) \quad (17g)$$

$$V_8 = -jZ_{0e}\,(i_{1e}\mathrm{Csc}\beta_e l + i_{2e}\mathrm{Cot}\beta_e l) - jZ_{00}\,(i_{70}\mathrm{Csc}\beta_0 l + i_{80}\mathrm{Cot}\beta_0 l) \quad (17h)$$

where

$$\begin{aligned} i_{1e} &= (I_1 + I_3 + I_5 + I_7)/4; & i_{2e} &= (I_2 + I_4 + I_6 + I_8)/4 \\ i_{30} &= (I_3 + I_5 + I_7 - 3I_1)/4; & i_{40} &= (I_4 + I_6 + I_8 - 3I_2)/4 \\ i_{50} &= (I_5 + I_7 - I_1 - I_3)/2; & i_{60} &= (I_6 + I_8 - I_2 - I_4)/2 \\ i_{70} &= (3I_7 - I_1 - I_3 - I_5)/4; & i_{80} &= (3I_8 - I_2 - I_4 - I_6)/4 \end{aligned} \quad (18)$$

The boundary conditions for a 4-strip interdigital line are :

$$\begin{aligned} I_2 &= -I_6; & V_2 &= V_6 \\ I_3 &= -I_7; & V_3 &= V_7 \\ I_4 &= -I_5 = 0 \end{aligned}$$

On solving the above equations we get an open circuit (Z) matrix between the input and output ports :

$$\begin{bmatrix} V_1 \\ V_8 \end{bmatrix} = \begin{bmatrix} Z_{11} & Z_{18} \\ Z_{81} & Z_{88} \end{bmatrix} \begin{bmatrix} I_1 \\ I_8 \end{bmatrix} \quad (20a)$$

where

$$Z_{11} = Z_{88} = -j/4[Z_{0e}\mathrm{Cot}\beta_e l + Z_{00}\{4\mathrm{Csc}(2\beta_0 l) - 3\mathrm{Cot}\beta_0 l] \quad (20b)$$

$$Z_{18} = Z_{81} = -j/4\{Z_{0e}\mathrm{Csc}\beta_e l + Z_{00}\mathrm{Cot}\beta_0 l\} \quad (20c)$$

and

$$Z_{it(4I)} = \sqrt{Z_{88}^2 - Z_{18}^2} \quad (21a)$$

and dispersion

$$\theta_{(4l)} = \text{Cos}^{-1}\left(\frac{Z_{88}}{Z_{18}}\right) \tag{21b}$$

5-Coupled Microstrip Interdigital Line

Fig. 4 shows the interdigital line structure made up of 5-coupled microstrips. Here also we apply the current sources from both sides of microsrips. The terminal voltage can be written as :

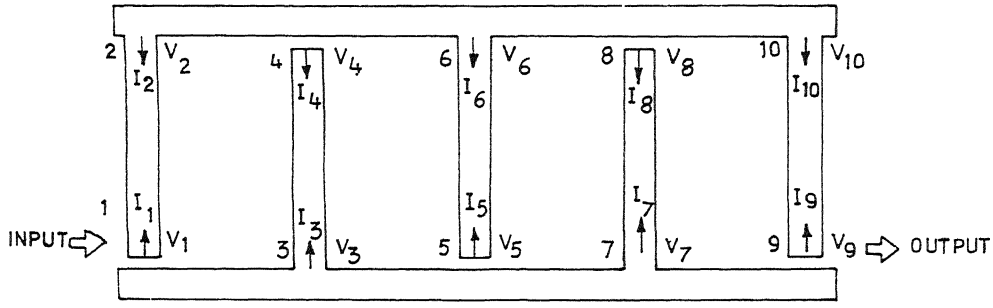

Fig. 4–Interdigital line structure for 5-coupled microstrips

$$V_1 = -jZ_{0e}(j\eta_e \text{Cot}\beta_e l + i_{2e}\text{Csc}\beta_e l) + jZ_{00}(i_{30}\text{Cot}\beta_0 l + i_{40}\text{Csc}\beta_0 l) \tag{22a}$$

$$V_2 = -jZ_{0e}(Z_{ie}\text{Csc}\beta_e l + i_{2e}\text{Cot}\beta_e l) + jZ_{00}(i_{30}\text{Csc}\beta_0 l + i_{40}\text{Cot}\beta_0 l) \tag{22b}$$

$$V_3 = -jZ_{0e}(i_{1e}\text{Cot}\beta_e l + i_{2e}\text{Csc}\beta_e l) + jZ_{00}[(i_{50} - i_{30})\text{Cot}\beta_0 l + (i_{60} - i_{40})\text{Csc}\beta_0 l] \tag{22c}$$

$$V_4 = -jZ_{0e}(i_{1e}\text{Csc}\beta_e l + i_{2e}\text{Cot}\beta_e l) + jZ_{00}[(i_{50} - i_{30})\text{Csc}\beta_0 l + (i_{60} - i_{40})\text{Cot}\beta_0 l] \tag{22d}$$

$$V_5 = -jZ_{0e}(i_{1e}\text{Cot}\beta_e l + i_{2e}\text{Csc}\beta_e l)$$

$$+jZ_{00}\,[(i_{70}-i_{50})\mathrm{Cot}\beta_0 l+(i_{80}-i_{60})\mathrm{Csc}\beta_0 l] \tag{22e}$$

$$V_6=-jZ_{0e}\,(i_{1e}\mathrm{Csc}\beta_e l+i_{2e}\mathrm{Cot}\beta_e l)$$

$$+jZ_{00}\,[(i_{70}-i_{50})\mathrm{Csc}\beta_0 l+(i_{80}-i_{60})\mathrm{Cot}\beta_0 l] \tag{22f}$$

$$V_7=-jZ_{0e}\,(i_{1e}\mathrm{Cot}\beta_e l+i_{2e}\mathrm{Csc}\beta_e l)$$

$$+jZ_{00}\,[(i_{90}-i_{70})\mathrm{Cot}\beta_0 l+(i_{10_o}-i_{80})\mathrm{Csc}\beta_0 l] \tag{22g}$$

$$V_8=-jZ_{0e}\,(i_{1e}\mathrm{Cot}\beta_e l+i_{2e}\mathrm{Csc}\beta_e l)$$

$$+jZ_{00}\,[(i_{90}-i_{70})\mathrm{Csc}\beta_0 l+(i_{10_o}-i_{80})\mathrm{Cot}\beta_0 l] \tag{22h}$$

$$V_9=-jZ_{0e}\,(i_{1e}-\mathrm{Cot}\beta_e l+i_{2e}\mathrm{Csc}\beta_e l)+jZ_{00}(i_{90}\mathrm{Cot}\beta_0 l+i_{10_o}\mathrm{Csc}\beta_0 l) \tag{22i}$$

$$V_{10}=-jZ_{0e}\,(i_{1e}\mathrm{Csc}\beta_e l+i_{2e}\mathrm{Cot}\beta_e l)+jZ_{00}(i_{90}\mathrm{Csc}\beta_0 l+i_{10_o}\mathrm{Cot}\beta_0 l) \tag{22j}$$

where

$$i_{1e}=(I_1+I_3+I_5+I_7+I_9)/5; \qquad i_{2e}=(I_2+I_4+I_6+I_8+I_{10})/5$$

$$i_{30}=(I_3+I_5+I_7+I_9-4I_1)/5; \qquad i_{40}=(I_4+I_6+I_8+I_{10}-4I_2)/5$$

$$i_{50}=[2(I_5+I_7+I_9)-3(I_1+I_3)]/5; \qquad i_{60}=[2(I_6+I_8+I_{10})-3(I_2+I_4)]/5$$

$$i_{70}=[3(I_7+I_9)-2(I_5+I_3+I_1)]/5; \qquad i_{80}=[3(I_8+I_{10})-2(I_6+I_4+I_2)]/5$$

$$i_{70}=(4I_9-I_7-I_5-I_3-I_1)/5; \qquad i_{80}=(4I_{10}-I_8-I_6-I_4-I_2)/5 \tag{23}$$

The boundary conditions for the 5-coupled strips interdigital line shown in Fig. 4 are :

$$I_2=-I_6; \qquad V_2=V_6$$

$$I_3=-I_7; \qquad V_3=V_7$$

$$I_6=-I_{10}; \qquad V_6=V_{10}$$

$$I_4=I_5=I_8=0 \tag{24}$$

Substituting (23) into (22) and using (24) we get an open circuit [Z] matrix between the input and output quantities as given below :

$$\begin{bmatrix} V_1 \\ V_9 \end{bmatrix} = \begin{bmatrix} Z_{11} & Z_{19} \\ Z_{91} & Z_{99} \end{bmatrix} \begin{bmatrix} I_1 \\ I_8 \end{bmatrix} \tag{25a}$$

where $Z_{11} = Z_{99} = -jZ_{0e}/5[\text{Cot}\beta_e 1 + \text{Csc}(2\beta_e 1)]$

$$+ jZ_{00}/5\{4\text{Csc}(2\beta_0 1)\beta_0 1 - 4\text{Cot}\beta_0 1)\} \tag{25b}$$

$$Z_{19} = Z_{91} = (-jZ_{0e}/5)\ \text{Cot}\beta_e 1) + (iZ_{00}/5)\text{Cot}\beta_0 1 \tag{25c}$$

The interative impedance Z_{it} and dispersion θ are then obtained from :

$$Z_{it(5I)} = \sqrt{Z_{99}^2 - Z_{19}^2} \tag{26a}$$

$$\theta_{(5I)} = \text{Cos}^{-1}\left(\frac{Z_{99}}{Z_{19}}\right) \tag{26b}$$

B. Coupled Microstrip Meander Lines

Crampagne and Ahmadpanah[3] had published the Z_{it} and θ curves for a 'unit cell' BCDEF of coupled microstrip meander as shown in Fig. 5. The meander BCDEF is a series connection of BCD and which are uncoupled. Agrawal[1] on the other hand showed the calculated curves for the meander ABCDE whose input and output ports are located at $x = -L/2$ instead of $x = 0$. These curves for a pair of coupled microstrip meanders are shown in Figs. 6(a) and 7(b). The curves obtained by Agarwal (solid lines) reveal that they are not independent of x, the location of the input and output ports of the unit cell. According to Weiss[2] and Crampagne and Ahmadpanah[3] the phase θ had been assumed to be the same for all x, i.e.,

$$V_3(x) = V_1(x)e^{j0} \tag{27}$$

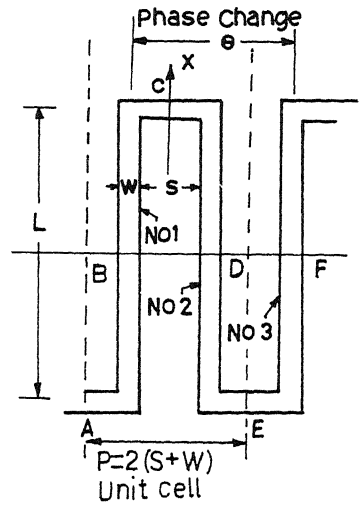

Fig. 5–A unit cell of the periodic array of meanders.

Agrawal[1] showed that their assumption was invalid (by taking all the couplings between the meanders into account and) obtained the Z_{1t} and θ curves for meanders consisting of both the even n and odd $(n-1)$ numbers of lines.

In this paper the same line dimensions and the same variations of Z_{0e}, Z_{00}, v_e, v_0, β_e, β_0 with respect to frequency as assumed by Crampagne and Ahmadpanah[3] have been taken which were plotted with respect to frequency as shown in Fig. 8 by Agrawal[1]. The strip length 1 was 0.01836m. The Z_{it} and θ curves as obtained from the above analysis of intergdigital lines have been compared with the corresponding complementary meanders of Agrawal[1]. The results are discussed below.

Results

3-Microstrip Interdigital Line

Fig. 6 shows the Z_{it} curves of 3 strip interdigital line and 2 (solid curves) and 4 strip meanders, and Fig. 7 shows the θ curves. The 3-strip interdigital line resembles the 2-strip meander except that the pass band of interdigital line is less broad and cut off is sharp. The pass band of 4-strip meander is smallest, and in this case there are two pass bands, within the frequencies of interest. Also, the Z_{it} curves of 4 strip meander are in the opposite sense.

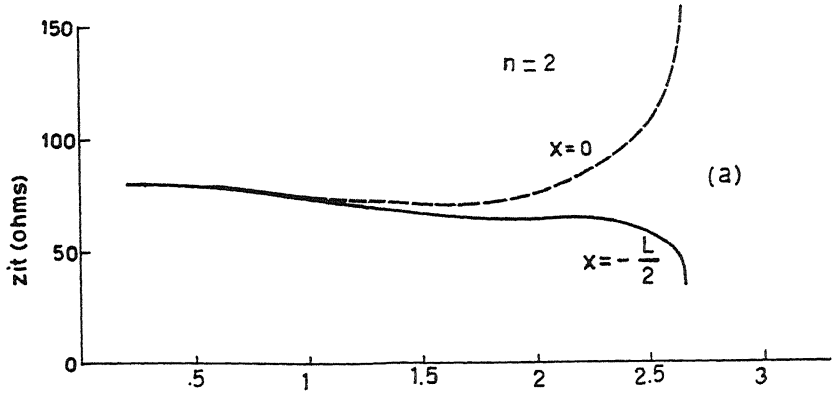

Fig. 6(a)

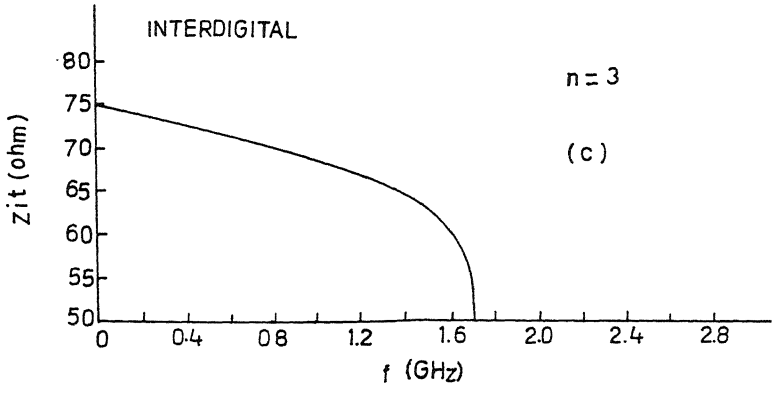

Fig. 6(c)

(Fig. 6b same as Fig. 11(a))

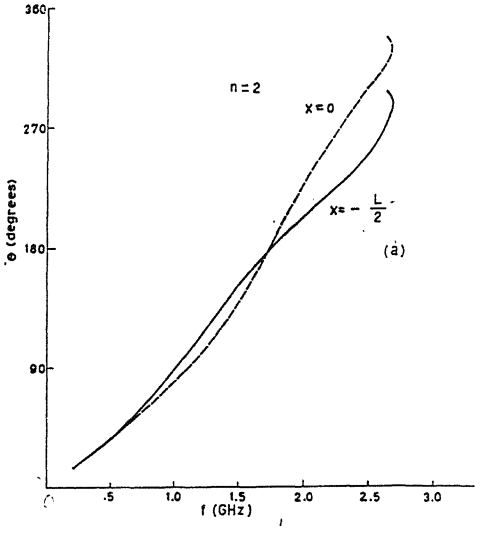

Fig. 7(a)

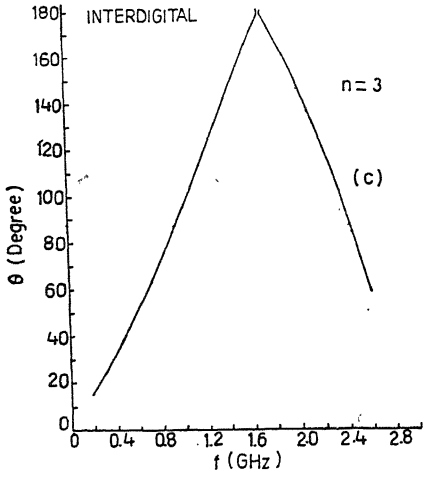

Fig. 7(c)

Figs. 6 & 7–Iterative impedance Z_{it} vs. frequency plots of 3-strip interdigital line compared with 2- and 4-strip meanders; and corresponding dispersion θ vs. frequency plots.

(Fig. 7b same as Fig. 12(a))

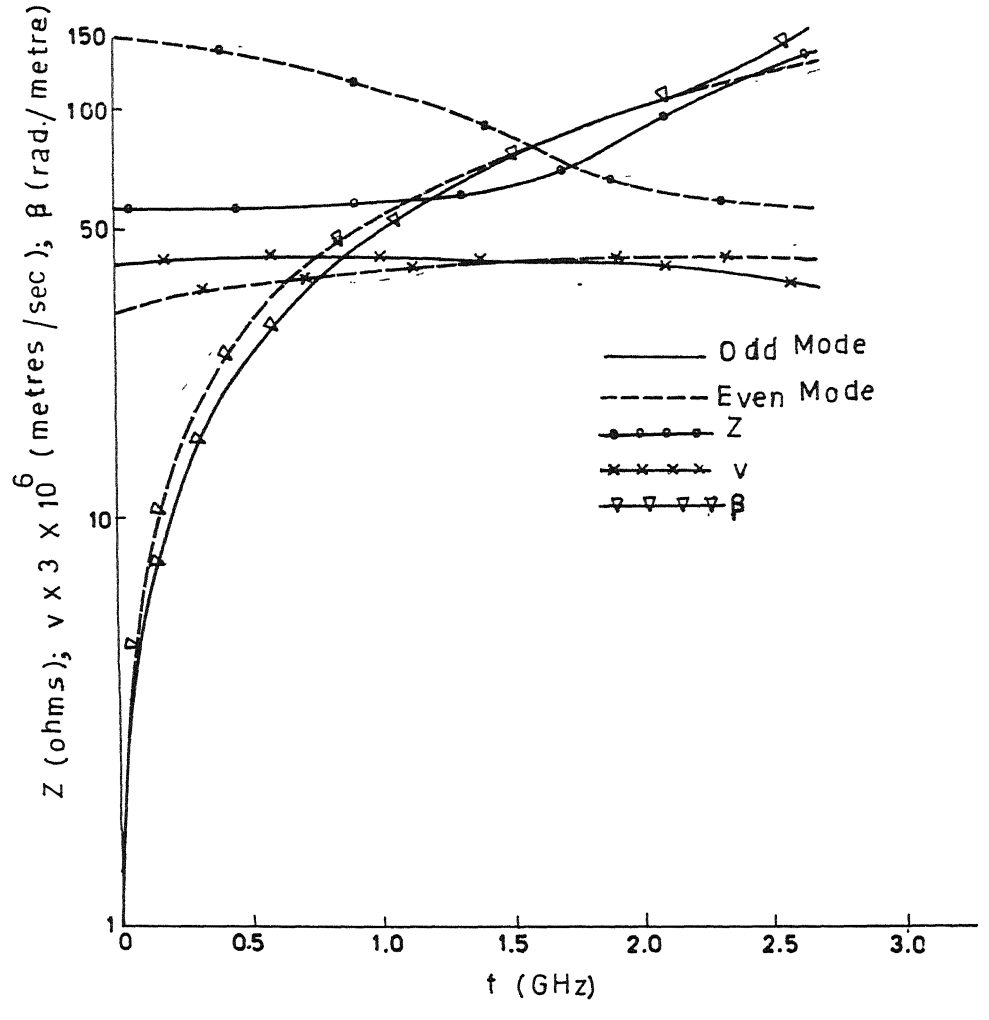

Fig. 8–The characteristic impedance, phase velocity and phase shift constant of the unit cell vs. frequency.

4-Microstrip Interdigital Line

Figs. 9 & 10 show the comparison of 4-strip interdigital line with 3 and 5 strip meanders. The interdigital line has 2 very narrow pass bands. The 3-strip meander has very wide pass bands. The curves for meanders are very different from that of the interdigital line. The number of passbands increases with number of strips. The interdigital lines have sharp cutoff.

Fig. 9(a)

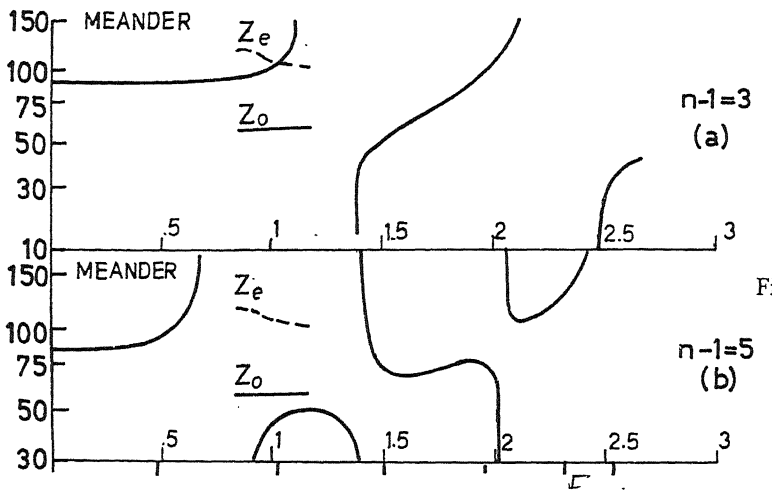

Fig. 9(b)

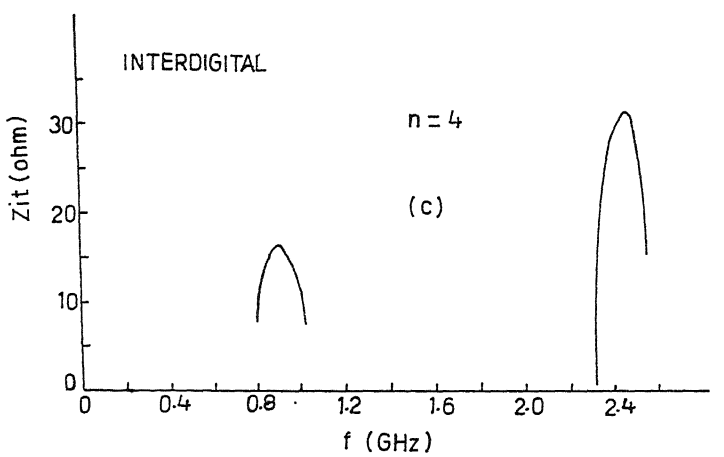

Fig. 9(c)

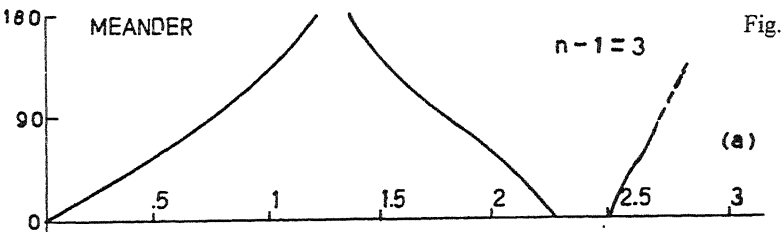

Fig. 10(a)

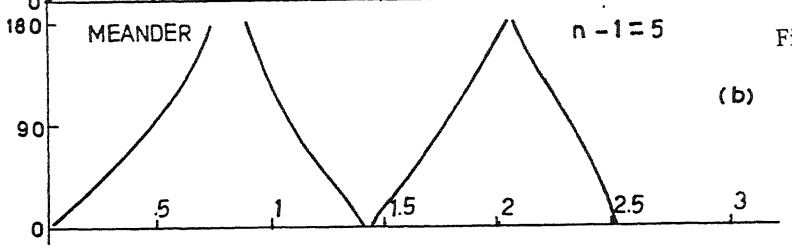

Fig. 10(b)

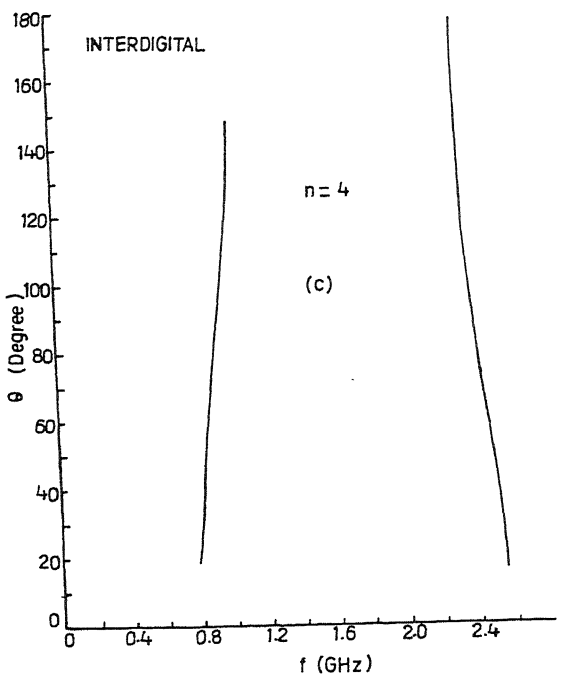

Fig. 10(c)

Figs. 9 & 10–Iterative impedance Z_{it} vs. frequency plots of 4-strip interdigital line compared with 3- and 5-strip meanders; and corresponding dispersion vs. frequency plots.

5-Microstrip Interdigital Line

Figs. 11 and 12 show the comparison of 5-strip interdigital line with 4 and 6 strip meanders.

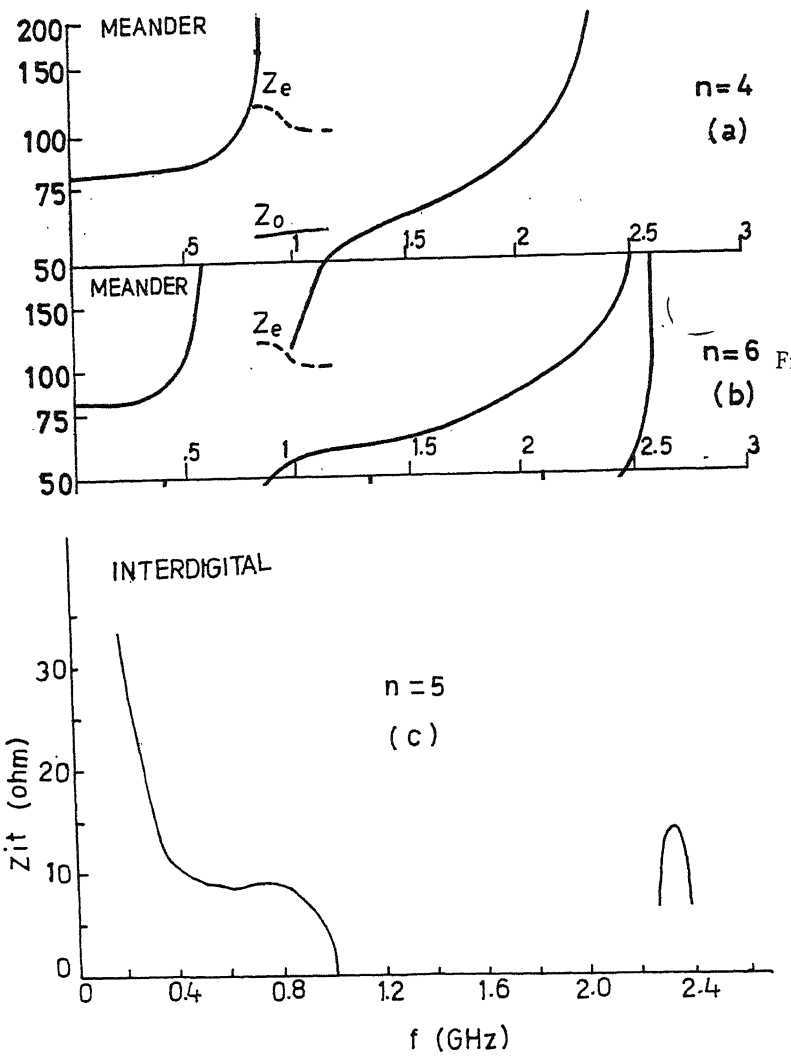

Fig. 6(b)
Fig. 11(a)
Fig. 11(b)

Fig. 11(c)

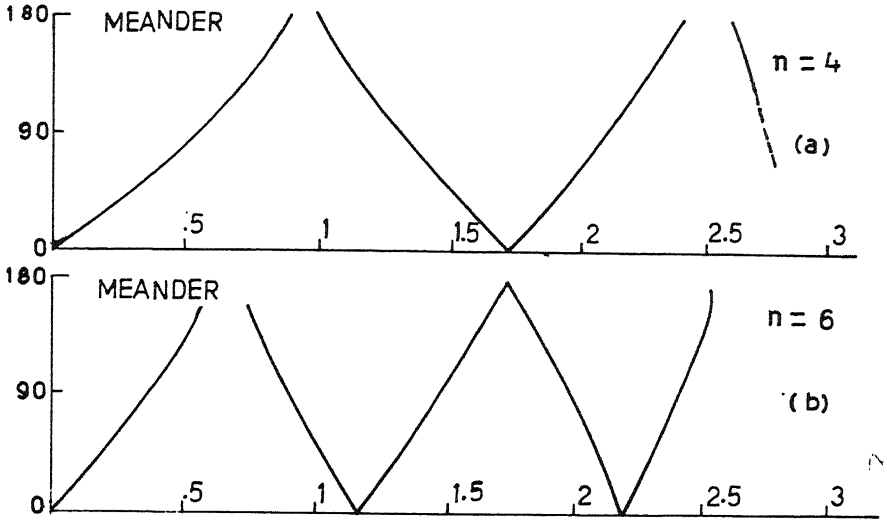

Fig. 7(b)
Fig. 12(a)

Fig. 12(b)

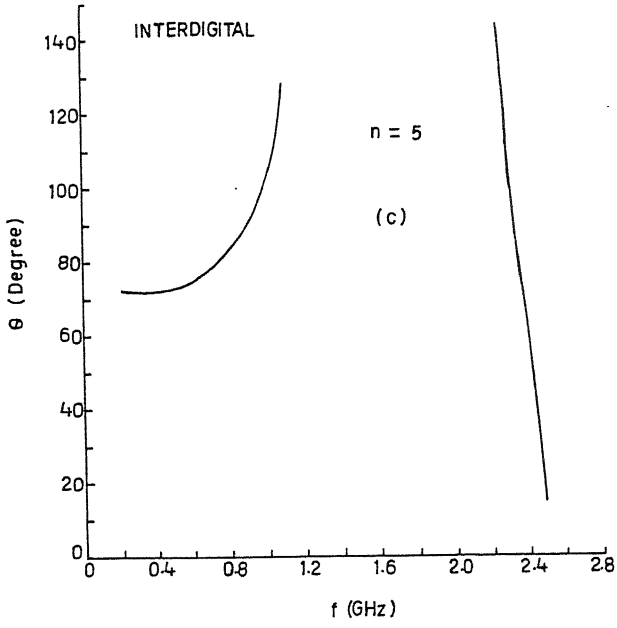

Fig. 12(c)

Figs. 11 & 12– Iterative impedance Z_{it} vs. frequency plots of 5-strip interdigital line coupled with 4- and 6-strip meanders; and corresponding dispersion θ vs. frequency plots.

Here also the interdigital line has a very large stop band and its curve does not resemble those for the complementary meanders, being of opposite sense. The 6-strip meanders has the widest pass band. The interdigital line has the narrowest passband and very sharp cutoff characteristics.

The aforesaid results can be summarised as follows :

As compared to the corresponding complementary meanders the curves for interdigital lines are of opposite sense. By increasing the number of strips the numbers of pass and stop bands increase in both the meanders and interdigital lines. The latter has less number of pass bands in comparison. Odd pairs (2,6,10) of meanders have wider pass bands and even numbers of interdigital lines have narrow pass bands and wide stop bands. These results can be used in the design of filters and other periodic structures. Typical Z_{it} values as a function of frequency are given in the table below—

Number of Strips	Z_{it} (ohms)								Z_0	Z_e
	Interdigital line			Meander line						
$f(GH_Z)$	3	4	5	2	3	4	5	6		
0.5	71.5	∞	9.5	79	88	82	94	∞	57	132
1.0	68.5	10	1.4	72.5	114	∞	44	56	58	109
1.5	62.25	∞	∞	67	52	62	72	63	63	83
2.0	75	∞	∞	64	104	88	71	86	87	62

References

1. Agrawal, A. K. (1980), *IEEE Trans, Microwave Theory Tech. MTT* **-28** : 927.
2. Weiss, J. A. (1974), *IEEE Trans, Microwave Theory Tech. MTT* **22** : 1194.
3. Crampagne R. & Ahmadpanah, M. (1977) *Int. J. Electronics,* **43** : 19.
4. Libbey, W. M. (1973), *IEEE Trans. Microwave Theory Tech. MTT* **-21** : 483.
5. Jones, E.M.T. & Bolljahn, J.T. (1956), *IRE Trans, Microwave Theory Tech. MTT* **-4** : 75.
6. Matthaei, G. L., Young, L. & Jones, E.M.T. (1964), "*Microwave Filters, Impedance matching networks & coupling structures*", McGraw Hill : 49.
7. Rizzi, P. A. (1988), "*Microwave Engineering-Passive Circuits*", Prentice Hall : 190
8. Collin, R. E. (1992), "*Foundations for microwave Engineering*", McGraw Hill : 125.
9. Bhat, B. & Koul, S. K. (1989), "*Strip like transmission lines for microwave integrated circuits*", Wiley Eastern : 566.

PROC. NAT. ACAD. SCI. INDIA, 73 (A), I, 2003

Statistical study of molecular ordering in MBA : A nematic liquid crystal

S. N. TIWARI, M. MISHRA and NITISH K. SANYAL*

Department of Physics, D.D.U. Gorakhpur University, Gorakhpur-273009, India.

**Vice-Chancellor, U. P. Rajarshi Tandon Open University, Allahabad-211001.*

Received April 26, 2001; Revised March 27, 2002; Accepted June 20, 2002

Abstract

The peculiar changes - characteristics of mesomorphic behaviour which occur at phase transitions, are primarily governed by the intermolecular interactions acting between sides, planes and ends of a pair of liquid crystalline molecules. In view of this fact, intermolecular interactions between a pair of MBA molecules have been evaluated using modified second order perturbation treatment along with multicentred-multipole expansion technique. An all valence electron method, CNDO/2, has been employed to compute the net atomic charge and corresponding dipole moments located at each atomic centre of the liquid crystal molecule. Using the results of stacking and in-plane interaction energy studies, probability calculations at varied angular and positional configurations in a molecular pair of MBA, have been carried out using Maxwell-Boltzmann formula. An attempt has been made to elucidate the nematogenic behaviour of 4′-methoxybenzylidene – 4 – acetoxyaniline (MBA) molecules.

(**Keywords** : nematic liquid crystal / molecular ordering / mesogen / CNDO / multicentred - multipole)

Introduction

Liquid crystalline phases are stable condensed phases in which molecules pack together with an order that is intermediate between the three-dimensional order of a crystalline solid and the disorder of an isotropic (ordinary) liquid. Liquid crystalline phases always have partial orientational order of the molecules and some liquid crystalline phases also have partial positional order of the molecules. The partial molecular ordering that is a characteristic of liquid crystallinity occurs frequently in natural and synthetic materials. Thus, liquid crystals are of considerable basic and applied interest[1,2].

The peculiar changes-characteristics of mesomorphic behaviour which occur at phase transitions, are primarily governed by the nature and strength of various types of intermolecular interactions acting between sides, planes and ends of a pair of

molecules[3]. In view of the key role of molecular interactions in mesogenic compounds, semi-emperical calculations have been emphasized by several workers to explain liquid crystallinity[4]. Perrin and Berges have employed PCILO, INDO, CNDO etc. methods to analyse (i) the internal rotations, (ii) possibilities of motion in aromatic core as well as in the terminal chains, and (iii) the influence of conjunction between the oxygen lone pairs and the benzene ring on the internal rotations in several mesomorphic compounds[5, 6]. Tokita *et al*[7] used Lennard – Jones potential to evaluate intermolecular interactions between a couple of pure nematogens and attempted to correlate their results with those of the molecular field theory[8] . However, it has been observed that '6-exp' type of potential functions are found to be more effective in explaining the molecular packing instead of 'Lennard – Jones' potentials[9].

Using Buckingham '6-exp' type of potential function, intermolecular interaction energy studies have been carried out in case of some mesogens in our laboratory[10-14]. It has been observed that the pair potential between such molecules is anisotropic in nature which is in general regarded as the prime requirement for the mesophase formation in thermotropic liquid crystals[15]. The minimum energy configurations obtained through such theoretical calculations correspond to the crystallographic structure of molecules in the solid state. Similar observations have been reported by others also[16]. Although considerable progress has been made in understanding the liquid crystalline phases using computer simulation techniques[17-20], it seems pertinent to study simple models in detail with an aim to elucidate the nature and strength of molecular forces, molecular ordering, orientational freedom etc. Since mesogenic properties are related to molecular aggregation in a specific manner, probability distribution calculations based on interaction energy results are expected to provide information about most probable molecular aggregation and tendency to retain translational/orientational order at different transition temperatures.

In the light of the above facts, relative probabilities of various configurations obtained through interaction energy calculations have been examined in case of some mesogens[21-23]. The present paper embodies the results of probability studies carried out in case of 4′-methoxybenzylidene – 4 – acetoxyaniline (MBA). The thermodynamic parameters reveal that MBA shows crystal to nematic transition at 358.2 K and nematic to isotropic melt at 382 K[24].

Method of Calculation

The molecular geometry of MBA has been constructed using crystallographic data from literature and standard values of bond lengths and bond angles[25]. Net charge and corresponding dipole moment components at each of the atomic centres of the

molecule have been computed by CNDO/2 method[26]. Modified Rayleigh-Schrodinger second order perturbation theory alongwith multicentred-multipole expansion technique as developed by Claverie and coworkers has been used to calculate intermolecular interaction energy between a couple of MBA molecules. According to this method, the total interaction energy (E_{TOT}) between two molecules is expressed as[27]:

$$E_{TOT} = E_{EL}+E_{POL}+E_{DISP}+E_{REP} \quad (1)$$

where E_{EL}, E_{POL}, E_{DISP} and E_{REP} represent electrostatic, polarization, dispersion and repulsion energy components respectively. The formulae for various energy terms are given as under.

Electrostatic energy :

According to the multicentred-multipole expansion method[28], the electrostatic energy term is expressed as :

$$E_{EL} = E_{QQ}+E_{QMI}+E_{MIMI} +..... \quad (2)$$

where E_{QQ}, E_{QMI} and E_{MIMI} etc. represent monopole-monopole, monopole-dipole, dipole-dipole and interaction energy terms consisting of multipoles of higher orders respectively. However, consideration up to the first three terms has been found to be sufficient for most of the molecular interaction problems[28,29]. Hence, only three terms have been included in the present calculation.

Polarization Energy :

The polarization energy of some molecule (say, s) is obtained as a sum of the polarization energies for the various bonds :

$$E_{POL} = C(-1/2)\sum_{u}^{(s)} \varepsilon_u^{[S]}.A_u^{(S)}.\varepsilon_u^{[S]} \quad (3)$$

where $$\varepsilon_u^{[S]} = \sum_{t\neq s}\sum_{\lambda}^{(t)} q_\lambda^{(t)} R_{\lambda u}/(R_{\lambda u})^3 \quad (4)$$

is the electric field created at the bond u by all surrounding molecules and A_u is the polarizability tensor of this bond. $R_{\lambda u}$ is the vector joining the atom λ in molecule (t) to the 'centre of polarizable charge' on bond *u* of molecule (s).

Dispersion and Repulsion Energy:

Dispersion and repulsion terms are calculated together using Kitaigorodskii type of formula as given below [30,31]:

$$E_{DISP} + E_{REP} = \sum_{\lambda}^{(1)} \sum_{\nu}^{(2)} E(\lambda, \nu), \tag{5}$$

where

$$E(\lambda, \nu) = K_\lambda K_\nu (-A/z^6 + Be^{-\gamma z}) \tag{6}$$

and

$$z = R_{\lambda\nu} / R^0_{\lambda\nu} = \sqrt{(2R^w_\lambda)(2R^w_\nu)} \tag{7}$$

where R^w_λ and R^w_ν are the van der Waals radii of atoms λ and ν respectively. The parameters *A*, *B* and γ do not depend on the atomic species: this necessary dependence is brought about by $R^0_{\lambda\nu}$ and the factors K_λ and K_ν which allow the energy minimum to have different values according to the atomic species involved[32]. The values of these various parameters and of the van der Waals radii have been given by Caillet and Claverie[33,34].

The energy minimization has been carried out for both stacking and in-plane (side to side and end to end) interactions separately. One of the interacting molecules is kept fixed throughout the process while both lateral and angular variations are introduced in the other in all respects relative to the fixed one. The first molecule has been assumed to be in the *X*-*Y* plane with *X*-axis lying along the long molecular axis while the origin is chosen approximately at the centre of mass of the molecule. The second molecule has been translated initially along the *Z*-axis (perpendicular to the molecular plane) and subsequently along *X*-and *Y*-axes. Variation of interaction energy with respect to rotation about *Z*-axis has been examined in the range of $\pm 60^0$.

Accuracies up to $0.1A^0$ in sliding (translation) and 1^0 in rotation have been achieved. The details of the mathematical formalism and optimization process may be found in literature [10, 14, 27].

The calculation of probabilities have been carried out using Maxwell-Boltzmann formula [35] as given below:

$$P_i = \exp(-\beta\varepsilon_i) / \sum_i \exp(-\beta\varepsilon_i) \quad (8)$$

where Pi stands for the probability corresponding to the configuration i; $\beta = 1/kT$, where k and T are Boltzmann constant and absolute temperature respectively and ε_i represents the energy of configuration i relative to the minimum energy value in a particular set for which the probability distribution is being computed. Molecular charge distribution, stacking and in-plane (side to side) interaction energy results are published elsewhere[11]. In this paper, results obtained from probability distribution calculations have been reported.

Results and Discussion

The molecular geometry of MBA has been shown in Fig. 1. The variation of probability with respect to translation of one of the stacked molecules along the Z-axis corresponding to four sets of axial rotation viz. $X(0^0)Y(0^0)$, $X(0^0)Y(180^0)$, $X(180^0)Y(0^0)$ and $X(180^0)Y(180^0)$ has been depicted in Fig. 2. It is observed that configuration $X(0^0)Y(180^0)$ and $X(180^0)Y(180^0)$ show a sharp peak at the same inter-planar separation, $4.0A^0$ with nearly equal probability i.e. 91%. Below $4.0A^0$, the probability of occurrence of these configurations reduces to zero. The configuration $X(0^0)Y(0^0)$ and $X(180^0)Y(0^0)$ show their maxima at $4.5A^0$ with probability values nearly 70% and 60% respectively. An analysis of the relative probability of being at maximum point corresponding to four temperatures *viz.* 300K (room temperature), 358.2K (solid to nematic), 382.0K(nematic to isotropic) and 500K (above room temperature), is shown in Table 1. As evident from this table, the configuration $X(180^0)Y(180^0)$ has almost 66% probability of occurrence at nematic to isotropic transition temperature while configurations $X(0^0)$ $Y(0^0)$ and $X(0^0)$ $Y(180^0)$ have nearly probabilities 7% and 27% respectively. The remaining one configuration namely, $X(180^0)Y(0^0)$ possesses negligible probability. This indicates that in a stacked pair of MBA molecules, the probability of the configuration in which one of the molecules is rotated by 180^0 both about X and Y-axes relative to the other, is maximum.

Table 1– Comparative probability of the minimum energy stacked complexes of MBA molecules with respect to translation along Z-axis corresponding to various rotational sets

Configuration	Separation (A^0)	Energy (kcal/mole)	Probability (%)			
			T= 300K	T= 358.2K	T= 382K	T=500K
$X(0)Y(0)$	4.0	-6.90	3.98	5.95	6.74	10.30
$X(180)Y(0)$	4.5	-4.71	0.10	0.27	0.37	1.13
$X(0)Y(180)$	4.0	-7.97	23.64	26.42	27.28	29.97
$X(180)Y(180)$	4.0	-8.63	72.27	67.34	65.59	58.50

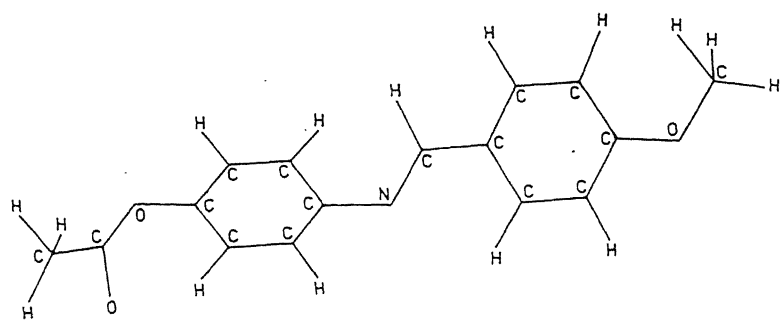

Fig. 1–Molecular geometry of 4′-methoxybenzylidene-4-acetoxyaniline (MBA).

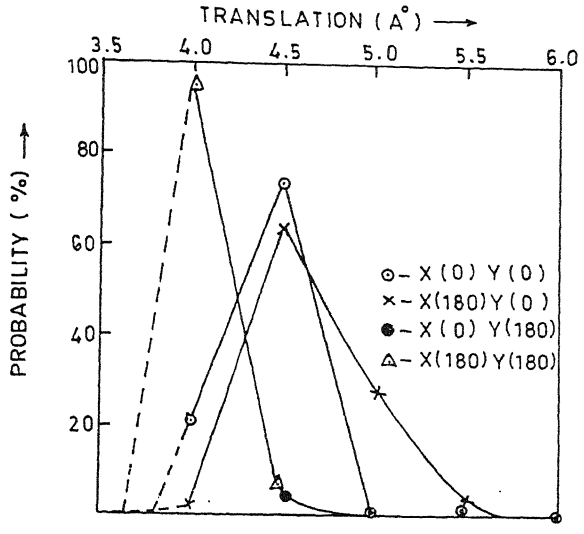

Fig. 2–Variation of probability with respect to translation of one of the stacked molecules along Z-axis corresponding to four distinct rotational sets namely $X(0^0)Y(0^0)$, $X(0^0)Y(180^0)$, $X(180^0)Y(0^0)$ and $X(180^0)Y(180^0)$ at 300K.

Fig. 3 represents the variation of probability with respect to translation of one of the stacked molecules along the long molecular axis (X-axis) for configuration $X(180^0)$ $Y(180^0)$ in the range of $\pm$ 10A^0 corresponding to three selective rotations about Z-axis by 0^0, 90^0 and 270^0 .The inter-planar separation between the molecules is 4.0A^0. The energy obtained in case of $Z(180^0)$ is always repulsive. Hence, probability is found to be zero at each point in this case. It may be observed that configuration $Z(0^0)$ shows a relatively sharp peak with a maximum probability of 52% at room temperature while $Z(90^0)$ and $Z(270^0)$ curves exhibit lesser values. Comparative probability of minimum energy stacked complexes with respect to translation along X-axis, is shown in Table 2 which shows that configuration $Z(0^0)$ has maximum probability of occurrence, 97% at nematic to isotropic transition temperature.

A graphical representation of the probability distribution with respect to translation of one of the stacked molecules along an axis perpendicular to the long molecular axis and lying in the molecular plane (Y-axis) in the range of $\pm$2.0A^0 has been shown in Fig. 4 which indicates an overlapped structure as most probable one. Since the peak is not very sharp, translation along this axis in a very small range (<0.5A^0) is probable at increased thermal agitations. Fig. 5 exhibits the variation of

probability with respect to rotation about *Z*-axis in the range of $\pm 60^0$ at 300K. It is evident from this figure that maximum probability (approximately 61%) lies at perfectly aligned structure.

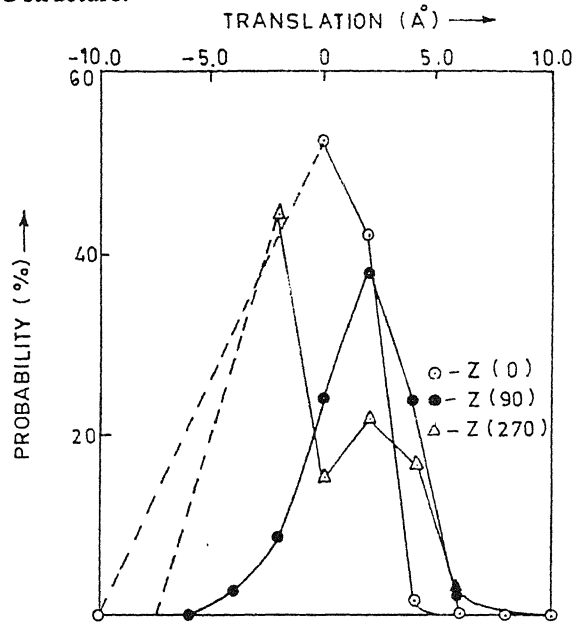

Fig. 3–Variation of probability with respect to translation along the long molecular axis (X-axis) in the range of $\pm$ 10.0A^0 corresponding to three selective rotations about Z-axis *viz.* $Z(0^0)$, $Z(90^0)$ and $Z(270^0)$. The inter-planar separation between the molecules is 4.0A^0 at 300K.

Table 2– Comparative probability of the minimum energy stacked complexes of MBA molecules with respect to translation along the long molecular axis corresponding to four selective rotations about *Z*-axis

Rotation about *Z*-axis	Energy (kcal/mole)	Probability (%)			
		T=300K	*T*=358.2K	*T*=382K	*T*=500K
0^0	-8.63	99.07	97.81	97.13	92.64
90^0	-5.58	0.58	1.33	1.73	4.28
180^0	–	–	–	–	–
270^0	-5.24	0.33	0.84	1.12	3.07

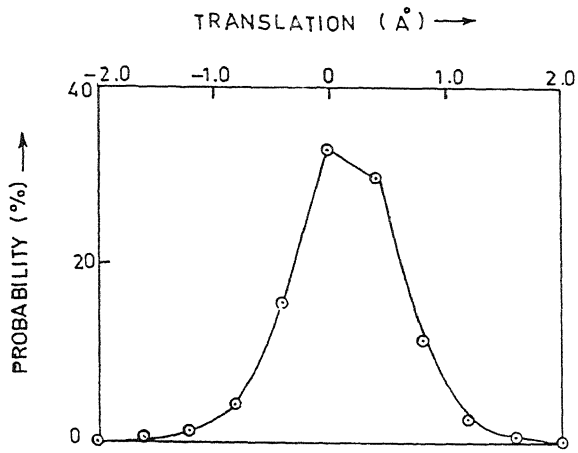

Fig 4–A graphical representation of the probability distribution with respect to translation of one of the stacked molecules along an axis perpendicular to long molecular axis (*Y*-axis) in the range of ± 2.0A^0 at 300K.

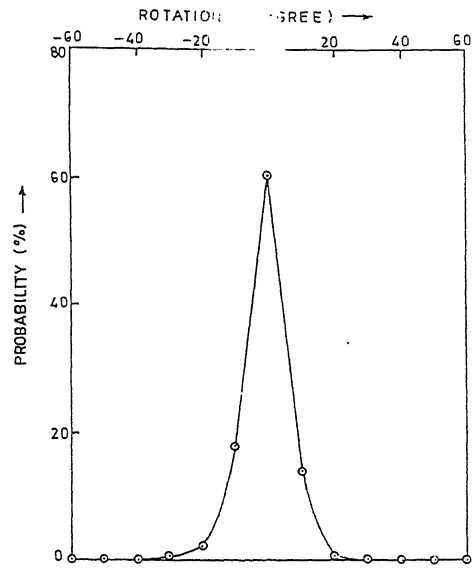

Fig. 5–Variation of probability with respect to rotation about Z-axis in the range of ± 60^0. One of the stacked molecules has *X*(180^0) *Y*(180^0) *Z*(0^0) configuration with respect to other and is separated at an inter-planar distance of 4.0A^0 at 300K.

The variation of probability at 300K with respect to in-plane (side to side) translation of one of the interacting molecules along *X*-axis has been plotted in Fig. 6. The intermolecular separation along *Y*-axis is 7.0A^0 and one of the molecules possesses $X(0^0)Y(180^0)Z(0^0)$ configuration. As evident from this figure, maximum probability (nearly 30%) occurs when one of the interacting molecules is displaced by 6.0A^0 along *X*-axis with a simultaneous rotation of 180^0 about *Y*-axis. Fig. 7 shows a plot of probability distribution for translation of one of the interacting molecules along *Y*-axis during in-plane interactions at an interval of 0.2A^0. This figure shows a sharp peak at an intermolecular separation of 7.0A^0. Further, it may be observed here that like the case of stacking interactions, distinct maximum exists during in-plane interactions in both the cases (Fig. 6 & Fig. 7).

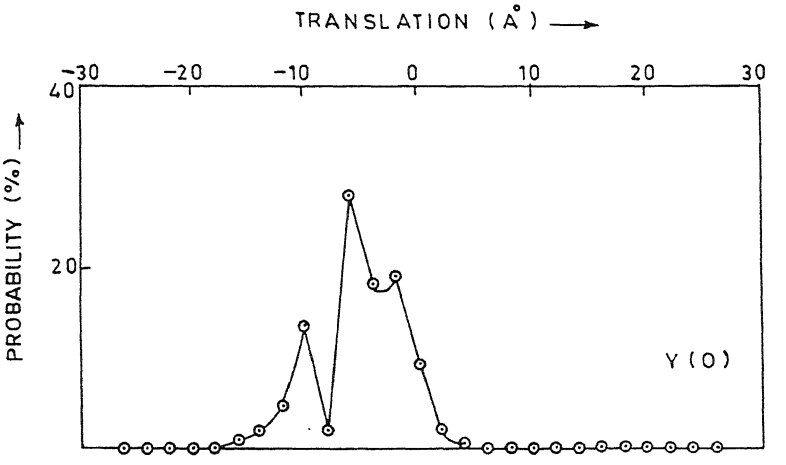

Fig. 6–A plot of probability distribution for in-plane (side to side) translation of one of the interacting molecules along *X*-axis. The intermolecular separation (along *Y*-axis) is 7.0 A^0 and one of the molecules possesses $X(0^0)Y(180^0)$ $Z(0^0)$ configuration at 300K.

The variation of probability with respect to change of inter-group separation during terminal interactions for the energetically most stable interacting terminal groups *viz.* (–OCOCH$_3$ .....H$_3$COCO–) configuration has been shown in Fig.8. It is observed from this figure that probability of any stable end to end configuration is very small (< 7 %) even at room temperature. The optimum end to end separation in this case (–OCOCH$_3$ .....H$_3$COCO–), is 3.03A^0 whereas the centre of mass positions of interacting MBA molecules are separated by 18.8A^0. Further other possible interacting groups i.e. (–OCOCH$_3$ .....H$_3$CO–) and (–OCH$_3$ .....H$_3$CO–) show negligible probability of occurrence.

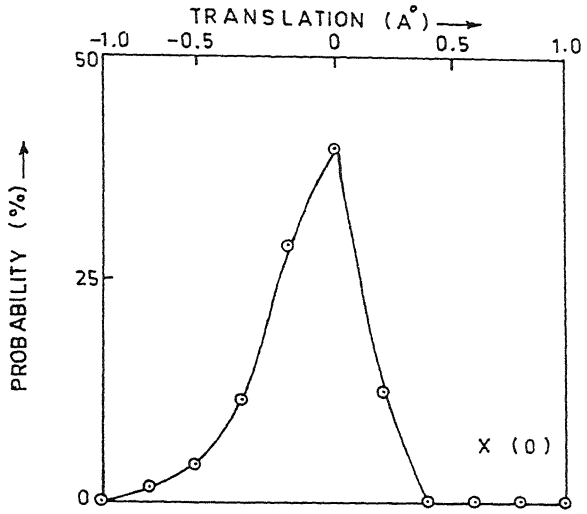

Fig. 7–A plot of probability distribution for translation of one of the interacting molecules along *Y*-axis during in-plane (side to side) interactions at an interval of $0.2A^0$. The initial value of intermolecular separation is 7.0 A^0 at 300K.

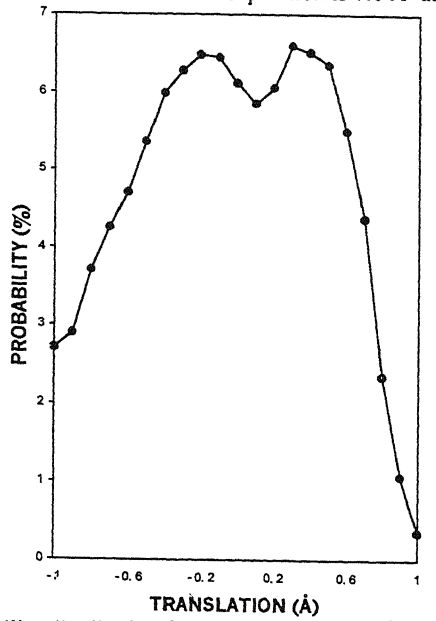

Fig. 8–A plot of probability distribution for translation of one of the molecules along *X*-axis during in-plane (end to end) interactions corresponding to -$OCOCH_3$-----H_3COCO- interacting groups at an interval of $0.1A^0$. The initial value of intermolecular separation is $19.0A^0$ while optimum end to end distance is 3.03 A^0. The calculation has been carried out at 300K.

Table 3– Translational and rotational rigidities corresponding to most probable configuration during stacking, in – plane (side to side) and terminal (end to end) interactions in case of a pair of MBA molecules at various temperatures.

Temperature (K)	Translational Rigidity						Rotational Rigidity about *Z*-axis ($\pm 10^0$)
	Stacking			In-plane (side to side)		Terminal	
	X-axis ($+2.0A^0$)*	*Y*-axis ($\pm 0.4A^0$)	*Z*-axis ($+0.5A^0$)**	*X*-axis ($\pm 2.0A^0$)	*Y*-axis ($\pm 0.2A^0$)	*X*-axis ($\pm 0.2A^0$)	
300.0	1.26	0.74	18.71	1.38	0.96	0.59	1.82
358.2	1.21	0.69	11.63	1.24	0.88	0.57	1.48
382.0	1.20	0.68	9.97	1.22	0.85	0.56	1.38
500.0	1.15	0.64	5.80	1.04	0.76	0.55	1.09

*At $-2.0A^0$ interaction energy comes out to be repulsive due to violation of van der Waal's contact distance and hence probability of the configuration vanishes as shown in Fig.3.

** At $3.5A^0$ interaction energy comes out to be repulsive due to violation of van der Waal's contact distance and hence probability of the configuration vanishes as shown in Fig.2

Translational and rotational rigidities corresponding to most probable configurations during stacking, in-plane and terminal interactions at different temperatures, have been shown in Table 3. It should be mentioned here that rotational rigidity has been defined as the probability ratio of being at maximum to that corresponding to $\pm 10^0$ of rotations. Translational rigidity has been defined as the probability ratio of being at maximum to that corresponding to $\pm 2.0A^0$, $\pm 0.4A^0$ and $\pm 0.5A^0$ of translations of one of the stacked molecules along *X*-, *Y*- and *Z*-axes respectively during stacking interactions. During in-plane (side to side) interactions translational rigidity has been calculated in a range of $\pm 2.0A^0$ for *X*-sliding and $\pm 0.2A^0$ for *Y*-sliding whereas the same has been considered in the range of $\pm 0.2A^0$ for translation along *X*-axis during in-plane (end to end) interactions. As evident from

Table 3, both rotational and translational rigidities decrease with increase in temperature in each case. The probability of any stable configuration during terminal interactions is poor. Similarly during stacking and in–plane (side to side) interactions, there is a lesser probability of existence of stable configurations corresponding to the translation along an axis perpendicular to the long molecular axis (*Y*-axis). Further, during translation of one of the stacked molecules along *X*- and *Z*-axes, interaction energy comes out to be repulsive at the intermolecular separation of $-2.0\ A^0$ and $3.5A^0$ respectively due to the violation of van der Waal contact distances in both the cases (Fig. 3 & Fig. 2). However, these results favour nematic behaviour of the system. Similar results have been obtained in case of para-azoxyanisole[21].

Conclusion

It seems that MBA exhibits a strong preference for aligned structure at transition temperature. In a stacked molecular pair both orientational flexibility and transitional freedom are found to be small corresponding to minimum energy configuration. Other configurations show greater translational flexibility alongwith their intrinsic preference for aligned structure which accounts for the nematic behaviour of the molecule

Acknowledgements

One of the author (SNT) thanks the UGC, New Delhi, for providing Minor Research Project.

References

1. de Gennes, P. G. & Porst, J. (1993) *The Physics of Liquid Crystals,* Clarendon Press : Oxford.
2. Chandrasekhar, S. (1992) *Liquid Crystals,* Cambridge University Press: Cambridge.
3. Gray, G. W. (1962) *Molecular Structure and Properties of Liquid Crystals,* Academic Press : New York.
4. Cotrait, M., Marsau, P., Pesquer, M. & Volpilhac, V. (1982) *J. Physique* **43** : 355.
5. Berges, J. & Perrin, H. (1981) *J Chim Physique* **78** : 873; (1984) *Mol Cryst Liq Cryst* **113** : 269.
6. Perrin, H. & Berges, J. (1982) *J Physique Lett* **43** : 531.
7. Tokita, K., Fujimura, K., Kondo, S. & Takeda, M. (1981) *Mol Cryst Liq Cryst Lett* **64** : 171.
8. Maier, W. & Saupe, A. (1958); (1959); (1960) *Z Naturforsch* **13A** : 568; **14A** : 882; **15A** : 287.
9. Pawley,G. S. (1987) *Phys Stat Sol* **20** : 347.
10. Tiwari, S. N., Roychoudhury, M. & Sanyal, N. K. (1987) in *Proc. Second Asia Pacific Physics Conference*, Chandrasekhar, S. ed., World Sci. Pub. Comp., Singapore, Vol. **2** : 1081.

11. Tiwari, S. N., Roychoudhury, M. & Sanyal, N. K. (1991) *Mol. Cryst. Liq. Cryst.*, **204** :111.
12. Tiwari, S. N. & Sanyal, N. K. (1999) in *Condensed Matter Physics*, eds., Agrawal, B.K & Prakash, H., Narosa Publishing House, New Delhi, p.182.
13. Tiwari, S. N. & Sanyal, N. K. (2001) *Proc. Nat. Acad. Sci., India*, **71A** : 53.
14. Tiwari, S. N., Mishra, M. & Sanyal, N. K. (2002) *Indian J. Phys.* **76B** : 11.
15. Bates, M. A., Luckhurst,G. R. (1997) *Chem. Phys. Lett.* **281** : 193.
16. Ojha, D. P., Kumar, D. & Pisipati, V. G. K. M. (2002) *Cryst. Res. Technol.* **37** : 83.
17. Smondyrev, A. M. & Phcovtis, R. A. (1999) *Liq. Cryst.* **26** : 235.
18. Luckhurst, G. R. & Romono, S. (1999) *Liq. Cryst.* **26** : 871.
19. Sarman, S. (2000) *Molecular Physics* **98** : 27.
20. Bharadwaj, R. K., Bunning, T. J. & Farmer, B. L. (2000) *Liq. Cryst.* **27** : 591.
21. Tiwari, S. N., Roychoudhury, M., Ojha, D.P.,& Sanyal, N. K.(1990) in *Advances in Statistical Physics of Solids and Liquids,* eds. Prakash, S. and Pathak, K. N.,Wiley Eastern Ltd., New Delhi, p .370.
22. Roychoudhury, M., Ojha, D. P. & Sanyal, N. K. (1994) *Indian J. Pure App. Phys.* **32** : 440.
23. Tiwari, S. N., Mishra, M. & Sanyal, N. K. (2002) in preparation.
24. Barrell, E. M. & Johnson, J. F. (1974) in *Liquid Crystals and Plastic Crystals,* eds. Gray, G. W. & Winsor, P. A., John Wiley, New York, p.254.
25. Bar, I. & Bernstein, J. (1977) *Acta Cryst,* **B33** : 738.
26. Pople, J. A. & Beveridge, D.L. (1970) *Approximate Molecular Orbital Theory*, Mc-Graw Hill, New York.
27. Claverie, P. (1978) in *Intermolecular Interactions: From Diatomics to Biopolymers*, ed. Pullman, B., John Wiley , New York, p. 69.
28. Rein, R. (1973) *Adv. Quant. Chem.* **7,** 335.
29. Rein, R. (1978) in *Intermolecular Interactions: From Diatomics to Biopolymers*, ed. Pullman, B., John Wiley, New York, p. 307.
30. Kitaigorodski, A. I. (1961) *Tetrahedron* **14** : 230.
31. Kitaigorodski, A. I. & Mirskaya, K. V. (1964) *Kristallografia* **9** : 174.
32. Huron, M. J. & Claverie, P. (1974) *J. Phys. Chem.* **78** :1862.
33. Caillet, J & Claverie, P. (1974) *Biopolymers* **13** : 601; (1975) *Acta Cryst.* **A31** : 448.
34. Caillet, J., Claverie, P. & Pullman, B. (1976) *Acta Cryst.* **B32** : 2740.
35. Tolman, R. C. (1938) *The Principles of Statistical Mechanics*, Oxford University Press, London.

CONTENTS

Published by Professor H.C. Khare, General Secretary for the National Academy of Sciences, Allahabad and printed by National Graphics, Allahabad.

Managing Editor – Professor S. L. Srivastava